Device Deployment Strategies for

Large-scale Wireless Sensor Networks

Kenan Xu

A thesis submitted to the
Department of Electrical and Computer Engineering
in conformity with the requirements for
the degree of

Doctor of Philosophy

Queen's University

Kingston, Ontario, Canada

January 2008

ABSTRACT

Planning device deployment is a fundamental issue in implementing wireless sensor network (WSN) applications. This design practice determines types, numbers and locations of devices in order to build a powerful and effective system using devices of limited energy supply and constrained capacities. The deployment plan decides the limits of many intrinsic properties of a WSN, such as coverage, connectivity, cost, and lifetime. In this thesis, we address the device deployment planning issues related to large-scale WSN systems.

We consider a typical deployment planning scenario in a heterogeneous two-tier WSN composed of sensor nodes and relay nodes. Sensor nodes form the lower tier of the network and are responsible for providing satisfactory sensing coverage to the application. Relay nodes form the upper tier of the network and they are responsible for forwarding data from sensor nodes to the base station. As so, relay nodes should provide reliable connectivity to sensor nodes for an extended period of time. We therefore address the sensor node deployment in terms of the sensing coverage and relay node deployment in terms of the communication connectivity and system lifetime.

For sensor node deployment, we propose a coverage-guaranteed sensor node deployment design technique. Using this technique, the sensing coverage is complete even if sensor nodes are randomly dispersed within a bounded range from its target locations according to a given grid pattern. In order to curb the increased cost due to extra sensor nodes that are used in the coverage-guaranteed deployment, while still maintaining a high-quality sensing coverage, we further study the probabilistic properties of the grid-based sensor node deployment in the presence of deployment errors.

For relay node deployment, we propose to extend the system lifetime by distributing relay nodes according to a density function, which is optimized in response to the energy consumption rate, so that the energy is dissipated at an approximately same rate across the network. We further craft the deployment density function to reconcile the needs of balanced energy consumption and strong sensor node connectivity.

The techniques proposed in this thesis fill the blank of available literature and can serve as guidelines for WSN designers, solution providers and system integrators of WSN applications.

ACKNOWLEGEMENTS

No single person affects a student's graduate experience more than his advisors. I am very fortunate to have had my advisors professor Hossam Hassanein and professor Glen Takahara. Professor Hassanein has guided me with his broad experience and pioneering vision. Not only does he teach me on specific technical issues, but only he points me to big pictures within which a certain subject exerts the greatest value. Professor Takahara mentors me with his extremely comprehensive knowledge of mathematics and exceptional skills of modelling. He also shows me a great deal of articulation in research, and spares no efforts to ensure that research is conducted in the most accurate and effective way. I believe such a combination will turn me into a successful researcher in years to come. In addition, they both are dedicated and very generous with their time, knowledge, and experience, which has been invaluable. In addition to their professional guidance, both my professors help me to grow personally throughout the up-and-down time. Professor Hassanein has been always positive, supportive and humorous. Professor Takahara has been always considerate, patient and sympathetic.

This thesis is dedicated to my mom, Xingkai Chen. Even though she was thousands of miles away during the course of my program, as always, I continually felt her boundless

support, love, understanding and unfaltering approval. I am forever indebted to her. While I regret that my father, Ling Xu, was never able to see the completion of my Ph.D, I am comforted by the knowledge of the pleasure it would have given him. His education and care was primal in awaking a desire for learning within me that I hope will never expire.

This thesis is also dedicated to my dear wife, Yuanyuan Feng. I feel extremely lucky to have her, a beautiful, bright, considerate lady, be my life-long partner. She has always been supportive to my career development since we knew each other. Her genuine love and strong support have been a powerful propel that brings me to this stage.

I would like to thank my other family member, especially to my cousin Hong Xu. She has given me a lot of support and care since the very early time. She has always been there for me and the family so that I can concentrate on my research.

I felt regretful to learn of the recent passing of Yinghong Fan, a telecommunication research lab alumnus and my close friend, during the end of my thesis writing. Yinghong, along with many other friends, past and present, has helped me to become the person I am today. They have taught me much, and their advice, feedback and friendship have made my postgraduate experience both more educational and more fun. I feel grateful to Dr. Quanhong Wang, my colleague in the telecommunication lab. We had great collaboration on a lot of research work. It has been said many times that a person is only as good as those who surround him and I am indeed fortunate.

I wish to thank the faculty of the Department of Electrical and Computer Engineering at Queen's University for their excellent instruction and dedication. I would also like to express my gratitude to the respectful graduate program staffs in the department, including Ms. Bernice Ison and Debie Fraser. I feel privileged to have their consistent support during my stay in Queen's.

Finally, I gratefully acknowledge the financial support of Queen's University, Natural Science and Engineering Research Council and Ontario Centers of Excellence.

TABLE OF CONTENTS

LIST OF TABLES

LIST OF FIGURES

LIST OF ABBREVIATIONS AND ACRONYMS

2CRNDC	2-Connected RN Double Cover
BECR	Biased Energy Consumption Rate
BER	Best-Effort-Relaying
BLUE	Best Linear Unbiased Estimator
BS	Base Station
CDF	Cumulative Distribution Function
CH	Cluster Head
CPLOAD	Collaborative Placement with Locally Optimal Traffic Allocation
CRNSC	Connected RN Single Cover
CUB	Central Utility Support Building
ECI	Energy Consumption Intensity
FPRN	First Phase RN
GPS	Global Positioning System
ID	Identification
ILP	Integer Linear Programming
MAC	Medium Access Control
MINLP	Mixed-Integer Non-Linear Programming
MSIS	Multiple Sensor Indoor Surveillance

NTBF	Nearest-To-BS-First
OEM	Original Equipment Manufactor
PTZ	Pan/Tilt/Zoom
RF	Radio Frenquency
RFD	Reduced Function Device
RN	Relay Node
RSSI	Received Signal Strength Indication
SMART	Movement-Assisted sensoR deploymenT method
SMT-MSPBEL	Steiner Points and Bounded Edge Length problem
SPINDS	Smart Pairing and Intelligent Disc Search
SPRN	Second Phase RN
SN	Sensor Node
ToA	Time-of-Arrival
VFA	Virtual Force Algorithm
WSN	Wireless Sensor Network

LIST OF IMPORTANT SYMBOLS

x_d	Signal strength arriving at a sensor that is at a distance *d* from the originator
d	Distance
θ	Signal strength at the originator
n	Noise strength
α	Signal decay exponent.
K, M, N	integer
ε , η	Real number
P	Path from source to destination
$r_s , r_s^{'}$	Sensing radius of sensor nodes
r_c^{S}	Communication radius of sensor nodes
r_c^{R}	communication radius of relay nodes
r_c	communication radius of nodes
l	Packet length
l_{AG}	Packet length of an aggregated packet
$l_{AG}(l,n)$	Length of the aggregated packet from n packets of length *l*.
l_{relay}	Length of the packets received from inter-cluster communication
$E_{RX}(l)$	Energy spent by receiving a packet of length *l*.
$E_{RX}(l,n)$	Energy spent by receiving n packets of length *l*.
$E_{TX}(l,d)$	Energy spent by transmitting a packet of length *l* over a distance *d*.
$E_{AG}(l,n)$	Energy spent by aggregating *n* packets of length *l*.
g	Aggregation ratio
$\beta , \alpha_1 , \alpha_2$	Circuit specific energy parameters.

m	Radio signal decay exponent.
E_{intra}	Energy used for intra-cluster communication and data processing.
E_{inter}	Energy used of r inter-cluster traffic relay.
q	Minimum percentage of SNs with connectivity in a newly deployed network
σ	Connection probability of an individual SN
σ_0	Minimum connection probability of an individual SN
N_{SN}	Number of SNs
r_{obj} , r'_{obj}	Disk radius of an object
L	Size length of a square field
A, F	Sensing field
$s_i\,(i=1,\ldots,N)$	SN node i
$d(x,s_i)$	Distance from a point x to s_i
$d_{\min}(x)$	Minimum distance from a point x to a SN.
$d_{\max\min}(y)$	MaxMin distance of the sensing field.
$p_i\,(i=1,\ldots,N)$	A convex polygon
e_h	Horizontal misalignment
e_v	Vertical misalignment
r	Distance between consecutive SNs
$V_{\min}$	Minimum vertical misalignment
$V_{\max}$	Maximum vertical misalignment
R	Random error radius
X	Covered area of a sensing field
$X_i\,(i=1,\ldots,N)$	Covered area of a triangle area of Δ_i
p_c	A pre-specified proportion of coverage of a sensing field
$p(x)$	Probability that a point x is covered by at least one SN.
$A_m\,(m=1,\ldots,N)$	Event that a point is covered by SN s_m
$B_m\,(m=1,\ldots,N)$	Event that either a point x or y is covered by SN s_m

Z	Set of integers
Z^d	d-dimensional integer lattice
$\{Y_a\}_{a\in Z^d}$	Family of random variables indexed by elements of Z^d
$\Im$	Set of all finite subsets of Z^d
V	A set
$\|V\|$	Number of elements in V
$D(V_1, V_2)$	Distance between set V_1 and V_2.
$\Phi(\cdot)$	Standard normal cumulative distribution function
ε_n	maximum absolute difference between the probability distribution function of $S(V_n)/\sigma(V_n)$ and that of a standard normal random variable.
p_R	Probability that a sensor node reaches at least one relay node
$p_R(d,\theta)$	Probability that a sensor node at (d,θ) can reaches at least one relay node.
$N_{RN}^{u\{\min\}}$	Minimum number of relay nodes in order to satisfy connectivity requirement if they are deployed in a uniform manner.
$N_{RN}^{w\{\min\}}$	Minimum number of relay nodes in order to satisfy connectivity requirement if they are deployed in a weighted random manner.
h_{RN}	Effective communication radius of relay nodes
$N_{RN}^{w\{\min 1\}}$	Minimum number of relay nodes in order to satisfy connectivity requirement in sensing area A_1 if they are deployed in a weighted random manner.
$N_{RN}^{w\{\min 2\}}$	Minimum number of relay nodes in order to satisfy connectivity requirement in sensing area A_2 if they are deployed in a weighted random manner.
$N_{RN}^{w\{\min 3\}}$	Minimum number of relay nodes in order to satisfy connectivity requirement in sensing area A_3 if they are deployed in a weighted random manner.

Chapter 1. INTRODUCTION

Recent design developments in micro-processor, micro-sensor and radio frequency (RF) technology have made it feasible to develop low-power, inexpensive, and wireless-networking-enabled sensor devices. A wireless sensor device generates data from sensing physical characteristics such as temperature, pressure and sound, and then transmits this data to the base station via an onboard radio either periodically or on-demand. According to different application requirements, a wireless sensor network (WSN) may consist of just a few or as many as thousands of wireless devices, operating in a collaborative and coherent manner to fulfill a common task.

In this chapter, we will first highlight the major characteristics of WSNs, followed by an introduction of their applications. We then introduce challenges and technical approaches to address them. We further explain the research problems explored in this thesis, i.e., WSN deployment problems, and its importance to WSN applications. The thesis contributions are also summarized briefly. In the end, the organization of this thesis is outlined.

1.1. Characteristics

Compared to traditional wired sensing/data acquisition systems, WSNs exhibit the following characteristics which make them very attractive technology for many applications.

- Eliminated wires: Many advantages of WSNs stem from the fact that they require either less wire or no wire at all. First, this makes WSNs applicable to a very wide spectrum of applications, providing a convenient and effective alternative to their wired counterparts, in such application areas as home control systems [1], building automation systems [2], and industrial automation and monitoring systems [3]. This is particularly attractive if such a system is established on a temporary basis or it is retrofitted into a legacy environment. They also enable a series of new applications where wiring is not possible or highly undesired, such as commodity health care products (e.g., wearable health monitors [4]), large-scale natural environment monitoring and control (e.g., [5, 6]), and precision agriculture (e.g., the soil moisture monitoring system at Camalie Vineyards, California [7]). Second, a WSN is highly flexible. One can construct a WSN by just a few devices initially, and expand the network to as many as thousands of devices later, according to the application requirements and budget availability. Third, the characteristic of no/less wire also brings a significant reduction in both capital investment and operation cost, and there are also large savings in time and labor for system setup and system maintenance.

- Small size devices: Researchers and engineers have built small form factor wireless sensor devices. For example, both Mica nodes from Crossbow Technology [8] and Tmote nodes from Moteiv [9] have similar dimensions to a typical match box. A Micadot node is as small as a coin. They are illustated in Figure 1.1. Furthermore, the industry has tried to devise ever-smaller system-on-chip products, such as the MICAz OEM Module [8]. Coupled with the characteristic of no/less wire, the miniaturization of devices allows them to operate in close proximity to objects of interest in the least intrusive manner possible. Therefore, the measurement is potentially more accurate.

(a) A Mica node (58mm*32mm*7mm)

(b) A Tmote node (32mm*20mm*1.8mm)

(c) A Mica dot node (25mm*6mm)

Figure 1.1 An illustration of small-size devices

- High redundancy: The low cost of individual wireless sensor devices allows one to set up a WSN network including many redundant devices. The device redundancy provides greater system robustness and extends the system lifetime if devices are effectively scheduled to alternate between active and sleep states. While redundant sensor devices may generate redundant data, this data redundancy can actually enhance sensing accuracy if data from different sources are effectively analyzed and combined.

1.2. Applications of WSNs

Thanks to its desirable characteristics, partially discussed above, a WSN can provide effective solutions to a full spectrum of applications. It can be used in all kinds of environments; hostile and friendly, urban and suburban, civilian and military, industrial, agricultural and scientific. Instead of presenting a long list of its potential applications, we briefly describe a few representative applications with implementation examples. These applications are also summarized in Table 1.1.

Table 1.1 WSN Applications

Application types	Example deployments
Industrial automation	a. Monitor the vibration signature for preventive maintenance of equipment in fabrication plant [10].
Precision agriculture	a. Monitor the temperature and humidity of soil and control the irrigation in Camalie Vineyards, California, USA [7].
Natural environment monitoring	a. Study the micro-climate surrounding a redwood tree [5]. b. Study the habitat on the Great Duck Island, Maine [6].
Building structure monitoring	a. Monintor the golden gate bridge[11]. b. Structural health [12].
Civilian surveillance	a. MSIS system for civilian surveillance [13]. b. IrisNet demonstration parking space finding application [14].

- Industrial automation: Industry has long been the pioneer of new technology adoption. While wired sensing technology has been widely present in various stages of advanced state-of-the-art fabrication systems, there is a great need for automatic sensing and control solutions for legacy and/or less advanced equipment. A WSN can satisfy such needs effectively. For example, Krishnamurthy et al. [10] describe a trial deployment of WSNs in a central utility support building (CUB) at a

semiconductor fabrication plant to monitor the vibration of equipment for the purpose of preventive equipment maintenance [10]. Cost analysis demonstrates that WSNs can provide high quality data at a relatively low expendure in installation and operation. As a result, WSNs have broad applicability in predictive maintenance of mechinery, which may represent a killer application of the WSN technology.

- Precision agriculture: It is inherently difficult and expensive to set up and maintain wired sensing systems in agriculture applications because of their large coverage area and outdoor exposure. However, many such challenges are naturally overcome by wireless sensor devices. The fact that there is no or less wire largely simplifies installation and maintenance efforts, making WSNs particularly attractive to agricultural applications. For example, an advanced soil moisture monitoring system has been deployed in Camalie vineyards, California, USA [7]. The system, known as Camalie Net, consists of thirty Mica wireless sensor devices. Driven by the moisture information, the system can irrigate more effectively in an on-demand manner. As a result, water consumption and associated pumping energy costs are reduced while simultaneously improving grape quality and yield. For instance, yield per vine in 2005 was double that in 2004 for vines of the same age yet water consumption was constant. The increase in yield was stayed in 2006.

- Environmental monitoring: An important benefit of WSNs is that they enable non-intrusive and large-scale monitoring, which is critical to many environmental monitoring applications. In [6], Mainwaring and colleagues present a real-life experiment of deploying a 32-node WSN in a natural area-Great Duck Island,

Maine—to monitor the Leach's Storm Petrel for the short-term cycle (24 to 72h) usage pattern of nesting burrows and long-term changes (7 months) in burrow and surface environmental parameters. In [5], Tolle et al. present a case study of a WSN that monitors the micro-climate surrounding a 70-meter tall redwood tree, at an observation density of every 5 minutes in time and every 2 meters in space. Each node measures air temperature, relative humidity, and photosynthetically active solar radiation.

- Building structure monitoring: WSNs can be used to collect and analyze a building's frequency response to ambient or forced excitation. Such a system is an unprecedented tool for studying the structural integrity and also provides valuable information indicating the building's health status. A general paradigm of such applications is a data acquisition system that collects data using many distributed devices and processes them at a centralized location. In [12], Xu et al. explore the design and evaluation of a WSN system called Wisden for structural data acquisition. Novel mechanisms are reported to enhance the reliability of data transport and allow for asynchronous operation. Researchers also examined the applicability of wavelet-based compression techniques to overcome the bandwidth limitations imposed by low-power wireless radios. Again, the system is implemented on Mica nodes. Another WSN deployment of building structure monitoring is conducted in San Francisco, where 64 motes are used to track stresses on the Golden Gate Bridge [11]. By measuring the swing of the bridge, sensor nodes together can detect a potential weakness in structural integrity and alert engineers of possible risks.

- Civilian surveillance: Surveilling civilians for safety and information is another important application of networked embedded sensing with significant social and economical value. One example is to use WSNs for access control. Coupled with the emerging technology of wireless mesh networks [15], a wireless surveillance system is particularly attractive because of its wide coverage and abundant information. Accenture Technology Labs has worked on the Multiple Sensor Indoor Surveillance (MSIS) project, whose objective is to develop methods to coherently reason about security-relevant information of the environment based on the noisy inputs from 32 webcams, an infrared badge ID system, a PTZ camera, and a fingerprint reader [13]. Another example is a parking space finding application demonstrated in a research project called IrisNet [14].

In summary, the emerging WSN can provide a powerful and ubiquitous monitoring platform for a wide range of applications. Yet more deployments will be conducted in the coming years, and there remain a number of challenges which must be addressed in order for the great potential of WSNs to be realized.

1.3. Challenges and Technical Approaches

Generally speaking, the research and development of WSN technology has aimed at an effective, multi-functional and reliable monitoring platform formed by small devices. This is very challenging since most individual devices are subject to stringent resource constraints and highly limited capabilities, including power supply, computation

capability, storage, etc. Three major tasks are conducted by a typical WSN, namely, sensing, in-network data processing, and wireless communications. We explore the technical issues with each of these three functionalities and provide technical approaches that address these issues.

Sensing is the most essential and critical functionality of any sensing network. Individual wireless sensor nodes usually can detect events or monitor the environment only in their close proximity due to the very nature of the signal and the relatively inferior sensitivity of miniaturized sensory units. On the other hand, we often expect a WSN to serve a large area with satisfying sensing coverage quality. According to different application scenarios, sensing coverage objectives can be classified into three types: continuous area coverage, distinct point coverage, and crossing coverage. The quality of sensing coverage is measured by both the quantity, such as the size of the area covered, and the quality, such as the degree of coverage. A higher degree of coverage (e.g., two or more sensors monitoring one point) means better reliability and allows for localizing and tracking objects. To this end, a typical design problem is to satisfy a given coverage requirement with a minimum number of devices, or to provide the best coverage possible with a given number of devices. Furthermore, one may choose to intentionally deploy redundant sensing devices and have them operate in an alternative manner in order to prolong the system lifetime. An associated design problem in this case is an effective duty cycle scheduling mechanism so that a minimum number of sensors are active at any given time while providing satisfactory sensing coverage.

In-network data processing plays an important role in the operation of WSNs. The advancement of micro-processor technology has been much faster than that of battery technology. It has been recognized that sensor nodes will have significant processing capabilities but very limited energy [16]. Furthermore, wireless communication is orders of magnitude more expensive than local computation in terms of energy consumption [17]. This encourages the idea of processing and aggregating raw data locally where they are originally generated and therefore reducing the traffic volume inside the network. As a result, energy is saved and the network lifetime is prolonged. Another attractive benefit is that network congestion can be significantly reduced. In-network data aggregation and collaboration are enabled by means of classification, filtering, transformation and compression. For example, suppose a WSN is to find the minimum moisture reading in a sensing field. A filter will be associated with the humidity data, and when multiple data arrive at the node, the filter is triggered to select the highest reading from the set and then create and send a new message. In order to efficiently conduct data aggregation it is important to organize the network into a facilitating structure, such as clusters or data gathering trees. Efficient distributed topology control schemes are therefore critical.

While raw data are generated by sensing the environment and processed locally within the network, they are typically transmitted through the network via wireless media. Researchers have predominantly advocated multi-hop ad hoc networks as the communication architecture of WSNs. In contrast to the conventinal wireless system, an ad hoc network does not rely on a centralized infrastructure, such as a base station in a cellular network and an access point in a wireless LAN. Instead, communication devices

are self-organized into a connected network on the fly. If the distance between two devices are far, the packets are relayed through the intermediate nodes, which route the traffic based on a dynamically maintained routing table (cache). A detailed discussion of the characteristics of multi-hop ad hoc networks can be found in [18]. An infrastruct-based network and a multi-hop ad hoc network are illustrated and compared in Figure 1.3.

(a) An infrastructure-based wireless network (b) A multi-hop ad hoc wireless network

Figure 1.2 A comparison of infrastructure-based networks and multi-hop ad hoc networks

With an effective implementation, an ad hoc network architecture offers a range of benefits to WSNs, including energy-efficient network operation, fast and easy network deployment, high robustness, reliability, etc. Energy efficiency is the most important factor in WSNs as devices are highly energy-constrained. In a wireless ad hoc network, energy efficiency is to be achieved by using multi-hop wireless relays over short distances, low-power and low rate RF transceivers, energy-efficient MAC protocols, and energy-aware routing protocols. The key principles of designing energy-efficient MAC protocols are to eliminate transmission collisions, adjust the transmission power according to the signal attenuation, and put radio interfaces in a sleep state for as much as possible. For routing protocols, the main approaches include choosing the route based on energy factors, such as residual energy and energy consumption, and choosing routes with the least traffic load to avoid congestion. Easy and fast system setup is also critical

to the success of a WSN application. Using effective algorithms, sensor nodes are able to self-organize, self-coordinate, and self-configure into an effective network topology and start to function once they are deployed. This will result in significant savings in deployment cost. Reliability and robustness are also important, and ad hoc networks are resilient to single point of failure scenarios. Besides, ad hoc networks can adapt to network changes caused by node failure, link failure, additive node deployment, etc. Furthermore, scalability is important to a WSN, which may consist of thousands of nodes. In a WSN, scalability can be achieved by effectively organizing the network into a tiered architecture, such as clusters and data aggregation trees.

1.4. WSN Deployment Problems and Thesis Contributions

As discussed above, the sensing coverage quality, the network connectivity, and the system lifetime will fundamentally determine the effectiveness and practicality of a WSN application. On the other hand, individual devices have very limited capabilities and resources, such as short sensing radius, limited power supply, etc. As such, WSN solution designers confront the fundamental challenge of constructing a high-quality and long-lasting but affordable WSN system using resource-constrained devices. The solution rests on an effective deployment plan. The plan depicts a rational combination of different types of devices and their positions, so that the overall system can satisfy the application requirements, including sensing coverage, lifetime, connectivity and reliability, at the minimum cost possible.

Some previous studies have tried to solve the WSN deployment problem. However, the algorithms and tools suggested by these studies have their limits. Some of them do not scale and can only be used in small scale WSNs. Some assume deliberate device placement without addressing deployment errors, which are inevitable in many scenarios. Many of these studies only try to optimize one metric of WSNs, such as lifetime, while ignoring the negative impact on other metrics, such as sensing quality. None of them have proposed a unified deployment framework in which both sensing coverage and the long-lasting network connectivity are addressed. A discussion of the previous work in this area is presented in Chapter 2.

In this thesis, we propose a unified deployment framework for a two-tier large-scale WSN and a set of associated methodologies. The first tier of the network comprises sensing nodes (SNs) which sense the environment and generate data. Therefore, the deployment of SNs is mainly concerned with sensing coverage. The second tier consists of relay nodes (RNs) which form the communication backbone and relay data from SNs to the base station. The RN deployment should ensure sufficient connectivity to SNs of the lower tier and at the same time be concerned with balanced energy consumption throughout the network so that the system lifetime is prolonged. As we aim at large-scale WSNs, grid-based deployment and random deployment are two viable deployment approaches. To this end, this thesis has three major contributions.

Firstly, we propose a coverage-guaranteed grid-based SN deployment. Previous work has addressed grid-based SN deployment under the assumption that devices can be placed

exactly at the grid vertices. However, in practice, the accuracy of device placement may be subject to various errors which impair the sensing coverage. To overcome the negative impacts of these errors, the grid resolution and the number of devices to be deployed needs to be re-evaluated. We identify two deployment errors: misalignment and random errors. We derive the minimum number of sensors required to achieve guaranteed coverage when deployment errors of these types are present. Since the deployment can guarantee sensing coverage even if the worst-case deployment errors take place, we call it the coverage-guaranteed grid-based SN deployment.

Secondly, we found the number of SNs required by the coverage-guaranteed grid-based SN deployment increases dramatically as the deployment errors become large. In order to reduce the number of SNs to be deployed (and therefore the deployment cost), we further study the probabilistic properties of the sensing coverage area of a wireless sensor network (WSN), in which sensor nodes are deployed randomly around the grid vertices. This is very useful when the coverage-guaranteed grid-based SN deployment becomes prohibitively expensive and/or the application can tolerate the loss of sensing coverage to some extent. We prove the sensing coverage area of a WSN deployed in a grid pattern follows approximately a normal distribution. We further propose a generic approach to evaluate the parameters of the normal distribution, i.e., the average and the variance of the covered area of the sensing field. Our generic approach can be used with all types of grid-shapes, all kinds of random error distributions, and different sensing models. We apply the generic approach to one specific deployment scenario: a triangular grid-based deployment with bounded uniform random error. From the numerical results, we find that

a grid-based sensor deployment WSN is quite resilient to deployment errors in many cases. This is a very encouraging characteristic and serves as a strong basis for adopting grid-based deployment in practice.

Finally, we also investigate RN deployment methods so as to provide connectivity to SNs and to maximize lifetimes. Particularly, assuming SNs having been uniformly deployed on a sensing field, we investigate how an RN deployment density function affects the network lifetime of a WSN. We first examine the Biased Energy Consumption Rate (BECR) problem with a uniform random RN deployment in both single-hop and multi-hop communication scenarios. This problem results in low energy utilization of RNs and an unnecessarily short system lifetime. To overcome the BECR problem, we propose a novel deployment strategy called lifetime-oriented deployment so as to balance the energy consumption rate of RNs across the network. However, this method is shown to provide poor connectivity to SNs when the number of RNs is relatively small. We further propose a hybrid deployment method which balances the goals of connectivity and lifetime. Our performance study of these deployment strategies shows the new strategies significantly outperform uniform random deployment. All designs and performance studies have been conducted for both single-hop and multi-hop communication scenario.

In summary, this thesis provides guidelines for large-scale device deployment of typical heterogeneous WSNs.

1.5. Thesis Outline

The rest of the thesis is organized as follows. In Chapter 2, a comprehensive review of WSN deployment methods in the literature is conducted. The technical concerns of WSN deployment are examined and technical proposals are classified and compared. The motivation of the thesis research is explored by identifying unsovled problems.

In Chapter 3, models of the system are discussed. First, the composition of a heterogeneous WSN is described. Second, the sensing capacity of an SN is modelled in two ways, namely, the binary disk model and the distance-based probablistic model. Third, energy comsupiton due to data communication is modelled. Fourth, the definition of WSN system lifetime is presented. Finally, we explain that our deployment study does not depend on the availability of device location information.

In Chapter 4, the grid-based SN deployment is devised so as to provide complete sensing area coverage even in the presence of worst-case deployment errors. We first examine the different types of deployment errors and their impact on the sensing coverage. We then derive deployment parameters in order to eliminate the void areas caused by deployment errors.

In Chapter 5, we investigate the probabilistic properties of the sensing coverage area provided by SNs which are dispersed from the grid vertex due to random deployment errors. We first propose a generic approach to evaluate the average and variance of the sensing coverage area. We then prove that the sensing coverage area follows approximately a normal distribution. The generic evaluation approach is applied to a

specific deployment scenario. We also develop a procedure for designing cost-effective grid-based SN deployment for probabilistic sensing coverage.

In Chapter 6, we study the effects of random RN deployment strategies. We first discuss the biased energy consumption rate problem associated with uniform random RN deployment. This problem leads to insufficient energy utilization and shortened network lifetimes. To overcome this problem, we propose two new random deployment strategies, namely, the lifetime-oriented deployment and hybrid deployment. The former solely aims at balancing the energy consumption rates of RNs across the network, thus extending the system lifetime. The latter reconciles the concerns of connectivity and lifetime extension. Both single-hop and multi-hop communication models are considered.

Finally, Chapter 7 concludes the thesis and offers directions for future research.

Chapter 2. RELATED WORKS AND MOTIVATION

A critical aspect of the design of any monitoring system is device deployment planning, which consists of determining an appropriate placement of monitoring devices to accomplish the desired task. The art gallery problem studied by Hoffmann et al. in [19] was one of the early works in the literature. The objective of the art gallery problem is to use a minimum set of guards in a polygon such that every point of the polygon is watched by at least one guard, who is assumed to observe anything that is in the line of sight.

As for WSNs, device deployment planning is a process that determines the types, numbers, and locations of different devices, so that application performance requirements (such as a minimum sensing coverage, ensured communication connectivity, and/or a minimum system lifetime) are satisfied in the most cost-effective manner or so that system performance is optimized for a given cost (device) budget.

Device deployment planning is of paramount importance for WSNs as it decides the available resource and their configuration for system setup, which in turn fundamentally determines the WSN performance bounds. Many design efforts have been made to optimize the WSN performance at operation time, such as duty cycle scheduling algorithms that put as many sensor devices as possible into the sleep state while keeping

a satisfactory sensing coverage and a connected network, energy-efficient MAC protocols that minimize the energy wastage when wireless transceivers are in idle state and/or by data retransmission, and energy aware routing algorithms which route traffic through an energy-efficient data path. The surveys in [16, 20] present a comprehensive review of these efforts, which aim at improving the network operation efficiency and achieving the best performance possible for a given set of resources. However, even the best suite of run-time protocols will not be able to provide the required system lifetime if devices are not provisioned appropriately beforehand. For example, if the number of installed devices is insufficient or there are topological deficiencies due to ineffective device placement, the sensing coverage or system lifetime will be degraded, or, in the worst case, the system will be non-operational.

Due to the various constraints of wireless sensor devices discussed in the first chapter and the characteristics of wireless ad hoc networking, the emerging WSN presents many new challenges to the problem of device deployment planning not considered in the art gallery problem. First, the sensing range of a sensor device is normally finite, as compared to the infinite detection distance assumed in the art gallery problem. In the literature, a variety of sensing models have been proposed, such as the binary disk model and the distance-based probabilistic detection model. Moreover, different coverage objectives have been considered, such as area coverage, grid vertex coverage, and crossing coverage. Second, devices in a WSN can only connect to devices in their neighborhood. Therefore, communication connectivity can not be taken for granted as in the art gallery problem which does not address the communication issue between guards. In some applications,

K-degree connectivity, where *K*>1, may be required for fault tolerance and enhanced network capacity. Third, sensor devices are supplied with limited energy, so network lifetime is of key concern in the deployment planning problem.

The device deployment planning problem for WSNs is further complicated by the availability of multiple different types of devices. One should judiciously choose a combination of them. In the literature, three types of devices are considered, namely, Sensor Nodes (SNs), Relay Nodes (RNs), and Base Stations (BSs). An SN senses the environment, generates data, and transmits the data to an active neighbouring RN. An RN relays traffic from SNs to BSs in a single-hop or multi-hop manner. In some cases, an RN could work as a cluster head to coordinate the operations of associated SNs. RNs are optional in the construction of a WSN, because if they are unavailable, SNs can relay traffic for each other. A BS is the final destination of all data traffic.

Due to its importance, the device deployment planning problem for WSNs has attracted a lot of interest and research effort. Various combinations of constraints and objectives have led to a rich research field. In this chapter, we present a comprehensive survey of the recent research advances on this subject. Using the categorization creteria adopted in [21], we present technical approaches of WSN deployment in two groups, i.e., static device deployment and dynamic device deployment. In a static node deployment, devices remain at the same locations over the course of their lifetime. In contrast, in the dynamic deployment case the locations of devices will be adjusted after the initial deployment. For each case, we categorize proposals according to the types of devices involved. The

shortcomings of these proposals are pointed out where appropriate. We also present the motivation of our research by discussing unaddressed problems in the literature. In the following, we discuss the most important concerns addressed in the device deployment planning literature, namely coverage, connectivity and system lifetime.

2.1. Coverage, Connectivity and System Lifetime

Sensing and communication are two essential functionalities of a wireless sensor device. On the other hand, most devices can only function for a limited time period, constrained by the fixed onboard energy supply. As such, the sensing coverage, communication connectivity between devices, and system lifetime are the most important factors when addressing WSN device deployment problems.

Sensing coverage reflects how well objects or events are monitored, detected, and/or tracked by the group of distributed devices, on a continuous space, at distinct positions, or along paths connecting two points. To address the sensing coverage issue of a WSN, the sensing model is an important factor. Generally speaking, the sensing capability of individual SNs has been modeled in one of two ways: probabilistic models of signal decay or the deterministic binary disk model.

The probabilistic models capture the nature of signal attenuation and persistent environmental noise. The signal strength, x_d, arriving at a sensor which is at a distance *d* from the signal originator, can be modeled as

$$x_d = \theta / d^{\alpha} + n, \qquad (2.1)$$

where θ is the signal strength at the originator, n is the noise strength, and $\alpha > 0$ is the signal decay exponent. Based on the signal attenuation model, two different probabilistic sensing models have been proposed, depending on whether multiple signals from different sensors are processed cooperatively or not. In [22], a cooperative measurement model based on a well-known Best Linear Unbiased Estimator (BLUE) is studied. The estimator can process readings from K SNs and generate one result with smaller errors. With this model, a point is said to be (K, ε)-covered if a signal generated from this point can be estimated by K sensors such that the probability that the absolute value of the estimation error is equal to or less than a preset threshold is equal to or larger than ε $(0 < \varepsilon < 1)$. However, some implementation issues remain to be addressed when the cooperative signal processing model is developed in practice. For example, as the signal originators randomly occur on the sensing field, deciding which K sensor readings the cooperative signal processing is conducted on is a non-trivial problem. A probabilistic model that does not consider cooperative signal processing is proposed in [23], where the probability that a sensor detects an object depends only on the distance between them and the noise, neither of which are affected by other nodes.

The deterministic binary disk model can be considered as a simplification of the probabilistic mode without cooperative signal processing. According to this model a point is covered if it is within the fixed sensing radius of an SN; otherwise, it is not covered. The main limitation of the disk model is that it does not reflect the inherent uncertainty due to signal attenuation through space and because of environmental noise. Also, it does not consider the performance gain due to cooperative signal processing of

multiple neighboring sensors. Nevertheless, due to its simplicity, the binary disk model is by far the most used model in the literature.

Enabled by the sensing functionality of individual SNs, WSNs are formed to satisfy the coverage requirements of various applications. The coverage concerns can be classified into three major types: (continuous) area coverage, crossing coverage, and discrete point coverage.

Area coverage is straightforward and refers to coverage through a two- or three-dimensional continuous space. Generally, K-degree (K>0) coverage is achieved if every point of a given space is covered by K or more SNs. High degree coverage provides improved accuracy and fault-tolerance against single point failure [24]. In some applications, such as object tracking, SNs not only detect the object, but also determine the position of the signal originator. In such a case, a point is covered if the network can localize the point within predefined error bounds. This localization coverage variant is carefully studied in [25].

Crossing coverage assesses the coverage quality by evaluating the detectability of a target traveling across a protected (monitored) area. This metric is vital to an entire class of applications, such as border protection. In [26], detectability is related to the distance from a path P to the sensors. Two characteristic paths are defined for a network: the maximal breach path and the maximal support path. The maximal breach path is the path whose closest distance to a sensor is as large as possible (e.g., maximize the minimum

distance between the path and sensors). The maximal support path is defined as the path where the farthest distance of any point of the path from the sensors is minimized. In [27], Meguerdichian et al. advocate enhancing the measurement by incorporating the travel time into the measurement of the detection probability of the path. Clouqueur et al. propose the notion of the exposure of a path *P* to be the net probability of detecting a target that traverses the field using *P* [28, 29].

The notion of *K*-barrier coverage, proposed in [30], is another metric of crossing coverage. A given belt region is said to be *K*-barrier covered by a sensor network if all crossing paths through the region are *K*-covered, where a crossing path is any path that crosses the width of the region completely. A path is said to be *K*-covered if it intersects with the sensing disks of at least *K* distinct sensors. Note that this differs from *K*-degree area coverage where every point along all paths is covered by at least *K* distinct sensors. *K*-barrier coverage is thus a much weaker notion than *K*-degree area coverage.

Discrete grid vertex coverage is studied based on the concept of representing a continuous sensing field by a collection of two- or three-dimensional grid points. In turn, the sensing coverage concerns focus on these grid vertices. Thus, complex calculus computation are avoided. Quite often, the positions of SNs are chosen to be at grid vertices. Grid vertex coverage is broken down into two different concerns, namely, detection coverage and localization coverage. The latter means that the location of the target is identified by the unique subset of sensors which sense the same grid vertex [31].

Given different coverage criteria, it is important and non-trivial to effectively and efficiently evaluate the sensing coverage quality of a given deployment of wireless sensors. Next, we will briefly discuss a few evaluation methods in the literature.

In [24, 32], Huang et al. propose algorithms, which are polynomial-time in the number of sensors, to computationally determine whether a sensing field is *K*-degree (area) covered, (*K*-covered), for a given sensor deployment. An algorithm was first devised assuming all SNs have the same sensing radius, and then extended for the case where SNs have distinct sensing radius. Based on the geometrical analysis, determining whether a given sensing field is *K*-covered is converted to determining whether the perimeter of each sensing disk is *K*-covered, which can be done in polynomial time. Theorem 4 in [33] improves this algorithm by transforming the problem of determining the coverage degree of a region to determining the coverage degrees of all the sening-disk intersection points in the same region. It is obvious that it is much easier to determine the coverage degree of a point than the disk perimeter.

The area coverage evaluation methods discussed above require knowledge of the whereabouts of the SNs. In the case of uniform random deployment, SNs are randomly deployed across the sensing field. Their locations are not deliberately controlled or known. The evaluation of coverage quality for randomly deployed SNs is the concern of the research in [34, 35]. Both papers derive asymptotic sensing coverage probabilities.

In [26], Meguerdichian et al. propose polynomial time algorithms to find the worst-case crossing coverage (Maximal Breach Path) and best-case crossing coverage (Maximal Support Path) for a given sensor deployment (SN positions are known). The paper also explores an optimization method to add more SNs in order to improve the coverage quality.

In [28, 29], Clouqueur et al. propose the notion of exposure of a path *P* to be the net probability of detecting a target that traverses the field using *P*. This paper further proposes an approximation solution to evaluate the minimum exposure of a given sensor deployment. The solution is composed of two parts. The continuous sensing field is first divided into an arbitrary grid, and a path is considered to be a connected set of edges within the grid. The detection probability of each edge of the grid is calculated. Therefore, finding the minimum exposure path between two points is equivalent to finding a shortest path between them, which can be efficiently solved by Dijkstra's shortest path algorithm. However, the optimization of the grid size, which is closely related to the speed of the travelling object, is left open for further research.

In [30], Kumar et al. propose efficient algorithms to determine if a region is *K*-barrier covered. For an open belt region (a belt region with open ends), the problem is reduced to the problem of determining whether there exist *K* node-disjoint paths between a pair of vertices in a graph. Existing algorithms for testing the existence of *K* node-disjoint paths between two vertices can be applied to globally test *K*-barrier coverage. For a closed belt region (a belt region with two ends connected), the problem of determining *K*-barrier

coverage is reduced to the problem of determining whether there exist K node-disjoint cycles, each of which loops around the entire belt region, which can be done in polynomial time.

Compared to the complexities of evaluating area coverage and crossing coverage, it is trivial to evaluate the discrete point coverage quality in polynomial time simply by determining the number of sensor disks overlapping each grid point. There is no research on this issue.

Communication connectivity is another critical factor that decides the application effectiveness, as it is essential to ensure that data are delivered to the BS for processing. In the context of a WSN, K-degree (K>0) connectivity has two different meanings, namely, K-path connectivity and K-link connectivity. The former means that there are K independent paths between every pair of nodes, while the latter means that each node is directly connected to K neighboring nodes. The former implies the latter, but not vice versa. In fact, a WSN could be disconnected even if K-link connectivity is satisfied. Generally, with K>1 connectivity, the network can tolerate some node and link failures. At the same time, the higher degree connectivity improves communication capacity among nodes. In some cases, it may not be necessary to maintain K connectivity among all devices, but only among nodes which form the communication backbone of the network.

For the sake of clarity, we define some notation to be used in the following discussion:

r_s : the sensing radius of SN in the case of the binary disk sensing model,

r_c^S : the communication radius of the SN, and

r_c^R : the communication radius of the RN.

In the special case where $r_c^S = r_c^R$, we use a single notation r_c to represent the communication radius of all nodes.

As discussed in the first chapter, lifetime is a predominate factor in all aspects of WSN design. Not only should the energy efficiency of individual devices be improved, but the lifetime issue also needs to be addressed from a system perspective. Energy-efficient communication protocols have been identified as a key approach to extending the system lifetime. In recent years, the portfolio of low power communication protocols, including energy-efficient MAC [36-38] and routing protocols [20], has expanded at an unprecedented rate. However, even the best suite of algorithms and protocols will not be able to provide the required system lifetime if devices are not provisioned appropriately beforehand. In other words, the types, numbers, and locations of devices determine a bound on system lifetime. Thus, device deployment plays a critical role in extending the network lifetime.

In the following section we provide a comprehensive review of the technical proposals in the literature. Using the categorization creteria adopted in [21], these proposals can be categorized into two types: static device deployment and dynamic device deployment.

2.2. Static Device Deployment

In most practical applications, devices do not change their locations once they are deployed on the sensing field. We call this kind of deployment practice static device deployment. In the literature, static device deployment is typically implemented in one of three approaches: deterministic deployment, grid-based deployment (also called pattern-based deployment) or random deployment.

Deterministic deployment refers to the case where devices can be exactly placed at arbitrarily selected locations. It is preferred whenever the deliberate placement of devices is allowed since it usually minimizes the number of devices or achieves the best performance. However, this approach becomes very expensive or infeasible if a large number of devices are involved, such as thousands of devices to be deployed in a forest, or the environment is hostile, such as a battlefield. Grid-based deployment may be applicable to large-scale WSNs due to its simplicity and scalability. The most studied grid patterns are the equilateral triangle grid, the square grid, and the hexagonal grid. However, such an ideal grid-based deployment also requires that it be feasible to place the sensor devices on the grid vertices exactly, which is very difficult in practice for large-scale deployment. As such, it is of great practical importance to take into account the inevitable errors when designing a grid-based deployment, but little research has been conducted on this issue. Another approach to large scale deployment is random device deployment, where a density function is used to dictate the distribution of devices over the sensing field. The most common density function is the uniform density function. However, the underlying assumption that the deployment is completely random is

sometimes overly pessimistic [2]. As a result, the deployment design for a given application is subject to overengineering.

As explained earlier, a WSN may consist of three types of devices (or two types if RNs are not employed), each of which has different roles. In the following, we organize the survey of static deployment approaches according to the devices involved.

2.2.1. Sensor Node Deployment

The typical formulation of SN deployment is to minimize cost (e.g., the number of SNs) under a coverage constraint, or maximize the sensing coverage quality for a given budget. Some studies also take energy efficiency into consideration. The same approach was adopted by [21] as well.

In [39], Efrat et al. study an extended version of the art gallery problem using line-of-sight sensors. Assuming that the sensing field is cluttered with obstacles, they devise algorithms to minimize the number of SNs required in order to have each point well covered, where well covered is defined as each point being seen by two sensors that form an angle greater than a given value, or each point being seen by three sensors that form a triangle containing the point. The algorithm is based on the Clarkson set cover methodology studied in [40].

In [41, 42], Zhang et al. investigate the sensor placement problem from a data fusion point of view. They argue that there is always an estimation distortion associated with a

sensor reading which is usually eliminated by processing multiple samples cooperatively. They thus map the problem of finding the optimal sampling points in an area to that of determining the optimal rate for achieving a minimal distortion, which is extensively studied in the signal processing literature. In other words, the problem is transformed from the space to the time domain. The optimal sampling points are related to the sensor locations. The main idea is to partition the deployment area into small cells and then the optimal sampling rate per cell is determined for minimal distortion. Assuming that all SNs have the same sampling rate, the number of sensors required in each cell can be determined.

In [43], Ganesan et al. explore the joint optimization of SN placement and transmission structure for data gathering, where a given number of sensors need to be placed in a field such that the sensed data can be reconstructed at a sink within specified distortion bounds while minimizing the total energy consumed for communication. The optimization becomes complex as it involves an interplay between the spaces of possible transmission structures given transmission radius limitations, and feasible placements which satisfy distortion bounds. A simpler version of the problem in 1-dimension is first solved by an analytical derivation and the result extended into 2-dimensions. However, in a general case, minimizing the total communication energy does not translate into a maximum lifetime, which in [42] and many other studies in the literature, is bounded by the shortest lifetime of all SNs.

In [44], Liu et al. devise a sensor placement in order to maximize the coverage area of a WSN constrained by the system lifetime, the energy budget, and the number of the SNs. The authors formulated and solved two optimization problems with and without allowing for arbitrary energy allocation among different SNs. However, this study only applies to a line network topology.

In [25], Wang et al. study random sensor deployments to achieve localization coverage. The authors first derive the relationship between localization errors and network resolution, which is the minimum distance d such that the network can distinguish any pair of points when the distance between them is larger than d. They then propose two methods to derive the necessary deployment density in order to guarantee a given localization error bound over the sensing field. In the first method, the localization coverage problem is converted into the widely studied detection coverage problem. A notion of sector coverage is introduced to derive the second method, which gives more accurate results.

In [2], Leoncini et al. study the coverage property of grid-based sensor deployments with random errors, in which SNs are dispersed around their target locations randomly. The authors attempt to minimize the number of SNs to achieve a required coverage quality on a sensing field, which is the minimum coverage percentage with a quantified probability. The paper first divides the sensing field into small square cells, so that a cell is covered if at least one sensor is located inside the cell. Next, the coverage percentage of two deployment methods are derived for a four-cell area, based on either deploying one

sensor around the center of each cell or deploying four sensors around the center of the four-cell area. It was observed that the former is better than the latter when the dispersion factor is small, and vice versa. The paper further derives an upper bound on the minimum number of deployed sensors to achieve a given coverage quality for a relatively large sensor network, when the dispersion factor is small enough. However, the research in [2] is specific to the two deployment setup studied and cannot be used with large scale grid-based SN deployment directly.

While the research above is concerned with area coverage, other research considers the grid vertex coverage problem. In [31], Chakrabarty et al. explore two SN deployment problems relevant to grid coverage. The first problem is to minimize the cost of sensors deployed by optimally choosing two types of sensors (differing in sensing range and cost) and their positions on grid vertices, with constraints of the coverage degree of grid vertices. The problem is formulated into an integer linear programming (ILP) problem and solved by public domain solvers. The second problem is determining sensor placement in order to provide localization coverage. The problem is mapped to uniquely identifying vertices in graphs, and efficient sensor placement strategies based on coding theory principles [45] are developed.

In [46], Lin et al. address SN deployment to minimize the distance of two indistinguishable grid points when complete discrimination is not possible because of the limited number of sensors. The problem is formulated as a combinatorial optimization problem which allows for a solution of complete location discrimination or one that

minimizes the distance of two undistinguished grid points, depending on the cost limitation. An algorithm is proposed to solve the problem based on the simulated annealing approach.

In [47, 48], Dhillon et al. address the grid vertex deployment problem when the sensing capability of an SN is modeled by a probabilistic model. The objective is to minimize the number of sensors subject to the sensing coverage quality requirement, which is dictated by minimum sensing probabilities at grid vertices. The paper proposes a heuristic method to place SNs iteratively. At each step, a sensor is placed at the grid point which currently has the lowest coverage probability.

In [30], Kumar et al. devise a deployment pattern to achieve *K*-barrier coverage with a minimum number of SNs. The optimal deployment is to deploy *K* rows of sensors on the shortest path across the length of the region, where each row has consecutive sensing disks abutting each other. The optimality of the pattern is proven. In the case that sensors are to be randomly deployed, the paper then derives the critical conditions for *K*-barrier coverage with high probabilities. *K*-barrier coverage refers to the detection of intruders as they cross a barrier of stealthy sensors, whose locations are not known to the intruder. The critical conditions make it possible to quickly compute the number of sensors necessary to ensure *K*-barrier coverage of the region with high probability.

Some research considers both coverage and connectivity in the SN deployment. In [49], Kar et al. attempt to devise a deployment plan in order to provide coverage and

connectivity using a minimum number of SNs, assuming the communication radius and the sensing radius are the same. A strip pattern is constructed by lining up sensors so that each sensor is within the transmission radius of its left and right neighbouring sensors. Multiple rows of strips are then arranged to provide coverage over a given sensing field. Transmission connectivity between rows of strips is achieved by deploying a vertical line of sensors. The same problem is addressed by Iyengar et al. in [50]. A lower bound of the deployment density of sensors (Theorem 1) to provide coverage and connectivity is derived. The optimality of the strip-based deployment in [49] is proven by comparing it with the lower bound.

In [33], Xing et al. extend research in [49, 50] by devising an SN deployment pattern when the communication radius and the sensing radius are of arbitrary relation. In the case where $r_c \le \sqrt{3} r_s$ a deployment pattern similar to that of [49, 50] is advocated, namely, multiple rows of connected strips of sensors plus one column of sensors. In the case where $r_c > \sqrt{3} r_s$, the paper proposes sensors be deployed in a equilateral triangular grid. This paper also proposes deployment strategies to cope with obstacles and boundaries, which are often encountered in an indoor environment. The research in [51] extends the results of [33] and shows that the strip-based deployment pattern is not only near-optimal but asymptotically optimal for achieving both full coverage and connectivity. Moreover, its optimality holds not only for $r_c / r_s = 1$ but for all $r_c / r_s < \sqrt{3}$. Further, the paper devises an optimal sensor deployment to achieve coverage and 2-connectivity by adding an additional vertical strip to the deployment. The asymptotic optimality of the deployment pattern is proven for all values of r_c / r_s. However, SNs

deployed in a strip pattern to enable the network connectivity in all deployment designs become performance bottleneck in terms of data transmission capacity and system lifetime.

In [52], Biagioni et al. evaluate the number of sensors needed to satisfy the requirements of sensing coverage and communication connectivity for several regular grid based sensor deployments, including a square grid, an equilateral triangle grid, and a hexagonal grid in a 2-dimensional region; they even analyze deployment, paired deployment, and in-line deployment for a 1-dimensinal region.

SN deployment is examined from a lifetime perspective in [53] and [54]. Uniform SN deployment results in a short system lifetime as SNs close to the BS usually consume more energy to relay traffic than those far away. In both studies, the objective is to optimize the random deployment density function so that SNs are dissipated of energy at the same rate across the network. In both studies, the basic idea is to cut the sensing field into a finite number of levels based on the distance to the BS. Inside each level, SNs share the traffic load from those SNs which are further away. Therefore, a density function can be determined for each level of the sensing field. However, the increasing density of SNs towards the BS, which is devised to balance the energy consumption rate over the network, is naturally non-optimal from a coverage perspective.

The static SN deployment proposals discussed in this section are summarized in Table 2.1.

Table 2.1 Static SN deployment proposals in the literature

Ref.	Deployment	Node type	Objective	Constraints
[39]	Deterministic	SN	Min. number of SNs	Sensing coverage
[41, 42]	Deterministic	SN	Max. sensing quality	Given SNs
[43]	Deterministic	SN	Min. com. energy consumption	A distortion bound and given SNs
[44]	Deterministic	SN	Max. coverage area	System lifetime, given SNs
[25]	Random	SN	Min. number of SNs	Localization coverage
[2]	Grid-based with errors	SN	Min. number of SNs	Coverage
[31]-1	Deterministic	SN	Min. cost of SNs	Grid coverage quality (deg.)
[31]-2	Deterministic	SN	Min. number of SNs	Grid coverage quality (loc.)
[46]	Deterministic	SN	Max. grid coverage quality (loc.)	Given SNs
[47, 48]	Deterministic	SN	Min. number of SNs	Grid coverage
[30]-1	Deterministic	SN	Min. number of SNs	Crossing coverage
[30]-2	Random	SN	Min. density of SNs	Crossing coverage with high probability
[49]	Deterministic	SN	Min. number of SNs	Coverage and connectivity
[50]	Deterministic	SN	Min. number of SNs	Coverage and connectivity
[33]	Deterministic	SN	Min. number of SNs	Coverage and connectivity
[51]	Deterministic	SN	Min. number of SNs	Coverage and connectivity Coverage and 2-connectivity
[52]	Grid-based	SN	Min. number of SNs	Coverage and connectivity
[53]	Random	SN	Max. lifetime	Given number of SNs
[54]	Random	SN	Max. lifetime	Given number of SNs

Our proposed research is different from the static SN deployment proposals discussed above in several aspects. First, most deployment strategies or design algorithms assume that SNs can be deliberately placed on specific locations. This is infeasible or very expensive in terms of labor cost, especially for large-scale applications. Some research advocates random SN deployment for large-scale WSN applications for reasons of its simplicity and scalability. However, the underlying assumption that the deployment is completely random neglects human efforts to control sensor placement during deployment and is often overly pessimistic [2]. In this thesis, we study grid-based

deployment for large-scale WSN applications. In contrast to the grid-based deployment studied in [52], our study takes deployment errors into consideration; namely, SNs are dispersed randomly around their target vertices. This is a very common issue with a large-scale deployment. While research in [2] considers the deployment errors with grid-based deployment, the study is specific to small-scale deployment scenarios and errors are modeled by the normal distribution. Our research aims at large-scale deployment scenarios and a variety of deployment error distributions.

Second, our study on SN deployment is only concerned with sensing coverage, and we leave the issues of network connectivity and system lifetime to RN deployment, which is discussed in the next section. Efforts to deploy identical SNs in terms of sensing coverage, connectivity, and/or lifetime are problematic. For example, the strip-pattern deployment of SNs in [33, 49-51] is a bottleneck of the WSN in terms of network capacity and lifetime, whereas the deployments proposed in [53, 54] that maximize lifetime are non-optimal from a sensing coverage perspective. Often it the literature, a heterogeneous network splits the tasks of ensuring coverage and connectivity between SNs and RNs. We present several RN deployment proposals in the following section.

2.2.2. Relay Node Deployment

Given the number and locations of SNs, the main goal of RN deployment is to establish a communication backbone to facilitate effective data transmission from SNs to the BS throughout the required network lifetime. As such, the first concern of RN deployment is connectivity, such that all SNs are connected to the BS via RNs. For some applications,

enhanced fault-tolerance through multiple connections is required. Another important aspect of the problem is energy efficiency and lifetime extension. Generally speaking, the closer two communication devices are to each other, the less energy is consumed for data transmission. Both SNs and the communication backbone formed by RNs should be considered with respect to the lifetime concern so that the system functions for a given lifetime. The exact form of the problem varies based on the combination of the optimization objective and the design constraints, including the communication ranges of RNs and SNs, the transmission power control capability, the network architecture, whether deployment is random or deterministic, and numerous other factors.

In [55], Wang et al. attempt to find locations for a minimum number of RNs so that each SN can reach at least one RN in one hop (SNs lifetime is ensured by limiting their transmission range). By limiting the candidate locations of RNs to the so-called densest regions, the search space of optimal locations is largely reduced. The problem is then modeled by a minimum set covering problem, which is generally known to be NP-complete. A recursive algorithm is proposed to solve the problem optimally. The practical computational complexity of the proposed algorithm is much less than exhaustive search in most real-world design cases. Following a divide-and-conquer strategy, the overall minimum set covering problem is split into a series of minimum set covering problems of smaller size. Other optimal and suboptimal greedy algorithms to solve the minimum set covering problem can be found in [56].

Other studies consider the end-to-end connectivity of SNs. In [57], Cheng et al. aim to deploy a minimum number of RNs in order to establish connectivity among SNs, where the transmission range of SNs and RNs is the same. The problem is formulated as an NP-hard optimization problem named the Steiner Minimum Tree with Minimum number of Steiner Points and Bounded Edge Length (SMT-MSPBEL). Two approximate algorithms are proposed to solve the problem. Both algorithms give results within a constant factor of the optimal. Lloyd et al. extend the research by assuming that relay sensors have longer transmission ranges than SNs and allowing both SNs and RNs to act as forwarders on a routing path. Based on finding the minimum spanning tree, an approximate algorithm is developed, which requires at most 7 times of the minimum number of RNs.

Some work considers higher degrees of connectivity. In [58], Hao et al. attempt to minimize the number of RNs such that each SN can communicate with at least two RNs and the network of the RNs is 2-connected. The problem is called 2-Connected RN Double Cover (2CRNDC), which is shown to be NP-hard. A polynomial time approximation algorithm is proposed. This research is limited to the case where the transmission radius of RNs is no less than twice that of the SNs.

In [59], Tang et al. address two RN deployment problems, namely, Connected RN Single Cover (CRNSC) and 2CRNDC as above. Two polynomial time approximate algorithms are proposed for each problem and their complexities are analyzed. The basic idea of these algorithms is as follows. The sensing field is partitioned into cells and the algorithm first determines a minimum number of RNs in each cell so that every SN is connected to

some RN. The algorithm then adds additional RNs to ensure connectivity between all of the RNs. In this research, the communication radius of RNs is assumed to be no less than four times that of SNs.

In [60], Lloyd et al. address a generalized form of the CRNDC problem by assuming the transmission range of RNs is greater than that of SNs. The paper solves the problem by proposing a general framework combining an approximate algorithm for the minimum geometric disk cover problem and an approximate algorithm for the SMT-MSPBEL problem.

In [61], Bredin et al. extend the research above by considering *K*-path connectivity between all nodes in a homogenous network. They show that the problem is NP-hard and propose an algorithm that places an almost-minimum number of additional sensors to augment an existing network into a *K*-connected network, for any desired *K*. The algorithm's result is proven to be within a constant factor of the absolute minimum.

In [62], Han et al. attempt to minimize the number of RNs necessary to provide *K*-connectivity to SNs in a heterogeneous network. Two different levels of *K*-connectivity are considered. The first one, called full fault-tolerance RN placement, aims at establishing *K* vertex-disjoint paths between every pair of sensor and/or RNs. The second one, called partial fault-tolerance RN placement, aims at establishing K vertex-disjoint paths only between every pair of SNs. Due to the different transmission radii of SNs and RNs, these problems are further complicated by the existence of asymmetric

communication links between neighboring nodes, resulting in one-way and two-way paths, in which communication can occur in one direction, but not in the other. The paper develops approximate algorithms for both problems which are then further extended to *d*-dimension (d>2) networks.

The literature reviewed above only considers the connectivity of the network. However, the limited, fixed energy supply of the devices makes the lifetime of the system a significant concern. As such, RNs can only relay a limited amount of traffic within a confined range. The next several paragraphs outline papers [32, 63-67] that address the lifetime-oriented RN deployment problem.

In [63], Oyman et al. attempt to guarantee a required lifetime for SNs while placing a minimum number of RNs. In this study, they consider that disjoint groups of SNs form clusters around RNs using the *K*-means algorithm. To find the minimum number of RNs and their locations, an iterative algorithm is devised. In each iteration, the maximum system lifetime is estimated for different numbers of RNs, starting from 1 and incrementing by 1 at each step, finding the optimal locations for the RNs at each step. The algorithm ends at the first iteration which ensures the required sysem lifetime.

A two-phase RN placement approach is proposed in [64, 65] to address RN placement when concerned with the lifetime of the communication backbone formed by the RNs. In the first phase, a minimum number of RNs are strategically placed with the aim of providing connectivity support to the SNs. In the second phase, RNs are added to provide

a complete relay path for each existing RN. In both phases, the energy limitation of RNs must be considered. The RN placement in the first phase is similar to the problem described in [55]. However, due to the energy limitation on RNs, the amount of traffic that an RN can handle is also limited. The criteria for candidate RN placement locations are modified to accommodate energy constraints. Then the minimum set covering model is applicable to solve the First Phase RN (FPRN) placement problem. After the first phase placement, each SN has been assigned an FPRN to forward its traffic. More RNs are needed so that every FPRN is able to find the neighbour(s) via which its traffic is relayed to the BS. In the literature, the Second Phase RN (SPRN) placement problem has been formulated using several different constraints [32, 64, 66, 67].

In [32], Hou et al. formulate a combined RN placement and energy provisioning problem as follows. Given the placement, traffic load and initial energy of the FPRNs, how can one allocate an additional energy budget E at M locations (which can be either at existing FPRNs or newly added SPRNs) such that the system lifetime is maximized? Implicitly assuming RNs are able to control their transmission energy, the authors of [32] first model this problem as a mixed-integer non-linear programming (MINLP) problem, which is known to be NP-hard. For such a MINLP problem, a heuristic algorithm called Smart Pairing and Intelligent Disc Search (SPINDS) is proposed, which can produce a satisfactory solution in polynomial time. However, in order to make use of SPINDS, it is presumed that the total energy can be partitioned arbitrarily. In practice, a discretely quantized energy supply is more feasible (e.g.,, a discrete number of battery units are used). In such cases, the SPINDS scheme should be modified. A similar problem is

addressed by Iranli et al. in [66], except that FPRNs are replaced by SNs and SPRNs are replaced by RNs. Optimal and heuristic methods are devised to solve the problem in the cases of one dimensional and two dimensional networks respectively.

In [64, 67], Wang et al. formulate a complementary problem to that in [32]. That is, given the placement, traffic load and initial energy of the FPRNs, determine the number and positions of the SPRNs such that the total additional device cost is minimized while keeping the system lifetime above a pre-set threshold and ensuring that each RN has at least one feasible path to deliver its traffic to the BS. Depending on whether or not RNs are able to adapt their transmission power, the problem has two variants, which are treated in the references [63] and [66].

In [64], the scenario where RNs can only transmit at a fixed transmission power is considered. Under such a condition, an RN can only reach other RNs within its fixed transmission range. Moreover, when the initial energy and the transmission range of an RN are known, the traffic rate it can handle (receive and transmit) can be calculated, which is defined as the capacity of the RN. The lifetime of an RN is guaranteed as long as this capacity limitation is respected in the design. Differing in how an RN distributes its traffic to its neighboring nodes and how a new node is placed, two heuristic algorithms are presented, namely, the Nearest-To-BS-First (NTBF) and Best-Effort-Relaying (BER) algorithms. With NTBF, if the traffic load of an RN does not exceed the total residual capacity of its adjacent neighbors which are closer to the BS, its traffic load will be distributed to its neighbors by first filling up the capacity of the node nearest to the BS,

then of the node next nearest to the BS, and so on. If the existing neighbors cannot relay all of its traffic load, a new RN is introduced as its next hop relay, which is placed on the line joining the RN and the BS, at a point as close to the BS as possible.

In [67], a complementary scenario in which RNs can adjust their transmission power is addressed. In such a case, an RN is able to use the minimum transmission power necessary to reach its intended next hop RN. Compared with a fixed transmission power, the variable transmission power leads to better energy efficiency. For an RN with a limited energy supply, the total traffic it can handle is determined by its actual transmission range. In other words, an RN is allowed to transmit over a long distance if its traffic amount is small while an RN can only transmit over a small distance when its traffic amount is large. In [67], using the optimal transmission distance in terms of minimizing the total energy consumption from a source to the destination [68], a collaborative placement with a locally optimal traffic allocation (CPLOAD) scheme is proposed. It has three major components: (1) locally optimal allocation decisions, by which an RN will maximally use its energy resources to forward as much traffic as possible as close as possible to the BS; (2) new RN placement, which ensures that an RN can use up its energy supply to forward the traffic as close as possible to the BS; and (3) redundancy elimination, by which unnecessary RNs are deleted.

While the work above considers deterministic deployment, other research attempts to optimize random RN deployment, which is dictated by the deployment density function, in order to extend the network lifetime. In [69], Xin et al. formulate the density function

optimization problem with and without transmission power control. The key idea is to approximate the traffic load on nodes at a distance *d* from the sink by the traffic accumulation of all nodes which are further away. Then an appropriate deployment density is derived to reflect the traffic load characteristics (and therefore the energy consumption rate).

The static RN deployment proposals discussed in this section are summarized in Table 2.2.

Table 2.2 The static RN deployment proposals in the literature

Ref.	Deployment	Node type	Objective	Constraints
[55]	Deterministic	RN	Min. number of RNs	Connectivity
[57]	Deterministic	SN	Min. number of SNs	Connectivity
[58]	Deterministic	RN	Min. number of RNs	2-connectivity
[59]	Deterministic	RN	Min. number of RNs	1-connectivity and 2-connecitivity
[60]	Deterministic	RN	Min. number of RNs	Connectivity
[61]	Deterministic	SN/RN	Min. number of SNs	K-connectivity
[62]	Deterministic	RN	Min. number of RNs	K-connectivity
[63]	Deterministic	RN	Min. number of RNs	Lifetime of SNs
[64]	Deterministic	RN	Min. number of RNs	Lifetime
[65]	Deterministic	RN	Min. number of RNs	Lifetime
[32]	Deterministic	RN	Max. lifetime	Total power budget
[66]	Deterministic	RN	Max. lifetime	Given energy budget
[67]	Deterministic	RN	Min. number of RNs	Lifetime
[69]	Random	RN	Max. lifetime	Given number of nodes

Our research is different from the RN deployment proposals discussed above in several aspects. Most of the research above ([69] excepted) studies the deterministic RN deployment problem. Our research interest is random RN deployment, which is dictated by a deployment density function and is applicable to large-scale deployment practice. By adopting a hierarchical architecture composed of two types of devices, RNs only need

to provide connectivity for a given lifetime period. Our research has the same goal as [69]. However, our research takes different approaches to approximate the traffic volume and therefore the energy consumption rate. Moreover, the research in [69] assumes RNs can adjust their transmission power. However, such an adjustment is based on knowledge of other nodes' locations, which is expensive to obtain in some cases. Our research achieves better applicability by avoiding this assumption.

2.2.3. BS Deployment

The typical objectives of the BS placement problem are maximizing the overall network lifetime, minimizing the longest data path, and achieving the maximal data rate. Given the number of SNs and/or RNs, their locations, and their onboard energy supply, the location(s) of the BS(s) is optimized using techniques like (integer) linear programming, network flow and computational geometry. However, these optimization problems are generally difficult, known to be NP-complete [70]. Only very special cases have been investigated for optimal solutions, including single-hop communication between SNs and the BS [71]. In other cases, heuristic algorithms [72] and approximation algorithms [39, 70, 73] have been proposed in the literature. Note that some techniques for RN deployment are applicable to BS deployment, such as those discussed in [63].

In [74], Maulin et al. examine the optimal placement of SNs, RNs, and BSs in terms of sensing coverage, connectivity, and bandwidth. Four integer linear programming problems are formulated for four different objectives, namely, minimizing the number of SNs to achieve coverage, minimizing the overall device cost, maximizing the network

lifetime, and maximizing the network utilization. Public domain solvers are used to solve these optimization problems.

In [70], Bogdanov et al. show that the placement problem of multiple BSs so as to maximize network capacity is NP-hard. The paper shows how to compute the maximum rate for a fixed layout of BSs by a reduction to the maximum flow problem. An optimal solution is solved for the special case of regular grid networks.

In [39], Efrat el al. develop a (1-ε), where $0 < \varepsilon < 1$, approximation algorithm for BS placement. Using this algorithm, the network lifetime is guaranteed to be not less than (1-ε) times the maximum network lifetime possible. In [73], Hou et al. address the same problem by devising a four step procedure to design (1-ε) approximation algorithms. The paper proposes a general framework to transform the infinite search space to a finite-element search space with a performance guarantee. This procedure is then applied to solve the problem raised in [39], i.e., maximizing the network lifetime by devising the location for the BS and an associated transmission arrangement. The proposed method significantly reduces the computational complexity compared to the algorithm in [39]. The method has also been adopted to solve another optimal BS placement problem, namely, maximizing the weighted network capacity with the constraint of a required lifetime.

In [71, 75], Pan et al. attempt to optimize the locations of BSs algorithmically so as to achieve maximum network lifetime. Assuming the positions of the underlying SNs and

RNs are known and RNs transmit their traffic to a BS directly without inter-RN relaying, authors first develop geometric algorithms for a simple case where the initial energies of RNs are proportional to their average bit-stream rate (i.e. bit rate) in [75]. A more generic problem was investigated where the initial energy of RNs is not proportional to their average bit rate [71]. Upper and lower bounds of maximal network lifetime are derived as well.

The static BS deployment proposals discussed in this section are summarized in Table 2.3. Our approach does not address the BS deployment problem.

Table 2.3 The static BS deployment proposals in the literature

Ref.	Deployment	Node type	Objective	Constraints
[74]	Deterministic	SN, RN, BS	Min. SNs Min. device cost Max. lifetime Max. utilization.	Coverage Coverage and node capacity Given nodes and coverage Given nodes
[70]	Deterministic	BS	Max. data rate	Energy consumption rate on sensors
[39]	Deterministic	BS	Max. lifetime	Traffic and initial energy
[73]-1	Deterministic	BS	Max. lifetime	Traffic and initial energy
[73]-2	Deterministic	BS	Max. weight capacity	Lifetime
[75]	Deterministic	BS	Max. lifetime	Given devices & initial energy
[71]	Deterministic	BS	Max. lifetime	Given devices & initial energy

2.3. Dynamic deployment

The proposals described above compute the specific locations or the deployment densities for devices in a WSN. Once devices are placed, they remain at the same positions during the course of their lifetime. In contrast, some proposals have advocated repositioning devices dynamically in order to boost the system performance either

immediately after devices are deployed or when the system performance degrades after a period of network operation. The dynamic repositioning of devices is an effective approach to addressing changing dynamics during the operation of WSNs, such as traffic patterns, load variations, failure of devices due to energy depletion or random device damage by the environment.

The most common performance metrics of the repositioning algorithms are energy consumption, total travel distance, travel time, communication/computation cost, and convergence rate. Repositioning devices in WSNs may involve SNs, RNs, or even BSs.

2.3.1. Repositioning SNs

The typical goals of repositioning SNs are enhancing sensing coverage, improving the network capacity, or extending the system lifetime.

In [76], Zou et al. propose a virtual force algorithm (VFA) as an SN repositioning strategy to enhance the sensing coverage after an initial random placement of sensors. For a given number of sensors, the VFA algorithm attempts to maximize sensing area coverage. A judicious combination of attractive and repulsive forces is used to determine virtual motion paths and the rate of movement for randomly placed sensors. Once the most effective sensor positions, which enhance sensing coverage and incorporate the energy dissipation for future operation, are identified, a one-time movement is carried out, i.e., the sensors are redeployed to these positions.

In [77], Wang et al. attempt to maximize area coverage with a minimal overhead in terms of travel distance, transient time during which nodes are moving and inter-sensor message traffic. Each SN assesses the coverage in its vicinity after deployment and decides whether it should be moved to boost the coverage. Three methods are proposed and evaluated, namely, Vector-based, Voronoi-based and Minimax. The main idea of the Vector-based method is borrowed from electromagnetics where close particles are subject to a repelling force to keep them apart. In the context of WSNs, virtual forces are applied to an SN by its neighbours. In contrast, Voronoi-based and Minimax are pull-based algorithms by which SNs "pull" other SNs to their local maximum coverage holes.

In [78], Wang et al. design a bidding protocol for deploying a mix of static and mobile sensors. The movement of mobile sensors is conducted round by round. Each round is composed of three phases: service advertisement, bidding, and serving. Mobile sensors broadcast their base prices and locations in the service advertisement phase. Static sensors detect coverage holes and send bidding messages to the closest mobile sensors in the bidding phase. In the serving phase, mobile sensors choose the highest bid. Although the bidding protocol can be used to achieve high coverage, sensors may move in a zig-zag pattern and waste significant energy compared with a solution which would simply move the sensors directly to their final locations.

In order to eliminate this energy waste due to the zig-zag movement, in [79] Wang et al. improve their earlier work by proposing a proxy-based movement algorithm. Instead of moving iteratively, sensors calculate their target locations based on a distributed iterative

algorithm, move virtually, and exchange new virtual locations with their new virtual neighbors. Actual movement only occurs when sensors determine their final locations. In this way, the proposed protocol can significantly reduce the energy consumption.

In [80], Wu et. al propose a Scan-based Movement-Assisted sensoR deploymenT method (SMART) that uses scan and dimension exchange to achieve a balanced distribution of sensors across the sensing field, which is divided into identical cells. The objective of sensor movement is to ensure that each cell has the same number of sensors inside.

2.3.2. Repositioning RNs/BS

The main goal of repositioning RNs and/or BSs is to extend the system lifetime and enhance the timeliness of delay-constrained traffic.

In [72], in order to improve system performance in terms of lifetime, energy consumption, throughput, and transmission delay, Younis et al. present a heuristic search solution to relocating the BS. To find the best potential BS location, the product of traffic density and transmission power is used as the metric to decide when and where to relocate the BS. Reference [81] adopts a similar idea by moving the BS to the most heavily loaded SN.

In [82], Gandham et al. propose applying multiple and mobile BSs to prolong the system lifetime. The operation of the network is conducted in rounds. At the beginning of each round, the new locations of multiple mobile BSs are determined so that the maximum

energy consumption of SNs is minimized. In each instance, the BS location problem is formed as the integer linear programming problem.

The dynamic node repositioning proposals discussed in this section are summarized in Table 2.4.

Table 2.4 The dynamic node repositioning proposals in the literature

Paper	Node type	Objective	Constraints
[76]	SNs	Maximize coverage	Given SN initial deployment
[77]	SNs	Maximize coverage	Given SN initial deployment
[78]	SNs	Maximize coverage	Given SN initial deployment
[79]	SNs	Maximize coverage	Given SN initial deployment
[80]	SNs	Balance the coverage	Given SN initial deployment
[83]	SNs	Overcome the coverage hole caused by the random failure of SNs	Given SN initial deployment
[72]	BSs	Maximize lifetime	Given SN deployment
[81]	BSs	Maximize lifetime	Given SN deployment
[82]	BSs	Maximize lifetime	Given SN deployment

In general, repositioning devices is expensive, both in terms of hardware cost and energy consumption. A typical small experimental locomotive component costs 100-300 Canadian dollars each. As a compare, a non-mobile Mica series device [8] costs no more than 400 dollars. It is reasonable to expect a much higher expense for real deployment in a practical system. In addition to purchase cost, the energy cost to operate the locomotive device is high, and the feasibility and reliability of moving a device on unknown terrain to the desired location is extremely difficult to guarantee. In our research, we do not consider dynamic positioning of devices.

2.4. Motivation

As presented in this chapter, WSN deployment problems have attracted a lot of research interest in recent years. However, some critical problems remain for large-scale WSN deployment for two major reasons.

First, the majority of the research has assumed that a device can be placed exactly at a point as desired. Such practices generally allow for the optimal construction of an application system. However, it is infeasible or very expensive when a large-scale WSN is deployed in an outdoor environment. In some cases, such as a battleground, the deployment field is not human-accessible.

Second, much of the research in the literature implicitly or explicitly assumes homogeneous WSNs, in which identical wireless SNs are used for both monitoring and data transmission. We argue that heterogeneous WSNs are more practical and effective than homogeneous WSNs, especially for large-scale applications, in which scalability is of paramount importance.

Heterogeneous WSNs can achieve scalability by adopting a clustering hierarchy architecture, as illustrated in Figure 2.1. The cluster hierarchical WSN is organized into two tiers. The lower tier of the network is composed of SNs, whose major utility is to provide sensing coverage that satisfies the requirements of an application. SNs are grouped into clusters around RNs. Such clustering schemes can be found in [84, 85]. The upper tier of the network consists of RNs, which serve as cluster heads within clusters.

RNs also form the data communication backbone for wireless SNs to report their data to the base station for data processing. Moreover, a clustering hierarchy can easily facilitate data aggregation. A cluster head can conduct data aggregation on data received from its cluster member nodes. The aggregation diminishes redundant information from multiple nodes and reduces network traffic, which can lead to a significant reduction of both communication energy costs [86-88], and the possibility of network congestion [89].

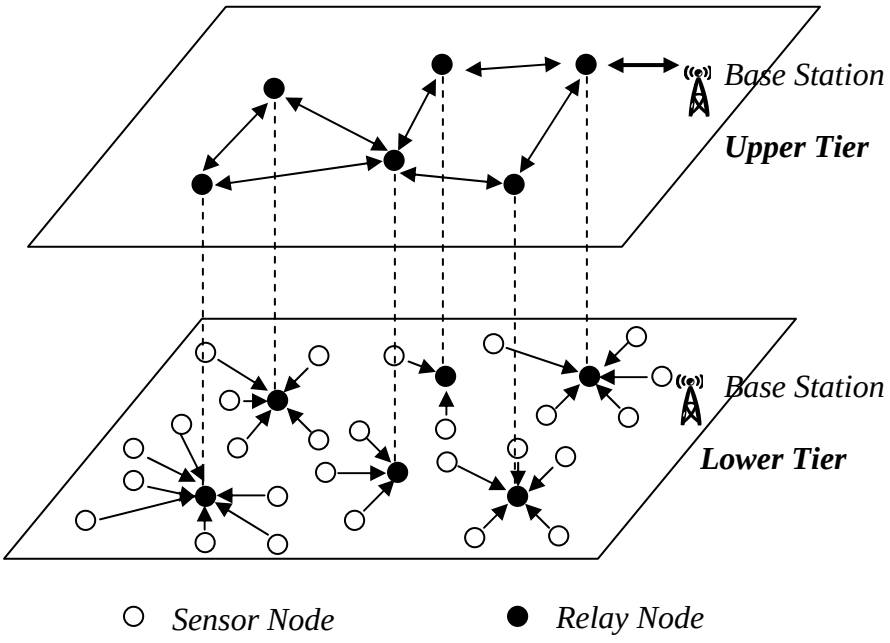

Figure 2.1 An illustration of clustered hierarchical WSNs

While it is possible to adopt the layered clustering architecture in a homogeneous WSN [90-94], such a system is either of insufficient capacity and performance, or subject to a very high cost. In contrast, if devices are specialized for their tasks, different devices can be chosen to meet the differing requirements, inherently imposed by the clustering hierarchy. The best combination of devices gives application solutions in a cost-effective manner, as observed in [95-97].

Moreover, from a device deployment perspective, heterogeneous WSNs allow for better network design and encourage design reuse. When a design is constructed for a homogeneous WSN, optimization of one metric often leads to degraded performance in terms of other metrics due to the inherent tradeoffs between metrics. For example, if one chooses to maximize sensing coverage by evenly spreading wireless SNs across the sensing field, the network will certainly suffer from the unbalanced energy consumption problem, as discussed in [98]. On the other hand, if one chooses to put more SNs close to the base station in order to extend the network lifetime, the sensing coverage quality will surely degrade with the distance from the base station. A two-tier heterogeneous WSN conceptually assigns different functionalities to different components of the network. Based on this functionality requirement, one can optimize the design of the lower tier for sensing coverage and optimize the design of the second tier for data communication. In this way, a design optimization conducted for one functionality will have fewer negative impacts on other functionalities. In fact, by decomposing the network into two logical tiers, the optimization can be done separately. This will encourage design reuse.

It is worth noting that the recent development of a variety of WSN platforms/devices makes heterogeneous WSNs feasible in practice. Examples of lower-tier SNs include MICA2 nodes from Crossbow [8], Tmote devices from Moteiv [9], etc., while examples of upper-tier RNs include STARGATE devices from Crossbow [8], motes from Intel [99], TC2001P from Zeevo [100], etc.

In this thesis, we aim at addressing the device deployment problem within a context of heterogeneous clustered hierarchical WSNs.

We will first examine grid-based SN deployment concerned with sensing area coverage with deployment errors considered. In particular, we are interested in optimizing the deployment parameters, such as the distance between SNs, so that satisfactory sensing coverage is achieved with a minimum number of SNs. This represents a major advance beyond previous research on grid-based deployment in [52], where deployment errors were not considered.

We will also optimize the random RN deployment density function in order to provide connectivity to SNs and have the network operate for as long as possible. Uniform RN random deployment is simple but inefficient from an energy perspective due to the biased energy consumption rate (BECR) phenomenon, described as follows. Consider a WSN composed of uniformly deployed SNs and RNs, and a fixed BS. Assume the traffic is uniformly generated over the sensing field and the initial energy is identical on every RN. In a single-hop heterogeneous WSN, where all RNs transmit data to the BS in one hop by adjusting their transmission power, illustrated in Figure 2.2(a), the RNs which are farther away from the BS will deplete energy faster than the RNs closer to the BS due to the larger transmission distance. As such, the nodes farther from the BS become unusable while a large portion of energy is still left on those close to the BS. In contrast, in a multi-hop heterogeneous WSN, where RNs adopt a fixed transmission power[1] and transmit data

[1] If RNs can adjust their transmission power, the BECR problem can be alleviated by efficient traffic distribution [175].

to the BS via multiple intermediate RNs, illustrated in Figure 2.2(b), RNs closer to the BS will consume energy faster than RNs farther away from the BS. This is because traffic builds up at RNs closer to the BS as traffic is relayed from far to near RNs. As such, near RNs become unusable earlier than those far from the BS.

It is essential to realize that the problem cannot be solved solely based on energy-efficient routing protocols. For example, the one-hop neighbors, as a group, will inevitably be exhausted sooner than the RNs using them for traffic relay since all traffic has to go through that set to the BS no matter which routing protocol is used. To this end, the study in this thesis is not coupled to any particular routing scheme. It only assumes that relay paths are always formed from far to near RNs to the BS, a property which is generally satisfied by most existing routing schemes.

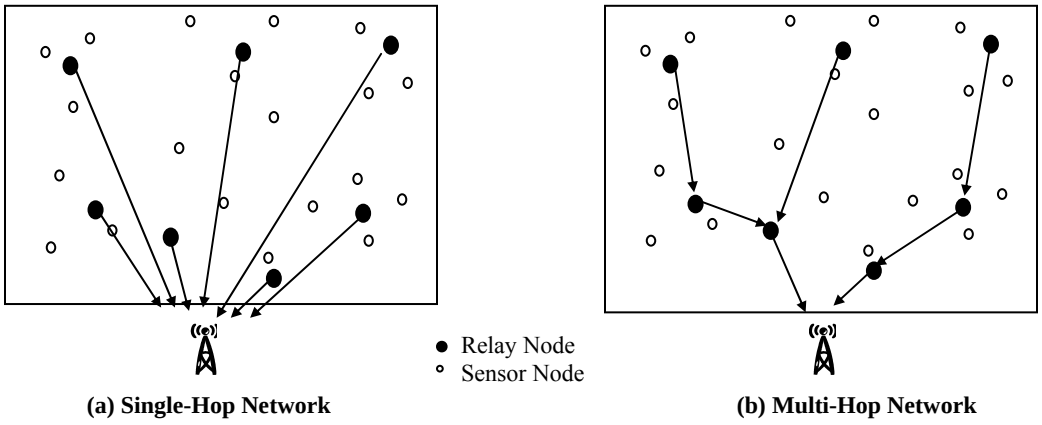

Figure 2.2 BECR Problem in Heterogeneous WSNs

The following chapters will address serveral of the gaps in the literature identified above, including the issue of coverage-oriented grid-based sensor node deployment in the face of deployment errors and lifetime-oriented random relay node deployment. In the next

chapter, we will first discuss the context of our research of WSN deployment problems in detail.

Chapter 3. SYSTEM MODELS

We consider hierarchical clustered WSNs composed of heterogeneous devices as depicted in Figure 2.1. In this chapter, we discuss the context of our research of WSN deployment problems in detail. We first describe the device composition of a WSN and how different devices work together to fulfill the joint sensing/monitoring task. We also present the sensing model of SNs, which is the key factor in determining sensing coverage quality and therefore SN deployment strategies. Moreover, we formulate the energy consumption for data communications, a decisive factor in determining system lifetime. In a large-scale WSN, the effectiveness of the overall system is little affected by the failure of one or a few devices. Therefore, the system lifetime does not end when only a few devices are exhausted of their energy. We explore an appropriate cutoff criterion for the system lifetime. Finally, as mentioned previously, our research does not assume the availability of device location information, and we explore the rationale for dispensing with this potentially valuable information.

3.1. Network Model

In this section, we discuss the heterogeneous devices in a WSN and how they operate. This model assigns different tasks to different devices, with SNs responsible for sensing and coverage, and RNs responsible for communication. In particular, we focus on how

communication traffic is treated after its generation, as this serves as a key factor in evaluating energy consumption. This is essential for optimizing RN deployment to extend the system lifetime. We consider that a large-scale heterogeneous WSN on a sensing field is composed of three types of devices, SNs, RNs and BSs.

An SN senses the environment, generates data, and transmits the data to an active RN in one hop. It has a limited energy supply and a fixed transmission radius r_c^S . The transmission radius is chosen so that SNs can last for a required lifetime (more details in Section 3.3). It has no relaying requirements—or at least traffic relaying is not a routine function of an SN—for several reasons. First, relaying traffic demands higher computational power and memory to accomplish complex tasks like traffic routing and communication security, which leads to higher device cost. Second, forwarding packets from other SNs leads to faster energy dissipation. Thus a relay-providing SN will inevitably deplete its energy faster than its beneficiary. When the number of hops on a relaying path becomes large, this effect is aggravated due to traffic accumulation. Without the necessity to relay, the SN can be a much simpler device. One example of an SN appropriate for our purposes is the Reduced Function Device (RFD) defined in the IEEE802.15.4 standard [101].

Based on the specific application, traffic is generated on SNs in a time-driven manner (periodically) or event-driven manner (sporadically), which is relayed back to the base station via RNs. The time-driven data delivery method is suitable for applications that require periodic data sampling. Event-driven data reporting can operate in a more energy-

efficient manner without negatively impacting the performance in some applications. For example, in object detection applications, meaningful data are transmitted only when an object is detected, which occurs in a sporadic manner. Event-driven data reporting can also be used in a condition-based data report scenario, in which the measurement data are transmitted only when they satisfy some preset conditions. In either the time-driven or the event-driven data transmission case, we assume that traffic is generated at the same long-term rate across the network.

RNs are dedicated to facilitate data communications without carrying out any monitoring functionality. An RN is also energy constrained. It works as a cluster head (CH) when active, grouping the SNs in its proximity into a cluster. It also coordinates and schedules MAC layer access within its cluster so that the energy overhead – for example because of retransmissions due to collisions—is minimized. After receiving data from its SNs, the RN aggregates the traffic. In the case of the single-hop communication model, an RN transmits data to the BS directly by adjusting its transmission power in order to avoid energy wastage. In case of the multi-hop communication model, an RN transmits data to its next hop RNs within its fixed transmission range r_c^R, where typically r_c^R is a few times larger than r_c^S. Note that the communication distance between two nodes are usually bounded by the smaller transmission distance, since an immediate acknowledgement packet is required from the receiver to the transmitter in a noisy communication environment. For example, in Figure 3.1, the SN on the left can not communicate with the RN even it is within the transmission radius of the RN. The SN on the right can communicate with RN since they are within the transmission radius of each

other. The aggregated traffic will not be aggregated again while passing through other RNs. We assume the traffic is light compared with the available bandwidth, or the traffic is well scheduled so that there is no traffic congestion in the network.

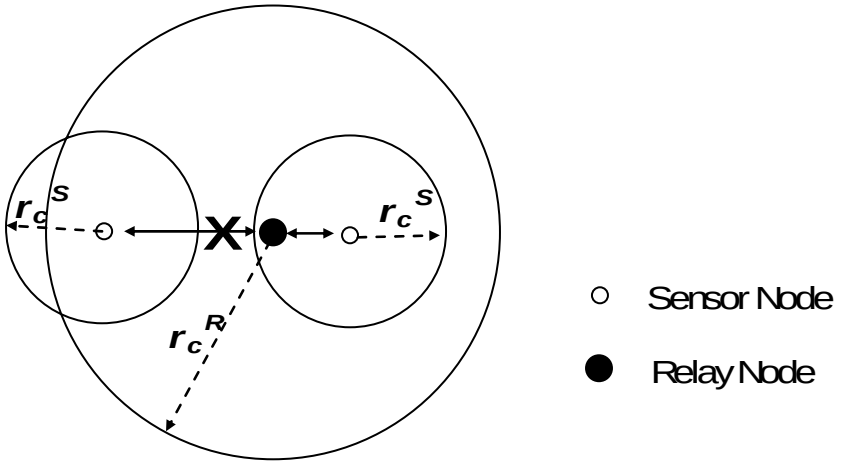

Figure 3.1 The communication distance of SNs and RNs.

We assume one BS is fixed somewhere in the sensing field (e.g.,, the corner or center). Without loss of generality, the position of the base station is marked as point (0, 0).

3.2. Sensing Model

The sensing model is a key factor that affects the SN deployment problem. In this thesis, we opt to model the sensing capability of individual SNs without considering cooperative signal processing. In particular, we consider the binary sensing disk model. While there are other sensing models in literature, such as probabilistic sensing model due to signal decay [23, 102, 103], the binary disk model is by far the most predominant due to its simplicity. Although we focus on the case of binary disk model in this thesis, much of our study applies to the probabilistic sensing model with trivial modification.

The binary disk model abstracts the sensing capability of an SN by a disk of sensing radius. A point is covered if it is within the sensing radius of an SN. Otherwise it is not covered at all.

3.3. Energy Model

In this section, we discuss how to quantify energy consumption due to data communications. This is essential to the RN deployment strategies to be developed in chapters 6 and 7.

We adopt an energy model similar to that in [104]. The energy spent by receiving a packet of length *l*, denoted by $E_{RX}(l)$, and transmitting a packet of the same length over a distance *d*, referred by $E_{TX}(l,d)$, are respectively

$$E_{RX}(l) = l\beta, \text{ and} \tag{3.1}$$

$$E_{TX}(l,d) = l(\alpha_1 + \alpha_2 d^m), \tag{3.2}$$

where β, α_1, α_2, and *m* are energy-related parameters.

For an SN, the energy is dissipated by both sensing and data communications. We assume the energy is well budgeted for both functionalities so that SNs can operate for a required lifetime period in respect to sensing. We will address the lifetime issue solely from the communication perspective.

The rate at which energy is dissipated by an SN for transmitting packets depends on transmission radius and the data traffic rate. As we assume that traffic is generated at the same long-term rate by SNs across the network and SNs do not relay traffic, one can fix the transmission radius of the SN according to (3.2) so that all SNs can last for a required lifetime period.

For data collection, the energy consumed by an active RN consists of two parts: the energy used for intra-cluster communication and data processing, denoted by E_{intra}, and the energy used for inter-cluster traffic relay, denoted by E_{inter}.

We have assumed that traffic is generated at the same long-term rate across the network. On average, an active RN receives n packets from member SNs during a given time period. The energy E_{intra} is composed of three parts; the energy cost of receiving n packets of length l, denoted by $E_{RX}(l,n)$; the energy cost of transmitting the aggregated packet of length l_{AG} to its next hop RN or the BS over a distance d, denoted by $E_{TX}(l_{AG}, d)$; and the energy cost of aggregating n packets of length l, denoted by $E_{AG}(l,n)$. According to the energy consumption model above, we have

$$E_{RX}(l,n) = nl\beta \ , \tag{3.3}$$

$$E_{TX}(l_{AG},d) = l_{AG}(\alpha_1 + \alpha_2 d^m) \text{ , and} \tag{3.4}$$

$$E_{AG}(l,n) = nl\gamma \ . \tag{3.5}$$

Letting g be the aggregation ratio, the length of the aggregated packet from n packets is

$$l_{AG}(l,n) = ngl \quad . \tag{3.6}$$

Replacing l_{AG} in (3.4) by (3.6), and adding (3.3), (3.4), and (3.5), we have

$$E_{\text{intra}} = \left(c_1 + g\alpha_2 d^m\right)nl \quad , \tag{3.7}$$

where $c_1 = (\beta + g\alpha_1 + \gamma)$

On the other hand, the energy spent on inter-cluster relay E_{Inter} consists of two parts, namely, the energy cost of receiving packets of total length l_{Relay} and transmitting them (as they are) over the distance *d*, resulting in the expression

$$E_{\text{inter}} = c_2 l_{\text{relay}} \quad , \tag{3.8}$$

where $c_2 = (\beta + \alpha_1 + \alpha_2 d^m)$.

Thus, the total energy spent by an active RN is

$$E_{RN}(d) = c_1 nl + ng\alpha_2 l d^m + c_2 l_{\text{relay}} \quad . \tag{3.9}$$

In the special case of single-hop communication, $l_{\text{relay}} = 0$, and if variable power RN communication is not possible, then the transmission distance is fixed, i.e., $d = r_c^R$.

3.4. Usability and Lifetime Model

The usability of a WSN is determined by both its sensing coverage and connectivity. Connectivity refers to how much of the generated data can be utilized, and can be measured by the percentage of SNs that can connect to the BS via RNs. As such, the coverage provided by SNs and the connectivity provided by RNs ultimately determine the effective coverage. As RNs get drained of energy, the connectivity becomes gradually weaker and so does the effective coverage, a process called *coverage aging* in [89]. In a two-tier hierarchical WSN, the network lifetime can be examined independently for the two tiers. For the lower tier, it is the time period during which sufficient SNs function to

maintain adequate coverage. The number of functioning SNs decreases as some SNs stop working due to energy depletion. As we assume that SNs function long enough (Section 3.2) so that coverage maintains during the course of network operation, the network lifetime is limited by the lifetime of the upper tier. As the upper tier is to provide connectivity from SNs to the BS, the system lifetime is the time period elapsed before the percentage of connected SNs is degraded to a given threshold q. A SN is connected if it can find a route to BS through RNs. A similar treatment of network lifetime can be found in [71].

It should be noted that the percentage of SNs with connectivity in a newly deployed network should not be less than q in order that the network functions. This can be achieved by ensuring that the probability that any SN connects to at least one RN is not less than a value σ_0, assuming that all RNs are well connected to the BS. This can be easily satisfied at the beginning of the network operation.. The relationship between q and σ_0 is explained as follows.

If the connection probability of any individual SN is σ, the probability that x out of N_{SN} SNs are connected has the binomial distribution with parameter (N_{SN}, σ). When $N_{SN}\sigma$ and $N_{SN}(1-\sigma)$ are big enough, this binomial distribution can be approximated by the normal distribution with mean $N_{SN}\sigma$ and standard deviation $\sqrt{N_{SN}\sigma(1-\sigma)}$. If we want the deployment to satisfy the functionality threshold q with a high probability (say

0.9999), the minimum connection probability of any individual SN, denoted by σ_0, can be obtained as a function of q.

In the rest of the thesis, the connectivity requirement is specified by the individual node connectivity probability σ_0.

3.5. Other Assumptions

Some device deployment research has assumed that devices are aware of their location information, such as [53, 54, 69]. Generally speaking, a device can make more informative decisions in terms of power and topology control if it knows its location and that of other key nodes. Device localization can be implemented by either Global Positioning System (GPS) receivers or distributed localization algorithms. The first choice will significantly increase the system cost. The second choice uses distance or angle measurements from a fixed set of reference points or anchor nodes and applies multilateration or triangulation techniques to find coordinates of other nodes [106, 107]. Distance estimates can be obtained from received signal strength indication (RSSI) or time-of-arrival (ToA) measurements. RSSI methods are not very reliable or accurate in non-uniform signal propagation environments. ToA methods have better accuracy, but may require additional hardware on SNs to determine for a signal that has a slower propagation speed than radio, such as ultrasound [108].

As such, our design of device provisioning does not assume the availability of location information.

We have discussed several key aspects of a WSN, which are essential to our study of WSN deployment problems. In the following chapters, we will address the SN and RN deployment problems in sequence.

Chapter 4. COVERAGE-GUARANTEED GRID-BASED SENSOR NODE DEPLOYMENT

Grid-based SN deployment is a practical and efficient coverage-oriented deployment approach for moderate to large scale WSN applications due to its simplicity and scalability. Previous research has devised grid-based SN deployment in order to provide complete sensing (area) coverage in an ideal circumstance where individual SNs are placed exactly at the grid vertices. However, in practice, it is often infeasible to guarantee exact device placement due to various errors. Placement errors may arise for a number of reasons, including natural or man-made obstacles in the terrain, timing errors in the deployment device mechanism, errors due to human factors, as well as environmental effects. For effectiveness, some deployment exercises may employ a low flying aircraft rather than a ground-based transportation tool, in which case these errors would be amplified. As explored in Section 4.2, when errors occur, the expected coverage quality, such as full coverage, can not be retained anymore. A coverage hole with equilateral triangular deployment is illustrated in Figure 4.1. Even though efforts could be made to minimize errors, errors are inevitable in many applications.

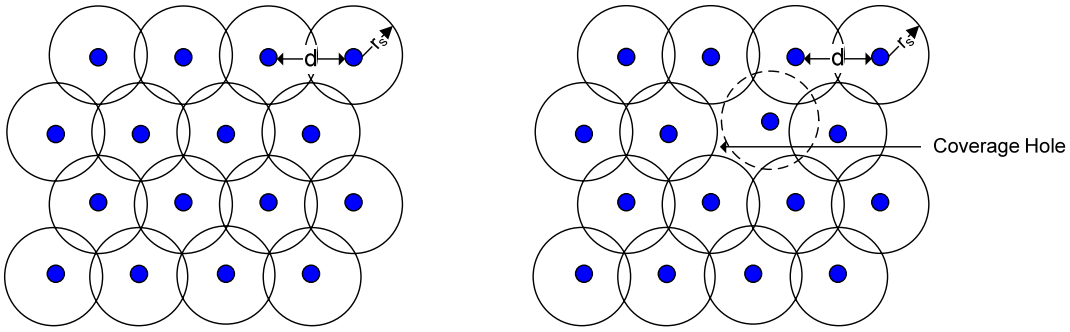

(a) An ideal case (When $d=\sqrt{3}r_s$, there is no coverage hole.)

(b) A coverage hole caused by errors

Figure 4.1 The equilateral triangular deployment

To retain the complete sensing area coverage in presence of deployment errors, the grid resolution and the number of devices to be deployed should be re-evaluated. In order to do so, the causes of the possible deployment errors and their properties are subject to a careful study. One should then arrange the SN deployment while taking these errors into consideration. To this end, the core contributions of this chapter are two-fold. First, we identify two types of deployment errors, namely, misalignment and random errors. We explore their impacts on the sensing area coverage. Second, we derive the minimum number of SNs required for guaranteed sensing coverage assuming the worst errors are bounded. The degree of discrepancy between the ideal deployment and the coverage-guaranteed deployment is quantified. To our best knowledge, this is the only research addressing guaranteed sensing coverage when deployment errors are taken into consideration. An abbreviated version of this chapter have appeared in [109].

The remainder of this chapter is organized as follows. In Section 4.1, the problem of grid-based deployment for full area sensing coverage is defined. The MaxMin criterion for determining sensing area coverage quality is proposed and ideal grid-based deployment is

reviewed. In Section 4.2, different placement errors are defined and coverage-guaranteed grid-based deployment is studied. In Section 4.3, the properties of both ideal grid deployment and robust deployment are summarized and compared. The chapter is summarized in Section 4.4.

4.1. Preliminaries

In this section, we discuss the issue of sensing coverage in details and define the objective of SN deployment in this research. We also propose an efficient computational method to determine whether a sensing field is fully covered or not. Lastly, we review ideal grid-based deployment.

4.1.1. Problem Definition

Recently, some papers have argued that partial sensing area coverage is sufficient in practice, as opposed to full sensing area coverage, in some WSN applications. As stated in [110], full coverage is either impossible or unnecessary in some applications. This is a result due to the combined effect of signal attenuation with distance, limited sensing sensitivity and the scale of applications. For example, the magnetic sensor HMC1002 used by He, et al. in [111] can only sense a small magnet at a distance of approximately 1 ft and slowly moving passenger cars at a distance of 8-10 ft. If such magnetic sensors are used to detect and track the movement of vehicles on a battleground, it is easy to imagine the difficulty of achieving full coverage. Furthermore, an excess deployment might seriously deteriorate the stealth character of the system. However, a partial coverage

problem can be reformulated as a "full" coverage problem. We explain our rationale in two situations.

In some applications, an important metric to measure the quality of partial coverage is the maximum distance from an uncovered position to the nearest SN. For example, some physical phenomena, such as temperature or air pressure, exhibit close spatial correlation, by which a reading at one point is negligibly different from readings in its surrounding area. To guarantee sensing fidelity, an application often only requires the distance from any uncovered point to its nearest SN to not exceed a certain design value. In such a case, the partial coverage problem becomes a full coverage problem by taking the maximum distance allowed as the effective sensing radius of a SN.

In other applications, the objects to be detected typically have a considerable size. As long as a SN can sense any part of an object, it is considered detected. Thus, the effective full coverage is achieved as long as no uncovered area can accommodate an object. If the size of the objects is modeled by a disk of radius r_{obj}, as long as a disk of radius r_{obj} at any point will intersect with some sensing disk of radius r_s, an effective full coverage is implied. We introduce the following equivalence condition for effective full coverage.

Lemma 1 (equivalence condition): A sensing field is fully covered by a deployment of SNs of sensing radius r_s, against an object disk of radius $r_{obj} \geq 0$, if and only if the sensing field is fully covered by the same deployment of SNs with sensing radius $r_s^{'}$, against a disk of radius $r_{obj}^{'} \geq 0$, where $r_s + r_{obj} = r_s^{'} + r_{obj}^{'}$.

Proof: Draw a sensing disk of radius r_s for each SN. If the sensing field is effectively covered by SNs of sensing radius r_s against a disk of radius $r_{obj} \geq 0$, a disk of radius r_{obj} at any point will intersect with one or more sensing disks. In other words, there is at least one SN within the distance $r_s + r_{obj}$ of any point in the field. Equivalently, there is at least one SN within the distance $r_s^{'} + r_{obj}^{'}$ from any point. Thus, for the same deployment of SNs, a disk of radius $r_{obj}^{'}$ will intersect with at least one sensing disk of radius $r_s^{'}$. The converse can be similarly proven. □

Therefore, we call $r_s + r_{obj}$ the effective sensing radius. With this effective coverage equivalence condition, we can convert a partial coverage problem with sizable objects into a full coverage problem with the effective sensing radius. For simplicity, we use r_s to denote the effective sensing radius in the rest of the chapter. In practice, the effective sensing radius could be much larger than the physical sensing radius.

We consider the SN deployment problem as follows. Given an $L * L$ square sensing field and an effective sensing radius r_s, what is the minimum number of SNs required in order to provide full coverage by using the grid-based deployment? We do not consider the connectivity explicitly in this chapter. However, it is implied by the full coverage if the transmission radius of a SN is not less than twice the sensing radius in a homogeneous network [33] or it can be provided by RNs in a heterogeneous network [64]. We will further address the connectivity issue in chapter 6 and 7 in detail.

4.1.2. Determining Coverage

In this part we explore how to effectively determine whether a sensing field is fully covered if the positions of SNs are given. Consider an arbitrary deployment of *N* identical SNs, $s_1, s_2, ..., s_N$ on an $L * L$ square sensing field *A*. Let $d(x, s_i)$ denote the distance from a point *x* to SN s_i and $d_{\min}(x)$ denote the minimum distance from a point *x* to a SN, i.e., $d_{\min}(x) = \min_{1 \le i \le N} d(x, s_i)$. Let r_s denote the fixed sensing radius of the SNs. If $d_{\min}(x) \le r_s$, point *x* is covered by at least one SN. If a point *y* on the sensing field has the maximum minimum distance, i.e., $d_{\max\min}(y) = \max_{x \in A} d_{\min}(x)$, and $d_{\max\min}(y) \le r_s$, the sensing field is fully covered. We call $d_{\max\min}(y)$ the MaxMin distance of the sensing field. As such, determining whether a sensing field is fully covered is equivalent to finding the MaxMin distance on the field and comparing it with r_s.

There are an infinite number of points on the sensing field and it would be computationally infeasible to calculate the minimum distance of each single point to determine if coverage was satisfied. We adopt the Voronoi diagram [112] to solve this problem. Figure 4.2 illustrates a Voronoi diagram formed around a group of *N* SNs, $s_1, s_2, ..., s_N$. The Voronoi diagram partitions the 2-D bounded plane set *A* into a set of convex polygons, denoted as $p_1, p_2, ..., p_N$ respectively. For any point in a convex polygon $p_i, i = 1, ..., N$, the corresponding SN s_i has the shortest euclidean distance to the point among all SNs. We introduce the following property of these convex polygons relevant to coverage.

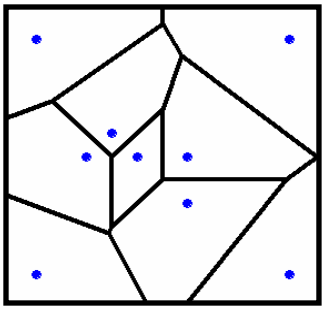

Figure 4.2 SN Deployment and Voronoi Diagram.

Lemma 2: If all vertices of the convex polygons formed from the Voronoi diagram corresponding to the SNs on the sensing field are covered by at least one SN, the sensing field is covered.

Proof: For any point x inside the convex polygon $p_i, d_{\min}(x) = d(x, s_i)$, i.e., s_i is the SN closest to x. Furthermore, on a polygon p_i, one of p_i's vertices has farthest distance to s_i. If all p_i's vertices are covered, the whole polygon is covered. Therefore, the sensing field is covered if all vertices of the convex polygons of the Voronoi diagram are covered. □

It is clear that the MaxMin distance must be associated with one of the vertices. With this property, we can determine the sensing coverage by checking a finite number of points on the sensing field, which leads to a significant reduction in complexity compared with the original problem.

4.1.3. Equilateral Triangle Grid-Based Deployment

There are three types of grid-based deployment corresponding to three regular shapes which can tile a plane without holes, namely, hexagon, square and equilateral triangle. According to the study in [52], the equilateral triangle grid will require the least number of SNs to cover a given sensing field in the ideal case, i.e. no deployment errors. We therefore choose to study the enhancement to equilateral triangle grid-based deployment in this chapter. However, all methodologies can apply to the other two grids with some trivial modifications. As a large-scale WSN is considered in this chapter, we will ignore the edge effect[2] when discussing deployment strategies in the rest of the chapter. Figure 4.3 illustrates the equilateral triangle grid deployment and its accompanying Voronoi diagram. Each polygon has six vertices and its associated SN has the same distance to all of them. To satisfy the coverage requirement, the distance should be no greater than r_s. This can be satisfied as long as the edge of any triangular tile is no longer than $\sqrt{3}r_s$. Ignoring the edge effect, the total number of SNs required to cover an $L*L$ square sensing field is approximately $2L^2/3\sqrt{3}r_s^2$ (the approximation is due to ignoring the edge effect and data rounding).

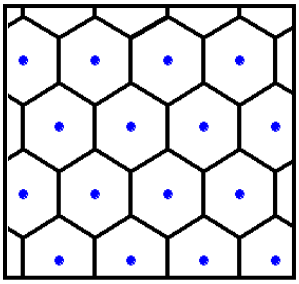

Figure 4.3 Ideal Equilateral Triangle Grid-based Deployment and Voronoi Diagram.

[2] Edge effect refers to the irregularity of the coverage property because of the boundary of the sensing field. If the sensing field is relatively large, it is of little importance in terms of the sensing fidelity and the number of SNs required to be deployed.

4.2. Coverage-guaranteed Equilateral Triangle Grid-based Deployment

Grid-based deployment is conducted by dropping SNs row-by-row using a moving carrier. The time interval between consecutive droppings is controlled to achieve the desired distance. However, often, this ideal deployment is not realistic due to placement errors. As SNs are placed away from the grid vertices, the polygons are distorted and some points on the sensing field may not be covered anymore. Previous work has not taken these inevitable errors into consideration [52]. Therefore, the deployment specifications, such as the distance between SNs and the number of SNs required, are either overestimated or underestimated, respectively. We will derive the adjustment of the deployment parameters in response to errors and quantify the degree of discrepancy between the ideal case and the non-ideal case. We also call the deployment design that can guarantee full coverage against errors a robust grid-based deployment.

In this research, we consider two sources of placement errors, namely, misalignment (correlated errors) and randomness (independent errors). Misalignment is a result of measurement approximations and errors, mechanical errors, human errors, etc. Randomness is the result of mechanical errors and environmental variations, such as obstacles on the ground. We first derive the robust deployment parameters in response of individual errors. We then combine multiple sources of errors and provide a general solution to the overall problem.

4.2.1. Horizontal Misalignment

Horizontal misalignment refers to the misplacement of one row of SNs relative to another row in the horizontal direction. Figure 4.4 illustrates horizontal misalignment in the case of equilateral triangle grid deployment. When a machine drops SNs row-by-row, the first SN may be placed at a point which is before or after where the grid specifies. However, the distances between consecutive SNs of the same row are as planned in advance. If the MaxMin distance on the sensing field is increased, the misalignment results in incomplete area coverage. Note that a left misalignment $-e_h$ is equivalent to a right misalignment $r - e_h$ in the sense that they lead to Voronoi polygons of the same shape, where r denotes the desired distance between consecutive SNs. Furthermore, consider two right misalignment cases, $e_h^1 > 0$ and $e_h^2 > 0$. They lead to the same Voronoi polygons as long as $\left(e_h^1 \bmod r\right) = \left(e_h^2 \bmod r\right)$. Without loss of generality, we only consider $0 < e_h < r$.

In Figure 4.4, point x_1 has the MaxMin distance to SNs. When $0 < e_h \le r/2$, the minimum distance from x_1 to SNs is,

$$d(x_1) = \sqrt{\frac{r^2}{4} + \frac{1}{3r^2}\left(e_h{}^2 + \frac{r^2}{2}\right)^2} \tag{4.1}$$

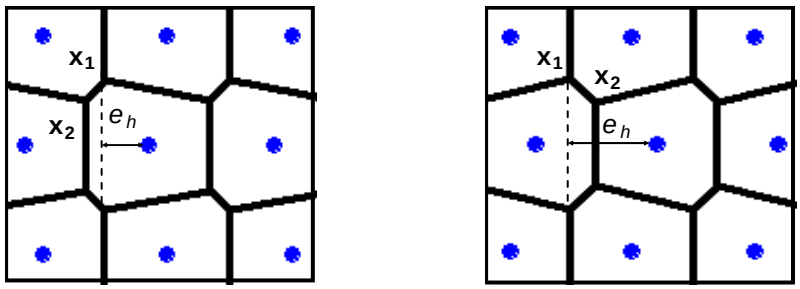

(a) $0<e_h<= r/2$ (b) $r/2<e_h< r$

Figure 4.4 An Illustration of Horizontal Misalignment with Triangular Grid Deployment.

To ensure coverage, let $d(x_1) = r_s$. When $e_h = 0$, we have $r = \sqrt{3} r_s$; when $e_h = r/2$, we have $r = \frac{4\sqrt{7}}{7} r_s$. Also, it is easy to prove that r is a decreasing function of e_h when $0 < e_h \le r/2$.

When $r/2 < e_h < r$, the minimum distance from x_1 to SNs is,

$$d(x_1) = \sqrt{\frac{r^2}{4} + \frac{1}{3r^2}\left(e_h{}^2 + \frac{3}{2} r^2 - 2re_h\right)^2} \tag{4.2}$$

To ensure coverage, let $d(x_1) = r_s$. When $e_h = r/2$, we have $r = \frac{4\sqrt{7}}{7} r_s$ and when $e_h = r$, we have $r = \sqrt{3} r_s$. Besides, r is an increasing function of e_h. Therefore, when a row of SNs are horizontally misaligned, the designed distance between SNs should be decreased and it should be $\frac{4\sqrt{7}}{7} r_s$ in the worst case. Therefore, an ideal triangular grid deployment (with $r = \sqrt{3} r_s$) is not able to maintain the area coverage. To be resilient to horizontal errors in the worst case, the edge length of the grid should be scaled back to $\frac{4\sqrt{7}}{7} r_s$ from $\sqrt{3} r_s$. The total number of SNs required is then approximately $\frac{7\sqrt{3} L^2}{24 r_s{}^2}$.

4.2.2. Vertical Misalignment

Vertical misalignment refers to the misplacement of one row of SNs in the vertical direction so that the distance between two rows is inappropriately wide or narrow. Figure

4.5 illustrates vertical misalignment in the case of the equilateral triangle grid-based deployment. In engineering practice, one can use fixed reference, such as marks on the ground, to determine the vertical coordinate of one row, or one can adopt a relative reference, such as the preceding row. There is no fundamental difference when calculating the worst-case MaxMin distance in these two cases. In this chapter, we consider the second case, namely, a row is deployed in reference to its preceding row. Vertical misalignment means the distance between two adjacent rows is not as specified. Again, the distances between consecutive SNs of the same row are intact. In this chapter, we use e_v to denote the vertical error. Ideally, the distance between neighboring rows is $\frac{\sqrt{3}}{2}r$. If $-\frac{\sqrt{3}}{2}r < e_v \le 0$, the distance between two rows is smaller than planned; if $e_v > 0$, the distance between two rows is larger than planned.

In Figure 4.5, point x_1 has the MaxMin distance to all SNs:

$$d(x_1) = \frac{\sqrt{3}}{2}r + e_v - \frac{1}{2e_v + \sqrt{3}r}\left(\frac{r^2}{2} + e_v^{\,2} + \sqrt{3}re_v\right) \tag{4.3}$$

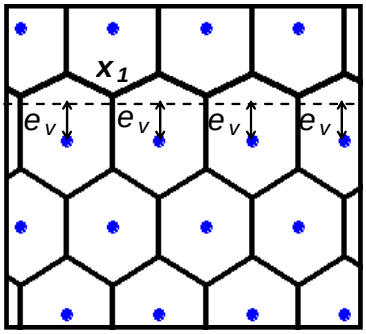

Figure 4.5 An Illustration of Vertical Misalignment with Triangular Grid Deployment.

Letting $d(x_1) = r_s$, we have

$$\frac{\sqrt{3}}{2}r + e_v - \frac{1}{2e_v + \sqrt{3}r}\left(\frac{r^2}{2} + {e_v}^2 + \sqrt{3}re_v\right) = r_s \tag{4.4}$$

and r is a decreasing function of e_v (technical proof is omitted). To ensure the equation is valid, the maximum value of e_v is set to $2r_s$.

Triangular grid deployments exhibit different resilience to the two kinds of misalignment. It is more resilient to the horizontal misalignment than the vertical one. When horizontal misalignment occurs, the grid deployment can always guarantee coverage by scaling back the designed distances between SNs. However, when vertical misalignment takes place, the grid deployment cannot guarantee full coverage if two neighboring rows are separated by more than $2r_s$, no matter how small the designed distance is between SNs. Thus, if we can limit the random vertical misalignment to a certain range $[V_{\min}, V_{\max}]$, where $V_{\min} > -\frac{\sqrt{3}}{2}r$ and $V_{\max} < 2r_s$, we can numerically solve for the desired length of the deployment grid that guarantees coverage in the worst case, referred to as $r(V_{\max})$, by plugging $e_v = V_{\max}$ into Eq.(4.4). At this length, one needs to deploy $L \cdot \left(\frac{\sqrt{3}}{2}r(V_{\max}) + V_{\min}\right)^{-1}$ rows. The total number of SNs to be deployed is then approximately $L^2 \cdot \left(\frac{\sqrt{3}}{2}r(V_{\max}) + V_{\min}\right)^{-1} \cdot r(V_{\max})^{-1}$.

4.2.3. Randomness

The misalignments discussed above lead to correlated deployment errors. We next discuss randomness, which refers to independent deployment errors of individual SNs. Randomness is modeled by a random error disk of radius R. The error disks are illustrated by the dashed circles in Figure 4.6.

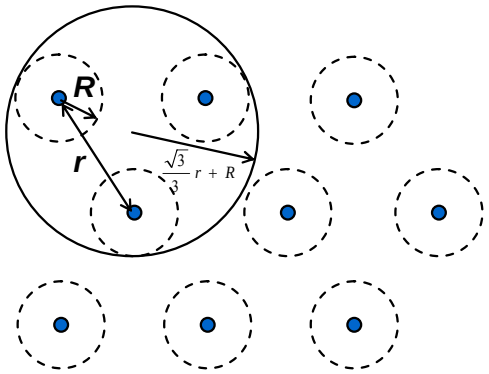

Figure 4.6 An Illustration of Random Error.

We can prove that if x_1 is the center of the disk which just contains three adjacent error disks (the solid circle in Figure 4.6), then x_1 has the MaxMin distance to SNs in all cases and

$$d(x_1) = \frac{\sqrt{3}}{3} r + R \tag{4.5}$$

Letting $d(x_1) = r_s$, we have

$$r = \sqrt{3}(r_s - R) \tag{4.6}$$

To ensure the validity of the formula, R should be less than r_s. The number of SNs to be deployed is $\frac{2L^2}{3\sqrt{3}(r_s - R)^2}$.

4.2.4. Compound Impacts of Misalignment and Randomness

In practice, both correlated errors (misalignments), modeled by a rectangle of $r \times (V_{\max} - V_{\min})$ and independent errors (randomness), modeled by a disk, are likely to happen. By combining the rectangle and the random error disk, we can model the overall deployment errors using a rounded corner rectangle as in Figure 4.7. Assume the vertical misalignment is bounded by $[V_{\min}, V_{\max}]$ and the random error is bounded by R. To ensure the feasibility of guaranteeing coverage, we require $R < r_s$ and $V_{\max} < 2r_s$. The worst case MaxMin distance is the sum of R and the MaxMin distance only due to compound misalignments.

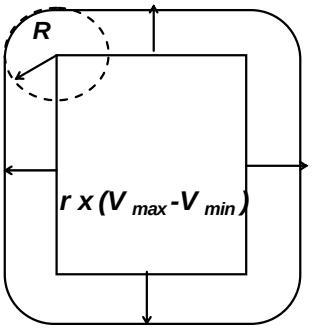

Figure 4.7 Model of Compound Impacts of Misalignment and Randomness.

The worst case MaxMin distance due to random error and compound misalignments is calculated as follows. If $e_h \le r/2$, then

$$d(x_1) = R + \sqrt{\frac{r^2}{4} + \frac{1}{\left(\sqrt{3}r + 2e_v\right)^2}\left(e_h{}^2 + \frac{r^2}{2} + e_v{}^2 + \sqrt{3}re_v\right)^2} \tag{4.7}$$

Letting $d(x_1) = r_s$, we get

$$\frac{r^2}{4} + \frac{1}{\left(\sqrt{3}r + 2e_v\right)^2}\left(e_h{}^2 + \frac{r^2}{2} + e_v{}^2 + \sqrt{3}re_v\right)^2 = (r_s - R)^2 \tag{4.8}$$

and, fixing e_v, r is a decreasing function of e_h. If $\frac{r}{2} < e_h < r$, we have

$$d(x_1) = R + \sqrt{\frac{r^2}{4} + \frac{1}{\left(\sqrt{3}r + 2e_v\right)^2}\left(\frac{3r^2}{2} + {e_h}^2 - 2re_h + {e_v}^2 + \sqrt{3}re_v\right)^2} \tag{4.9}$$

Letting $d(x_1) = r_s$, we have

$$\frac{r^2}{4} + \frac{1}{\left(\sqrt{3}r + 2e_v\right)^2}\left(\frac{3r^2}{2} + {e_h}^2 - 2re_h + {e_v}^2 + \sqrt{3}re_v\right)^2 = \left(r_s - R\right)^2 \tag{4.10}$$

Fixing e_v, r is an increasing function of e_h, and fixing e_h, r is a decreasing function of e_v. If the random vertical misalignment is limited to a certain range $[V_{\min}, V_{\max}]$, where $V_{\min} > -r$, $V_{\max} < 2r_s$, $R < r_s$, and $R + V_{\max}/2 < r_s$ (to keep Eq. (4.8) and (4.10) valid), full coverage is achievable by adjusting the designed distance between SNs. One can numerically solve for the length of the deployment grid, denoted by $r(V_{\max}, r/2, R)$, by plugging $e_v = V_{\max}$ and $e_h = r/2$ into either Eq.(4.8) or into Eq.(4.10). At this length, one needs to deploy $\frac{2\sqrt{3}L}{r(V_{\max}, r/2, R) + 2\sqrt{3}V_{\min}}$ rows. The total number of SNs one needs to deploy is then given approximately $\frac{2\sqrt{3}L^2}{\left(3r(V_{\max}, r/2, R) + 2\sqrt{3}V_{\min}\right)\cdot r(V_{\max}, r/2, R)}$.

4.3. Performance Evaluation

In this section, we compare the ideal grid-based deployment and robust grid-based deployments in terms of the maximum distance between SNs and the minimum number of SNs to be deployed to guarantee coverage. The formulas for the numbers of SNs and the distances in various deployment cases are listed in Table 4.1. As the general

formulations in some cases are not attainable, we solve for them numerically by assigning L=200, r_s=2, V_{min}=-0.2, V_{max}=0.4, R=0.3.

We have verified our deployment strategies according to Lemma 1 and we conclude that the robust deployment can be achieved by judiciously scaling back the space intervals by which SNs are dropped. In the case of compound errors from both misalignments and randomness, the number of SNs required to provide total coverage is much larger than the number of SNs required in the ideal case.

Table 4.1 Parameters of Grid-based deployment in different circumstances.

	The minimum number of SNs and the distance	**Numerical Results**
Ideal	$\frac{2L^2}{3\sqrt{3}r_s^2}\left[\sqrt{3}r_s\right]$*	3850[3.46]*
Horizontal Misalignment	$\frac{7\sqrt{3}L^2}{24r_s^2}\left\lfloor\frac{4\sqrt{7}}{7}r_s\right\rfloor$	5052[3.02]
Vertical Misalignment	$\frac{2\sqrt{3}L^2}{\left(3r(V_{\max})+2\sqrt{3}V_{\min}\right)\cdot r(V_{\max})}\left[r(V_{\max})\right]$	4799[3.22]
Randomness	$\frac{2L^2}{3\sqrt{3}(r_s-R)^2}\left[\sqrt{3}(r_s-R)\right]$	5328[2.95]
Compound Misalignment & Randomness	$\frac{2\sqrt{3}L^2}{\left(3r(V_{\max},r/2,R)+2\sqrt{3}V_{\min}\right)\cdot r(V_{\max},r/2,R)}\left[r(V_{\max},r/2,R)\right]$	9193[2.36]

*The formula and number in the square bracket refer to the distances between SNs.

4.4. Summary

In practice, the ideal grid-based deployment is difficult to be implemented and/or is not sufficient due to a variety of errors. Our research provides an insightful discussion of deployment errors and how they affect coverage properties of the WSN. We further propose and analyze the robust grid-based deployment design as a viable approach to

overcome such errors, by which the coverage is guaranteed even in the worst case. The research in this chapter represents pioneering work on practical grid-based deployment and has the potential to significantly advance the theoretically-merited grid-based deployment to a more practical stage. Our full-coverage-oriented deployment design can also be used to provide quality partial coverage due to the inherent connection between full coverage and partial coverage.

Chapter 5. COST-EFFECTIVE GRID-BASED SENSOR NODE DEPLOYMENT FOR PROBABILISTIC SENSING COVERAGE

In Chapter 4, we explored several types of possible deployment errors involved in a large-scale WSN deployment and their properties. The coverage-guaranteed SN deployment is devised by studying the impacts of these deployment errors and re-evaluating deployment parameters so that no area is left void even in the presence of worst-case errors. However, such a conservative deployment design may be prohibitively expensive in terms of the number of additional SNs required, which increases dramatically with the magnitude of errors. According to Table 4.1, the numbers of SNs to be deployed to cover a square sensing field in the cases of no error and random errors, which is modeled by a bounded disk of radius R, are approximately $\frac{2L^2}{3\sqrt{3}r_s^2}$ and $\frac{2L^2}{3\sqrt{3}(r_s-R)^2}$, respectively. Numerically, the number of SNs required to be deployed increases by 23%, 56% and 178% when $R=0.1r_s$, $R=0.2r_s$, and $R=0.4r_s$, respectively, compared to the ideal case of no errors.

The cost associated with a coverage-guaranteed SN deployment could unnecessarily impede WSN applications in some scenarios. On the other hand, full coverage may not be necessary in some applications. In order to curb the cost, one may want to leave the plan unchanged if it provides a high percentage of sensing coverage and the application can tolerate coverage incompleteness to some extent. Therefore, there is a strong need to understand how resilient the coverage of grid-based WSNs is against random deployment errors. A general question in this regard is what are the probabilistic properties of the sensing coverage area, such as average coverage, variance and probability distribution, given the shape and the size of the deployment grid and random error parameters? Furthermore, an application engineer needs an efficient method or tool to determine the SN deployment parameters, such as the length of grid edges and the number of SNs, such that the sensing coverage is met in the most cost-effective manner.

There is a more general form of error-involved grid-based deployment in which multiple SNs are to be placed "roughly" at the grid vertices to provide enhanced coverage. This situation is studied in [2]. In order to study the performance of deployment designs using different grid sizes, the paper proposed a derivative model to evaluate the average coverage of the square grid-based deployment, in which random deployment errors follow the normal distribution. Based on that, the minimum number of SNs required to achieve a given coverage requirement is evaluated. However, the derivative model can only be used with errors of the normal distribution. In addition, the study starts by cutting the sensing field into a group of cells, whose size is determined so that a cell is covered if an SN falls into it. Such an approximation is fairly rough and may lead to a pessimistic

evaluation of the coverage quality. Consequently, the evaluated minimum number of SNs tends to be greater than necessary. In an extreme case, if the requirement is to achieve guaranteed full coverage when the normal random parameter σ is 0, the minimum number of SNs required using the cell approximation is 2 times what is necessary.

For probabilistic coverage, a natural design goal would be to ensure that, in the face of random deployment errors, a prespecified proportion, say p_c, of the full sensing field is actually covered by the sensors with a high level of confidence. For such an objective, it is not sufficient that the actual proportion covered, say X, which is a random quantity, simply be equal to p_c on average. Rather, one needs to design the deployment so as to ensure that $P(X \geq p_c) \geq \eta$, where $100 \times \eta$ is a prespecified level of confidence, such as 95%. In order to design such a deployment, a designer needs more than just the mean of X for a given deployment. Ideally, one has the distribution of X, or a good approximation to the distribution.

The core contribution of this chapter is a generic approach to analyzing the probabilistic properties of the covered area of a WSN deployed in a grid pattern with random errors. Specifically, based on a central limit theorem for random fields, we prove that the sensing coverage area has approximately a normal distribution. Previously, we have developed methods to evaluate the average of the sensing coverage area in [113, 114]. In this chapter, we extend the methods therein to generic formulas to efficiently evaluate the two parameters of the normal distribution, i.e. the average and variance. The generic approach is applicable to all types of grid patterns, a wide range of random error distributions, and

different sensing models. To exemplify its usage, the generic approach is applied to a practical deployment scenario, namely, the triangular grid-based deployment with bounded uniform random errors and a binary disk sensing model. The sensing coverage distribution is computed using the normal approximation and verified by Monte-Carlo simulation for a range of deployment parameters. The numerical results show that the coverage provided by the grid-based SN deployment is resilient against deployment errors, which serves as a strong basis for adopting grid-based SN deployment in practice. To the best of our knowledge, this is the first research that studies the complete probabilistic properties of sensing coverage of a WSN using grid-based deployment. An important utility of our research is that we can use our study to address several practical deployment planning problems such as: given a deployment grid and the sensing capability parameters, what are the limits on the deployment errors such that the WSN is able to maintain a given coverage percentage $100 \times p_c$ with a high probability η? Or knowing a bound on the random errors and the sensing radius, what is the required density of SNs (the grid tile length) that would yield the desired coverage with a high probability?

The remainder of this chapter is organized as follows. In Section 5.1, the generic approach to evaluating the mean and variance of the covered area for a given deployment is proposed and its applicability is examined, and the normality of the covered area is proven. In Section 5.2, the generic approach is used to study the coverage properties of the triangular grid-based deployment with uniformly distributed random errors and the binary disk sensing model. In Section 5.3, numerical results are presented. Based on the

numerical results, some practical planning problems of grid-based deployment are examined and their solutions are demonstrated. In Section 5.4, a planning method for practical SN deployment problems is developed based on the generic analysis tool. Finally, the chapter is summarized in Section 5.5.

5.1. A Generic Approach

In this section, we first propose a generic approach to deriving the mean and variance of the covered area in a grid-based WSN deployment. This approach can be used with any type of grid-based deployment, including hexagonal, square and equilateral triangular. To make the discussion concise, we will assume the triangular grid-based deployment for the rest of the section. However, the discussion in this section can apply to other types of grid-based deployment with little modification. We then prove that the sensing coverage area of a large-scale WSN with grid-based deployment approximately has the normal distribution.

5.1.1. Derivation of the mean and variance of the covered area

Suppose a continuous sensing region F composed of M grid triangles is to be sensed by N SNs. We derive the mean and variance, respectively, of the sensing coverage area in the next two subsections.

5.1.1.1. The average sensing coverage area

The average sensing coverage area of the entire sensing field is the arithmetic sum of the average sensing coverage areas of the triangles making up the sensing field. In the following, we solve the average sensing coverage area for the i^{th} triangle Δ_i.

Let X_i denote the area of Δ_i covered by at least one SN. Then the average of X_i is

$$E[X_i] = \int_{\Delta_i} p(x)dx \tag{5.1}$$

where $p(x)$ is the probability that the point x is covered by at least one SN. Let A_m $(m = 1,...,N)$ denote the event that x is covered by SN S_m (for convenience, we suppress the dependence of A_m on x in the notation). Then we have

$$\begin{aligned} p(x) &= P(A_1 \cup A_2 \cup \cdots \cup A_N) \\ &= \sum_{m=1...N} P(A_m) - \sum_{m<n} P(A_m \cap A_n) + \cdots + (-1)^{N+1} P(A_1 \cap A_2 \cap \cdots \cap A_N) \end{aligned} \tag{5.2}$$

We assume that the deployment errors are independent so that the events $A_m (m = 1,...,N)$ are mutually independent. Thus, we have

$$p(x) = \sum_m P(A_m) - \sum_{m<n} P(A_m)P(A_n) + \cdots + (-1)^{N+1} P(A_1)P(A_2)\cdots P(A_N) \tag{5.3}$$

Therefore, to evaluate the average coverage of the sensing field, we need to evaluate the probability that a point x is covered by the SN S_m, for $x \in \Delta_i$ and $m = 1, \ldots, N$, and integrate Eq.(5.3) over the triangle as noted by Eq.(5.1).

There are two potential sources of complexity with the evaluation as described above. The first occurs if the integral in Eq.(5.1) must be evaluated numerically for each triangle in the grid and the grid size *M* is large. However, in typical grid-based deployments, even with random errors, a given point *x* will be sensed with non-negligible probability only by those SNs that are closest to the point, while the probability of its being covered by an SN not in its local neighborhood may be taken to be negligible or zero. Thus, we note that most of the terms in Eq.(5.3) can be safely set to zero, with only the terms involving SNs nearby to the point *x* retained. Moreover, if the errors are identically distributed then the integral in Eq.(5.1) will be essentially the same for all triangles in the grid, except possibly for edge triangles. In this case the integral in Eq.(5.1) needs to be computed just once, or plus at most a few extra times, corresponding to the number of distinct edge triangles.

The second potential source of complexity is in computing $P(A_m)$ in Eq.(5.3). In principal, we should always be able to compute it numerically with sufficient accuracy as a two-dimensional integral over a bounded region. While it is not infeasible to do this sufficiently many times so that the integral in Eq.(5.1) can be approximated with adequate accuracy, it is nonetheless desirable to have a closed-form expression for $P(A_m)$. If SN S_m is associated with the grid point (x_m, y_m) and $x = (u, v)$, then we have

$$P(A_m) = \iint_{\Re^2} P_s\left(\sqrt{(x_s - u)^2 + (y_s - v)^2}\right) f(x_s - x_m, y_s - y_m)\, dx_s dy_s \tag{5.4}$$

where $f(\cdot\ ,\ \cdot)$ is the bivariate density of the zero-mean placement error and $P_s(z)$, is the probability that an SN will properly sense a point a distance *z* away from it. Generally,

the integrand in Eq.(5.4) will be zero or negligible either everywhere (if the SN at (x_s,y_s) is far from the point (u, v)) or outside of a small bounded region. Several useful models are amenable to an explicit closed-form solution for the integral in Eq.(5.4), such as the binary disk sensing model with bounded uniform errors. This is to be explored further in Section 5.2.

5.1.1.2. The variance of the sensing coverage area

The variance of the covered area X of the entire sensing field F can be expressed by the variance of the covered area of individual triangles and the covariance of pairs of individual triangles as

$$VAR(X) = \sum_{i=1}^{N} VAR(X_i) + 2\sum_{\substack{i,j=1 \\ i<j}}^{N} COV(X_i, X_j) \tag{5.5}$$

where $VAR(X_i)$ is the variance of the covered area of the i^{th} triangle and $COV(X_i,X_j)$ is the covariance between X_i and X_j. The evaluations of the variance and the covariance are similar. We start from deriving the formula for the variance. $VAR(X_i)$ can be expressed as

$$VAR(X_i) = E[X_i^2] - E[X_i]^2 \tag{5.6}$$

Let $I(x)$ be the indicator function that the point x is covered. Thus we have

$$E\left[X_i^2\right] = E\left[\left[\int_{\Delta_i} I(x)dx\right]\left[\int_{\Delta_i} I(y)dy\right]\right]$$

$$= E\left[\int_{\Delta_i \times \Delta_i} I(x)I(y)dxdy\right]$$

$$= \int_{\Delta_i \times \Delta_i} P(x \cap y) dxdy \tag{5.7}$$

where $P(x \cap y)$ is the probability that both x and y (inside Δ_i) are covered. It is not straightforward to evaluate $P(x \cap y)$, but it can be further expressed as

$$P(x \cap y) = P(x) + P(y) - P(x \cup y) \tag{5.8}$$

where $P(x \cup y)$ is the probability that either x or y is covered. Let B_m $(m = 1,...,N)$ denote the event that either x or y is covered by SN S_m (for convenience, we suppress the dependence of B_m on the point x and y in the notation). Then we have

$$P(x \cup y) = P(B_1 \cup B_2 \cup \cdots \cup B_N)$$

$$= \sum_m P(B_m) - \sum_{m<n} P(B_m \cap B_n) + \cdots + (-1)^{N+1} P(B_1 \cap B_2 \cap \cdots \cap B_N) \tag{5.9}$$

We assume that the deployment errors are independent so that the events $B_m (m = 1,...,N)$ are mutually independent. Thus, we have

$$P(x \cup y) = \sum_m P(B_m) - \sum_{m<n} P(B_m) P(B_n) + \cdots + (-1)^{N+1} P(B_1) P(B_2) \cdots P(B_N) \tag{5.10}$$

Thus, evaluating the probability that x or y is covered is simplified to evaluating the probability that an SN $S_m (m = 1,...,N)$ covers x or y.

Next, the covariance of two triangles $COV(X_i, X_j)$ can be expressed as

$$COV(X_i, X_j) = E[X_i X_j] - E[X_i] E[X_j] \tag{5.11}$$

and we have,

$$E[X_i X_j] = E\left[\left[\int_{\Delta_i} I(x) dx\right]\left[\int_{\Delta_j} I(y) dy\right]\right]$$

$$= \int_{\Delta_i \times \Delta_j} P(x \cap y) dxdy \tag{5.12}$$

Plugging (5.8)-(5.10) into (5.12), we can obtain the covariance of two triangles. The difference is that *x* and *y* are in the same triangle Δ_i when evaluating the variance and they are in two different triangles Δ_i and Δ_j, respectively, when evaluating the covariance.

It is more computationally intensive to evaluate the variance than the average. There are a number of potential sources of complexity. First, the average has to be obtained in order to evaluate the variance and the covariance. The second source of complexity is related to the number of the integrals in Eq.(5.7) which are to be evaluated. Similar to the analysis on the complexity of evaluating the average, if the deployment errors are identically distributed, the integral in Eq.(5.7) will be essentially the same for all inner triangles. Thus, the integral in Eq.(5.7) needs to be evaluated at most a few times, depending on the number of distinct triangles. The third source of complexity is relevant to the covariance of triangle pairs in the grid. Again, due to the local nature of the sensing capability, only the triangle pairs which are close to each other will have non-negligible covariance. We can therefore safely set many covariance items in Eq.(5.11) to zero. Furthermore, ignoring the edge effect, the value of covariance depends only on the distance and the orientation of the triangles, and many different pairs of triangles will have the same covariance. Thus, the number of instances of evaluating the covariance can be significantly reduced. This reduction of complexity will be further demonstrated in the next section with examples. The fourth potential source of complexity is with computing $P(B_i)$. In principal, we can obtain a numerical result with sufficient accuracy as a four-

dimensional integral over a bounded region. Again, one can do this a sufficient number of times so that the integrals in Eq.(5.7) and Eq.(5.12) can be approximated with adequate accuracy. However, several useful models are amenable to an explicit closed-form solution for $P(B_m)$, such as the binary disk sensing model with bounded uniform errors, which we explore further in Section 5.2.

The derivation above does not assume any particular random error distribution, any particular grid shape, or the sensing model. As such, the generic expressions in Eqs.(5.1) – (5.12) are valid for any random error distributions, including normal, bounded normal, general bounded, bounded uniform, etc. It is also straightforward to modify them to work with any form of grid shape, including triangular, square, and hexagonal. In such cases, one can simply change the integration region accordingly.

5.1.2. The normality of the covered area

Since the covered area X of the sensing field F is a sum $X = X_1 + \ldots + X_M$, where X_i is the area covered in the i^{th} grid tile and M is the number of grid tiles in F, it is natural to expect that X is approximately normally distributed by virtue of some version of a central limit theorem. But we need to be a little bit careful. For one thing, the X_i's are not independent in general since X_i and X_j may be dependent on a common set of sensors, especially if tiles i and j are in close proximity. For another, the X_i's are not necessarily identically distributed, since tiles on the edge of the sensing field may have a different coverage distribution than tiles in the interior of the sensing field.

The set of random variables $\{X_1,\ldots,X_M\}$ is a subset of what is known as a *random field*, which means that the indices correspond to spatially distributed points in some topological space (in our case the 2-dimensional plane). Central limit theorems for random fields have been well studied in the probability literature, dating back at least to Rosen [115] and Bulinskii and Zurbenko [116]. In this subsection, we apply a theorem due to Takahata [117] which, in addition to implying asymptotic normality, gives an estimate on the rate of convergence. Throughout this subsection we assume that the deployment error distribution has bounded support and that the sensing range of all sensors is bounded. We note that this assumption holds for any physical system although mathematically we would like to allow certain unbounded error distributions, such as the bivariate normal. However, assuming boundedness greatly simplifies the mathematics, while not losing much generality, and so we choose to make the assumption. We first introduce some definitions and notation and state Takahata's theorem, then state and prove a corollary which is a weaker version of the theorem in terms of conditions more suited to the present context. We then state and prove a second corollary which gives the central limit theorem result for a sequence of increasing sensing fields, which is the case of interest for us. The limiting regime here is different than that given in Takahata's theorem, and so the result does require proof. We conclude with some discussion.

Let $\mathbf{Z}^d = \{(n_1,\ldots,n_d): n_i \in \mathbf{Z},\ i=1,\ldots,d\}$ be the d-dimensional integer lattice, where $\mathbf{Z}$ is the set of integers. Let $\{Y_a\}_{a\in\mathbf{Z}^d}$ be a family of random variables indexed by elements of

$\mathbf{Z}^d$. Such a family is called a *random field* on $\mathbf{Z}^d$. We assume that $E[Y_a]=0$ and $VAR(Y_a)<\infty$ for all $a \in \mathbf{Z}^d$. Let $\Im = \{V \subset \mathbf{Z}^d : |V| < \infty\}$ be the set of all finite subsets of $\mathbf{Z}^d$, where $|V|$ denotes the number of elements in V. For each nonempty $V \in \Im$, define

$$S(V) = \sum_{a \in V} Y_a \tag{5.13}$$

When dealing with a family of dependent random variables (such as $\{Y_a\}_{a \in \mathbf{Z}^d}$), one needs a measure of the strength of dependence between different subsets of the family in order to characterize conditions under which a central limit theorem will be valid. Such conditions are referred to as *mixing* conditions in the literature. However, because of the boundedness assumptions, we can avoid the technical definitions of mixing, and instead rely on the notion of *m-dependence*. First, we define a metric on $\mathbf{Z}^d$ by

$$|a-b| = \max_{1 \le i \le d} |n_i - m_i|, \tag{5.14}$$

where $a=(n_1,\ldots,n_d)$, $b=(m_1,\ldots,m_d) \in \mathbf{Z}^d$, and for two subsets V_1, $V_2 \in \Im$, the distance between V_1 and V_2 as

$$D(V_1, V_2) = \min\{|a-b| : a \in V_1, b \in V_2\}. \tag{5.15}$$

We say that the random field $\{Y_a\}_{a \in \mathbf{Z}^d}$ is *m-dependent* if the two sets of random variables $\{Y_a\}_{a \in V_1}$ and $\{Y_b\}_{b \in V_2}$ are mutually independent whenever $D(V_1, V_2) > m$.

With the notion of *m*-dependent defined, we now turn our attention to stating a central limit theorem result for the random field $\{Y_a\}_{a \in \mathbf{Z}^d}$ due to Takahata [124]. Let $\{V_n\}_{n=1}^{\infty}$ be

a sequence of elements of $\Im$ and let $\Phi(\cdot)$ be the standard normal cumulative distribution function; i.e.,

$$\Phi(x) = \int_{-\infty}^{x} \frac{1}{\sqrt{2\pi}} e^{-t^2/2} dt. \tag{5.16}$$

Define

$$\varepsilon_n(x) = \left| (P(S(V_n)/\sigma(V_n)) \le x) - \Phi(x) \right|, \tag{5.17}$$

where $\sigma(V_n) = \sqrt{VAR(S(V_n))}$, and

$$\varepsilon_n = \sup_x \varepsilon_n(x); \tag{5.18}$$

i.e., ε_n is the maximum absolute difference between the probability distribution function of $S(V_n)/\sigma(V_n)$ and that of a standard normal random variable. Then we have the following theorem, whose proof can be found in [124]:

Theorem 5.1 [Takahata, 1983]. Suppose that

(i) for some $M > 0$, $E|Y_a|^8 \le M < \infty$ *for all* $a \in \mathbf{Z}^d$;

(ii) the family $\{Y_a\}_{a \in \mathbf{Z}^d}$ *is m-dependent for some positive integer m;*

(iii) the sequence $\{V_n\}_{n=1}^{\infty}$ *satisfies* $|V_n| \to \infty$ *as* $n \to \infty$*; and*

(iv) $\liminf_{n \to \infty} VAR(S(V_n))/|V_n| > 0$.

Then $\varepsilon_n = O(|V_n|^{-1/2})$.

Note that if conditions (*i*) - (*iv*) are satisfied, then not only is the distribution function of $S(V_n)/\sigma(V_n)$ converging pointwise to $\Phi(\cdot)$ as $n \to \infty$ (i.e., $S(V_n)/\sigma(V_n)$ is converging in distribution to a standard normal random variable), but also Theorem 5.1 gives an explicit rate of convergence.

Suppose that sensors are deployed at the vertices of an infinite grid but with deployment errors, where all errors are independent and identically distributed, and the sensing properties of all sensors are identical. Let the set of grid tile labels be $\mathbf{Z}^d$ with the natural correspondence between labels and grid tiles (i.e., label (i, j) corresponds to the grid tile in row *i* and column *j* of the grid). Let the sets $\{V_n\}_{n=1}^{\infty}$ be defined as in Theorem 5.1, X_a be the area that is covered by sensors in the grid tile with label *a*, and $Y_a = X_a - E[X_a]$. With $S(V_n) = \sum_{a \in V_n} Y_a$ defined as in Theorem 5.1, we have the following corollary.

Corollary 5.2. Suppose that

(i) the support of the deployment error distribution is bounded;

(ii) the sensing range is bounded;

(iii) the sequence $\{V_n\}_{n=1}^{\infty}$ *satisfies* $|V_n| \to \infty$ *as* $n \to \infty$*; and*

(iv) $\liminf_{n \to \infty} VAR(S(V_n))/|V_n| > 0$.

Then $\varepsilon_n = O(|V_n|^{-1/2})$.

Proof. We check the conditions of Theorem 5.1. Since the grid tile areas are bounded the random variables Y_a are all bounded and so condition (i) of Theorem 5.1 is clearly satisfied. By boundedness of the error distribution support and the sensing range, there is some $d_{\max} < \infty$ such that Y_a and Y_b are independent whenever the grid tiles with labels *a* and *b* are more than $d_{\max}$ away from each other in Euclidean distance. Therefore, it is easy to see that the family $\{Y_a\}_{a \in \mathbf{Z}^d}$ is *m*-dependent for $m = d_{\max}$, and so condition (ii) of Theorem 5.1 is satisfied. Conditions (iii) and (iv) of Theorem 5.1 are the same as conditions (iii) and (iv) of Corollary 5.2. ■

For our purposes we wish to consider a sequence of sensing fields $\{F_n\}_{n=1}^{\infty}$ of increasing size on the 2-dimensional plane, as opposed to an increasing sequence of subsets $\{V_n\}_{n=1}^{\infty}$ of a single infinite grid. One must note that Theorem 5.1 or Corollary 5.2 are not directly applicable to this situation because in the assumptions of Theorem 5.1 there is one underlying random field $\{Y_a\}_{a \in \mathbf{Z}^d}$ and so each of the subsets in the sequence $\left\{\{Y_a\}_{a \in V_n}\right\}_{n=1}^{\infty}$ are subsets of the same random field. However, when considering a sequence of sensing fields, the distributions of the random variables associated with the sensing field grid tiles may change slightly when going from one sensing field to the next (by adding a grid tile, for example), since the addition of new sensors potentially affects the coverage distributions of some existing grid tiles. In other words, while the sensing field F_n and the subset V_n refer to the same set of grid tiles, the coverage distributions of the tiles in F_n are affected only by sensors associated with grid vertices in F_n, while the coverage distribution of tiles associated with V_n are potentially affected by any sensors that have been placed on the infinite grid. However, only tiles at or close to the edge of V_n get affected by sensors outside the field, and this effect becomes diminishingly small as the size of the field grows.

Let us start with the setup in Corollary 5.2. The sensing field F_n is then the same set of indices as the set V_n, but the notation F_n implies that no sensors have been placed (with error) at grid vertices outside the field corresponding to F_n. We say that a grid tile is a

boundary grid tile of the sensing field associated with the subset V_n if there is a positive probability that at least one point in the tile can be covered by a sensor whose target grid vertex is outside the sensing field associated with V_n. We say that a grid tile is a boundary tile of the sensing field F_n if it is a boundary tile of the sensing field associated with V_n. Note that the distribution of the covered area for a non-boundary tile is the same whether we are considering the field associated with F_n or with V_n. Let X'_{na} denote the covered area of the grid tile associated with the index $a \in F_n$ and let $Y'_{na} = X'_{na} - E\left[X'_{na}\right]$, for $a \in F_n$; $n \geq 1$. Let $S(F_n) = \sum_{i=1}^{n} Y'_{na}$ and $\sigma(F_n) = \sqrt{VAR(S(F_n))}$. The result that we want is for $S(F_n)/\sigma(F_n) \to U$ in distribution, where U is normally random distributed. We assume that the conditions of Corollary 5.2 hold, so that $S(V_n)/\sigma(V_n) \to Z$ in distribution, where Z is a standard normal random variable. Let B_n denote the set of boundary indices of V_n (or F_n). Then we can write $S(V_n) = S_1(V_n) + e(V_n)$, where $S_1(V_n) = \sum_{a \in V_n - B_n} Y_a$ sums over non-boundary tiles and $e(V_n) = \sum_{a \in B_n} Y_a$ sums over boundary tiles. Similarly, we write $S(F_n)$ as $S(F_n) = S_1(F_n) + e(F_n)$, where $S_1(F_n) = \sum_{a \in V_n - B_n} Y'_{na}$ and $e(F_n) = \sum_{a \in B_n} Y'_{na}$. By the definition of the boundary set B_n the two quantities $S_1(V_n)$ and $S_1(F_n)$ have the same distribution. Therefore, if the following conditions hold:

$$\sigma(V_n)/\sigma(F_n) \to c \text{ as } n \to \infty, \text{ where } c \text{ is a constant} \tag{5.19}$$

$$e(V_n)/\sigma(V_n) \to 0 \text{ in distribution as } n \to \infty \tag{5.20}$$

$$e(F_n)/\sigma(F_n) \to 0 \text{ in distribution as } n \to \infty \tag{5.21}$$

then one can see that all of $S(V_n)/\sigma(V_n)$, $S_1(V_n)/\sigma(V_n)$, $S_1(F_n)/\sigma(F_n)$, and $S(F_n)/\sigma(F_n)$ will converge in distribution to a normally distributed random variable. The conditions (5.19)-(5.21) are not difficult to show if the number of boundary terms is of the same or smaller order than $\sigma(V_n)$, which is at least $O\left(\sqrt{|V_n|}\right)$ by condition (iv) of Corollary 5.2. This is a reasonable condition but depends on the shape of the sensing field. In practice, for large grids, we expect that the number of boundary tiles should be no more than a few times the square root of the total number of tiles in the grid.

5.2. Triangular Grid-based Deployment with Bounded Uniform Errors

In this section, we explore the coverage properties of a sensing field adopting triangular grid-based SN deployment assuming bounded uniform errors and a binary sensing disk model, by applying the general approach developed in Section 3. Let d denote the length of the side of a triangular grid tile and r_s denote the radius of the sensing disks. According to Chapter 4, in the ideal case (no errors), to achieve full coverage with a minimum number of SNs, d is set to $\sqrt{3}r_s$. However, due to random errors, SNs are uniformly deployed within error disks of radius R, centered at the grid vertices.

To evaluate the average and variance of the sensing coverage area, we have to evaluate the average and variance for individual triangles, and covariance for triangle pairs. As discussed in Section 3, for a sensing field composed of M triangles, we do not have to evaluate the average and variance for M times, or the covariance for C_M^2 times due to

locality of sensing coverage and uniformity of deployment errors. We next derive formulas for evaluating the average and variance of one triangle, and the covariance of two neighboring triangles.

Figure 5.1 illustrates a triangular area and three sensing disks corresponding to a deployment instance of three SNs. Note that more SNs may cover part of the triangle, depending on the error radius R.

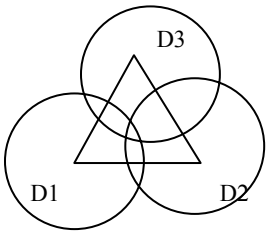

Figure 5.1 A triangle and three associated sensing disks

Both Eq.(5.3) and Eq.(5.10) are composed of $2^N - 1$ terms. The only potential source of complexity comes from the computation of the N terms of $P(A_m)$ in Eq.(5.3) and $P(B_m)$ in Eq.(5.10), $m = 1,\ldots,N$ (the remaining terms being obtained by multiplication). For bounded errors, not all N SNs will cover a given point (or two points in the case of $P(B_m)$) in the field. With some simple calculation, one can derive the number of SNs that could contribute to the coverage of points in a triangle. For example, if $R + r_s < \frac{\sqrt{3}}{2} d$, at most 3 SNs will provide coverage to points in a triangle; if $R + r_s < d$, at most 6 SNs will provide coverage to points in a triangle; if $R + r_s < \sqrt{3} d$, at most 12 SNs will provide coverage to points in a triangle, and so on. Therefore, out of all items in Eq.(5.3) and Eq.

(5.10), the first few terms would dominate and many of the rest become zero. This property can be used to further reduce the computation complexity. A nice feature of Eq.(5.3) and Eq.(5.10) is that we can obtain an error bound on the approximation if some terms are neglected in the computation.

The probability $P(A_m)$ is equal to the probability that the distance between the point *x* and the SN S_m is less than or equal to r_s. This is satisfied if S_m is within the intersection of the disk of radius r_s centered at (u,v), denoted by $O_{u,v}$, and the error disk centered at the grid vertex corresponding to S_m, denoted by E_m, as depicted in Figure 5.2.

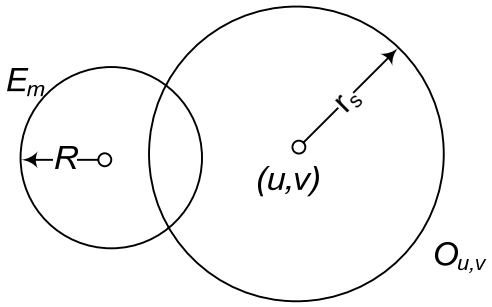

Figure 5.2 A disk centered at x and an error disk

Therefore we have,

$$P(A_m) = \frac{\text{area}(E_m \bigcap O_{u,v})}{\pi R^2} \tag{5.22}$$

As the area of the intersection of two circles of given radii has a closed form, $P(A_m)$ can be efficiently computed for any SN S_m and point *x*.

The probability $P(B_m)$ is equal to the probability that the distance from the point *x* and/or *y* to the SN S_m is less than or equal to r_s. This is satisfied if S_m is within the intersection of the disk of radius r_s centered at *x* denoted by O_x, and the error disk centered at the grid vertex corresponding to S_m, denoted by E_m, or the intersection of the disk of radius r_s centered at *y* denoted by O_y, and the error disk centered at the grid vertex corresponding to S_m as depicted in Figure 5.3.

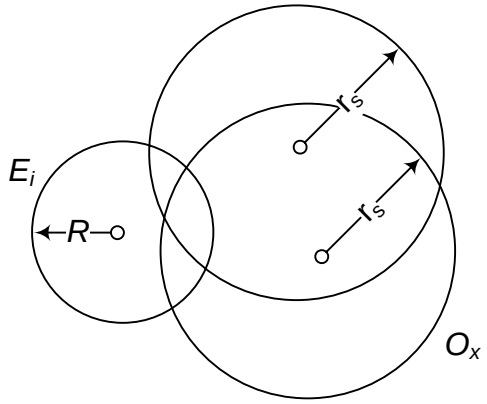

Figure 5.3 A disk centered at *x*, a disk centered at *y* and an error disk

Therefore we have,

$$P(B_m) = \frac{\text{area}(E_m \bigcap O_x) + area(E_m \bigcap O_y) - area(E_m \bigcap O_x \bigcap O_y)}{\pi R^2} \tag{5.23}$$

We derive the closed form formula to calculate the intersection of three disks in Eq. (5.23), $P(B_m)$ can be efficiently computed for any SN S_m, the point *x* and *y*.

Next, we further evaluate the covariance between pairs of triangle areas. As deployment errors of individual SNs are independent, two areas will have zero covariance if they do

not share any SN. For example, if $R + r_s < \frac{\sqrt{3}}{2} d$, a given triangle has non-zero covariance with 12 triangles, as demonstrated by Figure 5.4. Furthermore, we do not have to evaluate the covariance for a given triangle 12 times since the covariance only depends on the distance between triangles and their orientation. For example, in Figure 5.4 the triangles 1, 2 and 3 have the same covariance with the triangle in the center. The triangles 4, 5, 7, 8, 10, and 11 have the same covariance with the triangle in the center. So do the triangles 6, 9, and 12. We can group pairs of triangular areas into three types, as illustrated in Figure 5.4.

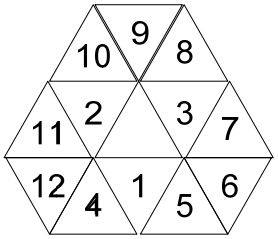

Figure 5.4 The neighbouring triangles and the calculation of their covariance

5.3. Numerical Results and Discussion

In this section, we present numerical results of the coverage properties of grid-based deployment with bounded uniform errors derived above. We verify the correctness of the average coverage and the variance of coverage obtained in Section 4 by simulating the grid-based deployment with random errors using Monte Carlo, in which *100,000* deployment instances are randomly generated. For each deployment instance, the covered area is obtained by conducting numerical integration over the sensing field. For the sake of conciseness, we use the coverage percentage to represent the sensing coverage quality.

We then develop the approaches to solving the practical design problem of finding the minimum number of SNs to obtain a given coverage percentage c at a probability p.

To verify the correctness of the derivations in Section 5.2, we consider a WSN composed of 11 rows and 11 columns of SNs. That is, the sensing field consists of 200 small triangular areas. We fix the sensing radius r_s at 10. Thus, the average coverage of the sensing field is a function of the error disk radius R and the length of the grid tile d. We first study how R impacts the average coverage. We conduct four groups of experiments by setting $d=16$, $d=18$, $d=20$ and $d=22$. In each experiment, the value of R varies from 0 to 8. The empirical CDF of the coverage percentage from simulations and the CDF of the coverage percentage generated from the parameters obtained by analytical programs are plotted in Figure 5.5. The average coverage percentage and the variance as a function of R are presented in Figure 5.6 and Figure 5.7, respectively.

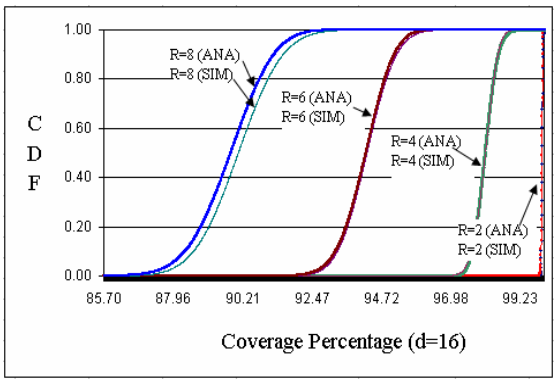

(a) CDF function of the sensing coverage when d=16

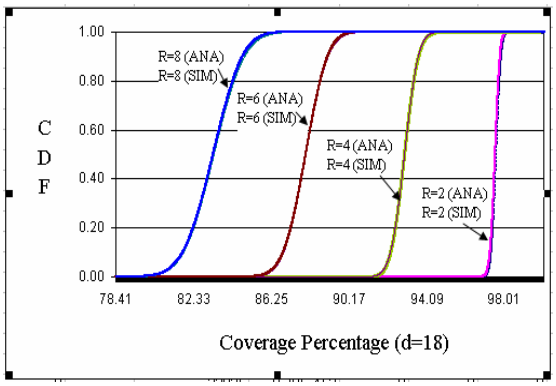

(b) CDF function of the sensing coverage when d=18

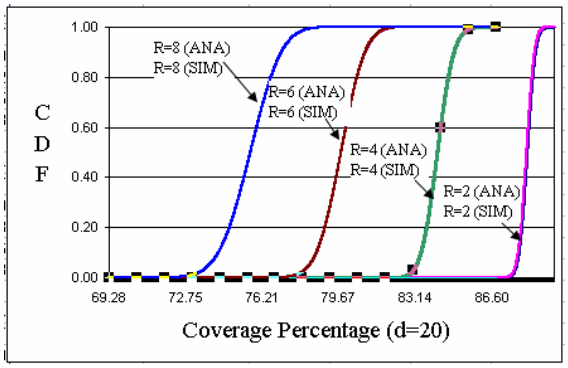

(c) CDF function of the sensing coverage when d=20

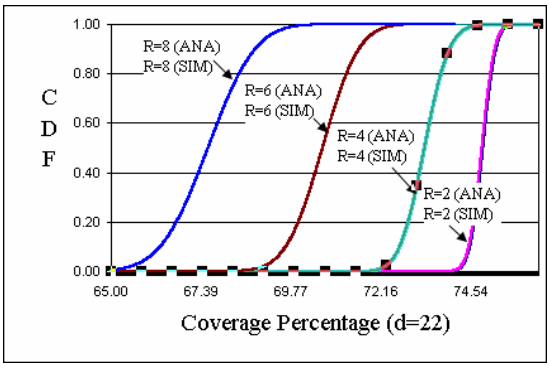

(d) CDF function of the sensing coverage when d=22

Figure 5.5 Comparison of empirical CDF and analytical CDF

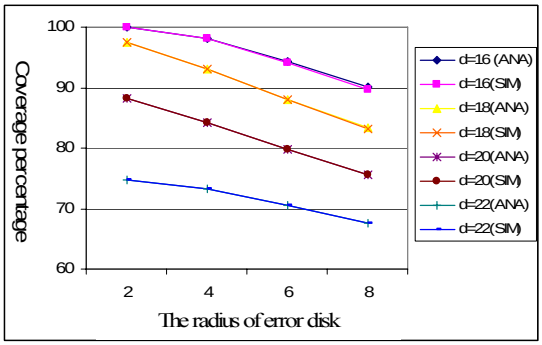

Figure 5.6 The average coverage percentage vs. the radius of the error disks

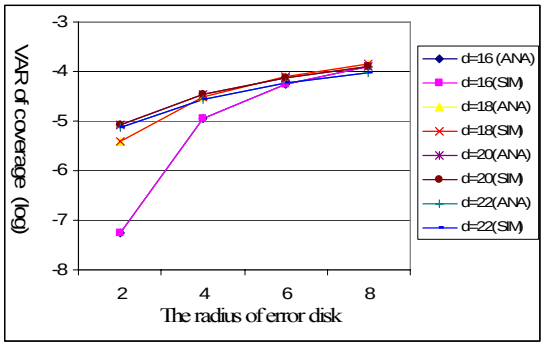

Figure 5.7 The variance of coverage vs. the radius of the error disks (log)

In Figure 5.6 and Figure 5.7, the results from the analytical derivations in Section 5.2 and from simulations match very well. Having demonstrated the accuracy of analytical

derivations, in the remainder of this section, we will only present the numerical results based on the analytical study of Section 5.2, which can be more efficiently obtained. Table 5.1 summarizes the average coverage percentage, the variance, the coverage percentage with different probabilities, i.e., 80%, 90% and 95%. We make the following observations of the sensing coverage properties.

Table 5.1 The coverage properties with four scenarios

Distance between SNs (d)	Error bound	Average Coverage Percentage	Variance	80% Coverage	90% Coverage	95% Coverage
16	2	99.93	5.57E-08	99.90	99.90	99.89
	4	98.08	1.12E-05	97.65	97.53	97.42
	6	94.25	5.66E-05	93.28	93.01	92.77
	8	90.07	1.30E-04	88.60	88.19	87.84
18	2	97.55	3.93E-06	97.30	97.23	97.17
	4	92.97	3.03E-05	92.26	92.06	91.89
	6	88.00	7.70E-05	86.87	86.55	86.28
	8	83.35	1.46E-04	81.80	81.37	80.99
20	2	88.18	8.51E-06	87.80	87.70	87.60
	4	84.13	3.40E-05	83.37	83.17	82.98
	6	79.79	7.38E-05	78.68	78.38	78.10
	8	75.63	1.24E-04	74.19	73.80	73.45
22	2	74.84	7.35E-06	74.49	74.40	74.31
	4	73.30	2.68E-05	72.64	72.45	72.29
	6	70.62	5.76E-05	69.64	69.37	69.13
	8	67.54	9.70E-05	66.27	65.92	65.61

First of all, the results show a very appealing feature of grid-based deployment, which is that the sensing coverage is rather resilient to random errors. For example, when $d = 18$ and $R = 2$, the coverage percentage is no less than 97% with probability 95%. Note that when $R = 2$, to achieve 100% coverage, 68% more SNs are required to be deployed [52]. In other words, 68% extra SNs can only increase the sensing coverage by no more than 3%. We conclude that sacrificing a little coverage can make the network much more

affordable. A similar observation has been made earlier for a randomly deployed WSN in [118].

In addition, the average coverage and the coverage percentages at different confidence levels monotonically decrease with R for the range considered. This is a useful characteristic to solve for the maximum R allowed for a given d and a given coverage requirement. For example, if the required coverage is 85% with probability 95%, and d is 20, the maximum R should be no greater than 3.52. The maximum R as a function of d (when the probability is 95%) is plotted in Figure 5.8. Note that when d is 20 (22), the coverage cannot reach 95% (85%) or more no matter how small R is.

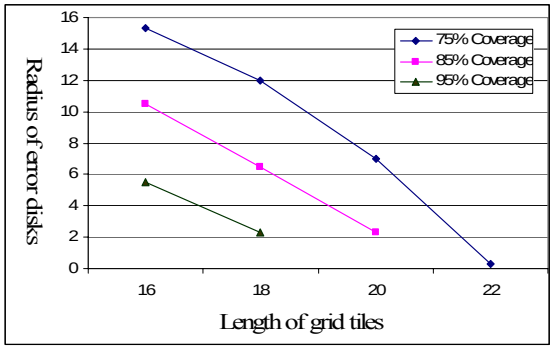

Figure 5.8 The maximum error radius vs. the length of grid tiles

As seen in results, the distance between SNs also affects the coverage properties. The average coverage percentage is a monotonically decreasing function of d. So are the coverage percentages at different confidence levels. This characteristic can be used to answer another practical question, namely, what is maximum d or what is the minimum deployment density in order to satisfy a given coverage percentage for a given d? The maximum d as a function of R (with probability 95%) is plotted in Figure 5.9.

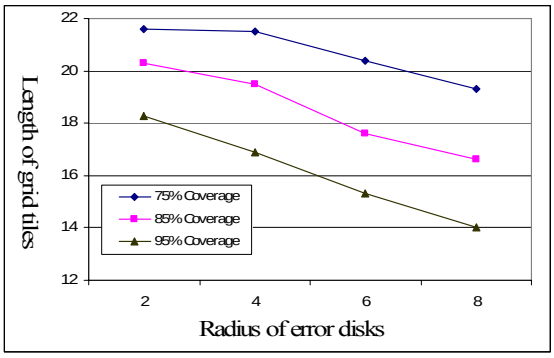

Figure 5.9 The maximum *d* vs. the radius of the error disks

5.4. Deployment Problem and Design Algorithm

In previous sections, we propose a generic analysis approach and demonstrate its usage in specific deployment scenarios. Another important utility of this generic tool is for designing practical grid-based SN deployment solutions.

A general grid-based SN deployment problem is to find the minimum number of rows and columns of SNs so as to provide high-quality sensing coverage over a given field. For example, one needs a SN deployment to provide no less than 85% coverage over a square field of 200*200 at 95% probability. We have two remarks on solving this problem. Firstly, the union of small triangles should encompass the square field, as shown in Figure 5.10. In case of a large-scale deployment, the coverage properties of the square area can be effectively approximated by the coverage properties of the union area of a large number of triangles. Secondly, to find the minimum number of rows and columns, we can start with some initial values of rows and columns that will provide a coverage property no better than the requirement. We then increment the values of row and/or column by 1 each time and evaluate the coverage property, until the coverage

requirement is satisfied. The efficiency of this method depends on how close the initial value of rows and columns is to the optimal value. This idea is implemented in the procedure as follow.

(1) Initialize *d* so that the coverage is surely worst than the required quality.

(2) Calculate the initial value of rows as $ROW=\left\lfloor 2\times\frac{200}{\sqrt{3}d}\right\rfloor+1$; the initial value of columns as $COL=\left\lfloor\frac{200}{d}+0.5\right\rfloor+1$;

(3) Evaluate the coverage property of a WSN with *ROW*, *COL* and *d*.

(4) If the coverage property does not satisfy the requirement,

Let $ROW=ROW-1;\ COL=COL-1;d=\max\left(\frac{200}{ROW-1}\times\frac{2}{\sqrt{3}},\frac{200}{COL-1.5}\right)$, calculate the value of rows as $ROW=\left\lfloor 2\times\frac{200}{\sqrt{3}d}\right\rfloor+1$; the value of columns as $COL=\left\lfloor\frac{200}{d}+0.5\right\rfloor+1$, return to (3).

Else

Done;

For the problem above, we can initialize *d* as 20 when R=4 by looking at the Table 5.1. Finally, we solve for the number of rows and columns as 13 and 12 respectively, and the distance between SNs is optimized as 19.25.

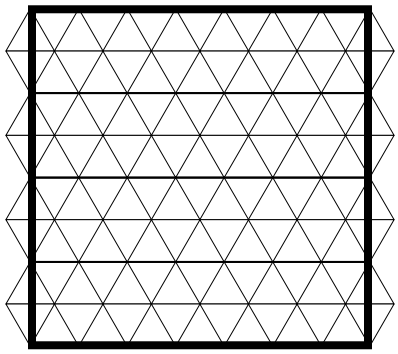

Figure 5.10 The square field is encompassed by the union of small triangles

5.5. Summary

In this chapter, we first propose a generic approach to evaluating the average and variance of the sensing coverage area, for a variety of deployment scenarios. The generic approach can be used with all types of grid shape, various random error distributions, and different sensing models. We further prove that the sensing coverage area of a grid-based large-scale WSN follows the normal distribution. We apply the generic approach to one specific case, namely, the triangular grid-based deployment with bounded uniform errors and a binary sensing disk model. We derive the closed form formulas to calculate the normal distribution parameters. Numerical results are obtained and verified by Monte Carlo simulation results. Our proposal can not only be used to analyze the sensing coverage properties of a given deployment scenario, it can also be used to solve practical problems of efficient grid-based SN deployment planning for sensing coverage. A design procedure is developed. This research provides a generic tool to plan large-scale WSN deployment in practice. In general, the grid-based SN deployment is resilient against deployment errors. We therefore advocate adopting this deployment method whenever possible in practice.

Chapter 6. NON-DETERMINISTIC RELAY NODE DEPLOYMENT STRATEGIES

In Chapter 4 and Chapter 5, we have investigated SN deployment approaches in concerns of sensing area coverage. In a heterogeneous two-tier WSN, RNs form a communication backbone to relay traffic from SNs to the BS.

RN deployment affects two important properties of a WSN, i.e., the communication connectivity and the system lifetime. Therefore, it is desired that the group of RNs can provide strong communication connectivity to SNs and such connectivity lasts for as long as possible. Assuming devices can be deliberately placed on the sensing field, some research efforts have attempted to minimize the number of RNs with constraints of network connectivity [55, 57-62], or minimize the number of RNs with constraints of network connectivity and system lifetime [63-65, 67]. However the methodologies and solutions therein are not applicable in situations where deliberate device placement is not feasible. For example, the sensing field is hostile or inaccessible to humans, or the sensing field is so large that a great number of devices are deployed. In such cases, devices can be deployed randomly according to a density function. As such, the positions of devices cannot be precisely known or controlled. A well designed deployment density function becomes a viable approach to efficient device deployment [69].

Uniform random deployment is the most commonly considered random deployment strategy in the literature. However, as described as in Chapter 2, it is inefficient from an energy perspective due to the biased energy consumption rate (BECR) phenomenon, when RNs operate in either the single-hop manner or the multi-hop manner. To solve the BECR problem associated with uniform random deployment, we propose two novel random deployment strategies for RNs in both communication models, namely, lifetime-oriented deployment and hybrid deployment. We then analyze and compare the three deployment strategies (uniform, lifetime-oriented, and hybrid). Both theoretical analysis and simulated evaluation show the new deployment strategies can effectively alleviate the BECR problem and extend the system lifetime. To the best of our knowledge, this is the first effort to optimize the random device deployment (by the density function) in order to extend the lifetime of a large-scale heterogeneous WSN. An abbreviated version of this chapter have appeared in [119, 120].

The remainder of this chapter is organized as follows. In Section 6.1, random RN deployment strategies are proposed for the single-hop communication case and the impact of RN deployment on connectivity and lifetime is explored. In Section 6.2, random RN deployment strategies are proposed for the multi-hop communication case. In Section 6.3, the performance of three RN deployment strategies is evaluated and compared. In Section 6.4, we discuss some practical issues, such as the extensibility of our work and the implementation methods. The chapter is summarized in Section 6.5.

In addition to assumptions and models presented in Chapter 3, in this chapter, we assume that SNs are uniformly deployed on the sensing field, either in a grid pattern or in a uniform random manner. The satisfactory sensing coverage is supported by the group of SNs.

6.1. Random Deployment Strategies in Single-hop Communication Case

In this section, we propose and examine deployment solutions for the following problem. Given a WSN as modeled in Chapter 3, how should one deploy a given number, N_{RN}, of RNs so that the network lifetime is maximized? We will address this problem assuming RNs communicate with the BS in a single-hop manner. In the next section, we will address the same problem in case that RNs communication with the BS in multi-hop manner. In the following of the chapter, we use polar coordinates to specify locations on the sensing field.

We will first study the pros and cons of the connectivity-oriented deployment strategy. We then propose two novel deployment strategies, namely, lifetime-oriented deployment and hybrid deployment.

6.1.1. Connectivity-Oriented Deployment

Uniform deployment is the mostly used deployment model in the literature [104, 121-125]. Assume N_{RN} RNs are deployed uniformly in a sensing site A of area $|A|$. For any SN, the probability that it can reach at least one RN in one hop is

$$p_R = 1 - \left(1 - \pi r_{SN}^2 / |A|\right)^{N_{RN}} \tag{6.1}$$

If a connectivity probability σ_0 for any SN is required, i.e., $p_R \geq \sigma_0$, the minimum number of RNs is expressed as:

$$N_{RN}^{u\{\min\}} = \ln(1-\sigma_0)/\ln(1 - \pi r_{SN}^2 / |A|) \tag{6.2}$$

Compared with other random deployments, this strategy provides identical and maximal connectivity everywhere in the WSN. In other words, for a given connectivity requirement σ_0, this strategy will require the least number of RNs (illustrated in Section 6.3). We therefore refer to it as the Connectivity-Oriented Deployment strategy. However, due to the BECR phenomenon discussed above, it suffers fundamentally from an energy efficiency perspective.

6.1.2. Lifetime-Oriented Deployment

We also refer to this strategy as a weighted random deployment. Consider two regions of a WSN, one far from the BS and another close to the BS. Assume there is the same number of nodes (SNs and RNs) in each of them. As the active RNs in the farther region dissipate energy faster than their peers in the closer region due to the longer transmission range, the overall system becomes unusable even though much energy is left in RNs in the near region. To allow nodes in both regions to function for the same length of time, the node deployment density should reflect the different energy dissipation rates. That is, more RNs should be deployed as one gets farther from the BS. When one CH dies, another RN can take over its role.

Denote the integral of $E_{RN}(d,0)$ over the sensing area A by $D = \int_A E_{RN}(u,0)ududv$. For the nodes in different regions of the network to function for the same period, the RN deployment density at a point $(d,\theta) \in A$ should be proportional to the energy dissipation rate of an active RN at a distance d from the BS. As such, the RN deployment density function is

$$f(d,\theta) = E_{RN}(d,0)/D = \left(c_1 + g\alpha_2 d^m\right)nl/D \qquad \text{if } (d,\theta) \in A \tag{6.3}$$

and $f(d,\theta) = 0$ otherwise. If N_{RN} RNs are deployed according to the density function (6.3), the probability that an SN at point (d,θ) can reach one or more RNs in one hop is

$$p_R(d,\theta) = 1 - \left(1 - \int_{O(d,\theta)} f(u,v)ududv\right)^{N_{RN}} \tag{6.4}$$

where $O(d,\theta)$ is a circle centered at (d,θ) with radius r_{SN}. If r_{SN} is relatively small, the probability can be approximated by

$$p_R(d,\theta) \approx 1 - \left(1 - \pi r_{SN}^2 f(d,\theta)\right)^{N_{RN}} \tag{6.5}$$

Assume the connectivity σ_0 is required. Then letting $p_R(d,\theta) = \sigma_0$ and using the approximation in (6.5), we have

$$1 - \left(1 - \pi r_{SN}^2 f(d,\theta)\right)^{N_{RN}} = \sigma_0 \tag{6.6}$$

Plugging (6.3) into (6.6) and solving for d, we get

$$d_0 = \left[\left(\frac{D \cdot (1-(1-\sigma_0)^{1/N_{RN}})}{ng\alpha_2 l\pi r_{SN}^2} - \frac{c_1}{g\alpha_2}\right)\right]^{1/m} \tag{6.7}$$

The formula (6.7) defines a cutoff distance in the sensing area. We define the region *B* as

$$B = \{(d,\theta) \mid (d,\theta) \in A, d < d_0\} \tag{6.8}$$

In this region, the probability of connectivity of an SN is less than σ_0, while an SN outside of *B* has connectivity probability higher than σ_0. Assuming a square sensing area with the BS at the center, the cutoff circle and region *B* are illustrated in Figure 6.1.

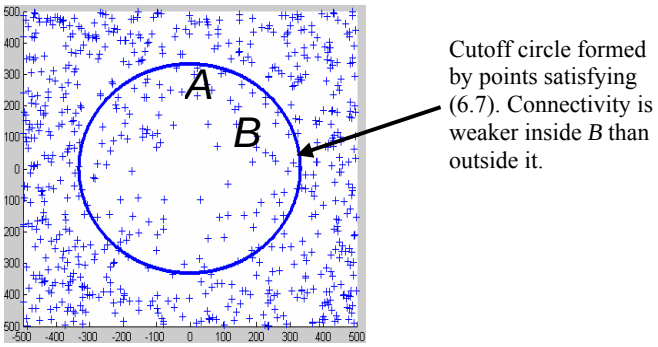

Figure 6.1 An illustration of weighted random deployment

If we set the right side of (6.7) equal to zero and solve for N_{RN}, we have

$$N_{RN}^{w\{\min\}} = \ln(1-\sigma_0)/\ln(1-c_1 nl\pi r_{SN}^2/D) \tag{6.9}$$

That is, if N_{RN} is less than $N_{RN}^{w\{\min\}}$, the deployment according to (6.3) will not be able to meet the connectivity requirement in the sub-area inside the cutoff circle.

Note that in order to obtain a numerical solution to a specific application scenario, one does not need to evaluate the number of SNs associated with one RN, n, which appears in many formulas above since it will be cancelled out from the denominator and numerator.

6.1.3. Hybrid Deployment

The weighted random deployment of RNs according to the density function (6.3) can counteract the BECR phenomenon. However, this benefit will be fully realized only if the connectivity of SNs is satisfied in the network. If the number of given RNs, N_{RN}, is less than $N_{RN}^{w\{\min\}}$, the number of SNs without connectivity may be too high for the network to function properly.

The objective of the hybrid deployment is to optimize RN deployment by balancing the concerns of connectivity and lifetime extension. If $N_{RN} < N_{RN}^{u\{\min\}}$, there is no way to guarantee the connectivity in the first place. If $N_{RN} \geq N_{RN}^{w\{\min\}}$, the weighted random deployment as defined by (6.3) can provide sufficient connectivity. If $N_{RN}^{u\{\min\}} \leq N_{RN} < N_{RN}^{w\{\min\}}$, the weighted random deployment alone will not be able to satisfy the connectivity. In this case, the hybrid deployment tries to maximize the system lifetime while satisfying the connectivity requirement. To this end, the hybrid deployment is designed in two steps. Firstly, we design the deployment of N_{RN}^{l} RNs to extend the lifetime in a weighted random manner defined by (6.3). Since the connectivity of an SN in the weak connectivity region *B* is less than σ_0, in the second step we arrange the deployment of N_{RN}^{c} RNs exclusively in *B* so as to meet the connectivity requirement everywhere in the network (overall, the RNs in *B* are deployed uniformly when the RNs deployed in the two steps are combined together). The number of RNs deployed in the

two steps should be equal to the given number N_{RN}. We next study how N_{RN} should be optimally split between N_{RN}^{l} and N_{RN}^{c}.

Allocation of RNs for the two steps is a constrained optimization problem. As N_{RN}^{l} increases, N_{RN}^{c} has to be decreased. However, if N_{RN}^{c} is too small, the connectivity of the sparse area of the network is at risk. In the following, we consider an arbitrary $n_{RN}^{l} < N_{RN}$ for the first step. To satisfy the connectivity in region *B*, we derive the number of RNs needed in the second step n_{RN}^{c} (enhance connectivity in region *B*) as a function of n_{RN}^{l}. By summing n_{RN}^{l} and n_{RN}^{c} (function of n_{RN}^{l}), we obtain the total number of RNs n_{RN} as a function of n_{RN}^{l}. We prove that n_{RN} is a non-decreasing function of n_{RN}^{l}. Therefore, we can easily solve for N_{RN}^{l} for a given N_{RN} numerically.

Assume that n_{RN}^{l} RNs have been deployed according to (6.3). We define the RN density at a position (d,θ) as the product of the number of RNs deployed and the density function $f(d,\theta)$. To make the connectivity in *B* meet the minimum requirement, the RN density in *B* should be leveled up to the RN density level of points (d_0,θ) on the boundary of *B*. The number of RNs needed in the second step is

$$n_{RN}^{c} = \left| \int_{B} \left(n_{RN}^{l} \cdot f(d_0,v) - n_{RN}^{l} \cdot f(u,v) \right) u\,du\,dv \right| \tag{6.10}$$

Plugging (6.3) into (6.10), we have

$$n_{RN}^{c} = \left| \frac{ngl\alpha_2 n_{RN}^{l}}{D} \int_{B} \left(d_0^{m} - u^{m} \right) u\,du\,dv \right| \tag{6.11}$$

Summing n_{RN}^{l} and n_{RN}^{c}, the total number of RNs deployed is

$$n_{RN} = n_{RN}^{l} + \left\lceil \frac{ngl\alpha_2 n_{RN}^{l}}{D} \int_{B} \left(d_0^m - u^m\right) u du dv \right\rceil \tag{6.12}$$

Lemma 1: n_{RN} is an non-decreasing function of n_{RN}^{l}.

Proof: Pick two integer numbers n_{RN}^{l1} and n_{RN}^{l2} where $n_{RN}^{l1} < n_{RN}^{l2}$. Consider two deployments in which n_{RN}^{l1} and n_{RN}^{l2} RNs are deployed in the first step, respectively. We have the following cases:

(1) If both deployments satisfy the connectivity requirement, i.e., $n_{RN}^{l2} > n_{RN}^{l1} \geq N_{RN}^{w\{\min\}}$, no RNs are needed for the second step, and the argument holds.

(2) If the first deployment does not meet the connectivity requirement, while the second one does, then $n_{RN}^{c1} \leq N_{RN}^{w\{\min\}} - n_{RN}^{l1} \leq n_{RN}^{l2} - n_{RN}^{l1}$ RNs are needed to be deployed to compensate for the density in the sparse areas, and the argument holds.

(3) If both deployments do not satisfy the connectivity requirement, then deploy n_{RN}^{c1} and n_{RN}^{c2} RNs, respectively, to satisfy the connectivity requirements according to formula (6.11). As illustrated in Figure 6.2, the average number of RNs in the area B_2 (B area for the second deployment) is the same for both deployments as they just meet the connectivity requirement. The number of RNs from the second deployment in the

area B_1 (B area for the first deployment excluding B_2) is more than that from the first deployment since the first deployment just meets the connectivity requirement, and the second deployment provides better connectivity. In the rest of the area, the number of RNs is determined by the first step of each deployment only and the first deployment will have fewer RNs. Summing the numbers of RNs in the three parts, the argument holds. ■

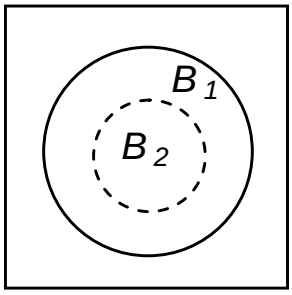

B_2 represents the area to be compensated in the second phase of both deployments. B_1, which does not include B_2, denotes the area that is only compensated in the second phase of the first deployment.

Figure 6.2 Comparison of two deployments

In the second step, $N_{RN}^{c} = N_{RN} - N_{RN}^{l}$ RNs will be deployed in the region B according to the density function in Eq.(6.13),

$$g(d,\theta) = \begin{cases} \dfrac{f(d_0,\theta) - f(d,\theta)}{\int_B (f(d_0,\theta) - f(u,v))\,du\,dv} & \text{if } (d,\theta) \in B \\ 0 & \text{otherwise} \end{cases} \tag{6.13}$$

After the second step, the RN density becomes uniform everywhere in B and the connectivity is satisfied everywhere. Finally, the overall deployment density function for one-time deployment can be written as

$$h(d,\theta) = \begin{cases} \dfrac{f(d_0,\theta)}{f(d_0,\theta)|B| + \int_{A-B} f(u,v)\,du\,dv} & \text{if } (d,\theta) \in B \\ \dfrac{f(d,\theta)}{f(d_0,\theta)|B| + \int_{A-B} f(u,v)\,du\,dv} & \text{if } (d,\theta) \in A - B \end{cases} \tag{6.14}$$

6.2. Random Deployment Strategies in Multi-hop Communication Case

In this part, we study the three random deployment strategies with the multi-hop communication model.

6.2.1. Connectivity-Oriented Deployment

The connectivity-oriented deployment in the multi-hop communication case is the same as the one in the single-hop case, in terms of the density function and connectivity property. It suffers fundamentally from an energy efficiency perspective due to the BECR phenomenon.

6.2.2. Lifetime-Oriented Deployment

Due to the aggregation effect of traffic relaying in the multi-hop communication model, deriving an optimal density function is more challenging than in the single-hop case. We present a derivation of a heuristic sub-optimal deployment density function. We show that the lifetime is increased by up to more than 3 times by using the heuristic weighted deployment compared to the uniform deployment in our experimental setup. We first consider a circular sensing field of radius R, with the BS fixed at the center. We discuss how to extend the methodology to an arbitrary convex sensing field in Section 6.4.

The average deployment density in a given area should depend on two factors, namely the average total energy consumption rate in the area and the size of the area. The energy consumption rate of an area is the total energy consumed by RNs in the area per round of

data collection. To overcome the BECR problem, the average density over an area should be proportional to the energy consumption rate and inversely proportional to the size of the area. For example, in Figure 6.3, consider two arbitrary shells, B_1 and B_2, with the BS at the center. The size of B_1 is larger than that of B_2. Due to the BECR phenomenon, suppose that RNs in B_1 and B_2 have the same energy consumption per round. Then B_2 should have higher deployment density so that the expected numbers of RNs are the same in the two areas.

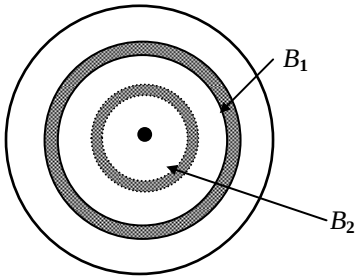

Figure 6.3 A sensing site: the density function is proportional to the energy consumption rate, and is inversely proportional to the size of areas.

We therefore define the *Energy Consumption Intensity* (ECI) of an area as the ratio of the energy consumption rate of the area to the size of the area. For an arbitrary point (d,θ) and a small positive value ε, we can form a disk of radius ε with (d,θ) at the center. We define the ECI of position (d,θ), i.e., $\mathrm{ECI}(d,\theta)$ as the limit of the ECI of the disk as ε goes to 0. In fact, as the traffic is symmetric with respect to the BS, $\mathrm{ECI}(d,\theta)$ does not depend on θ. The concept of $\mathrm{ECI}(d,\theta)$ is the basis for deriving the weighted random deployment density function. The principle is that the density function should be proportional to the ECI at any position.

To obtain the ECI, we next derive the amount of inter-cluster traffic and intra-cluster traffic at different parts of the network. We first define a parameter h_{RN} as $h_{RN} = h * r_{RN}$, where h is between 0 and 1. In Figure 6.4, we construct the shell A_m of width h_{RN} lying between the two dotted circles in the sensing field. The area which is outside of A_m (farther from the BS) is referred to as A_{out}, and the area which is inside of A_m (closer to the BS) is referred to as A_{in}. Three types of traffic relay (between RNs) are of interest, first from A_{out} to A_m, second from A_m to A_m, and third from A_{out} to A_{in} directly. When $h = 1$, the direct relay from A_{out} to A_{in} does not exist and some relay happens from RNs in A_m to other RNs in A_m. As h becomes smaller (the width of the shell decreases), the relay from A_{out} to A_{in} directly becomes more common and so more traffic from RNs in A_{out} will not be relayed by RNs in A_m. At the same time, less traffic from RNs in A_m will be relayed to other RNs in A_m. By empirically choosing the value of h appropriately, the amount of traffic relayed from A_{out} to A_{in} directly and the amount of traffic relayed between RNs inside the shell A_m are largely cancelled out by each other. In such a case, we can approximate the volume of inter-cluster traffic relayed by RNs in the shell A_m by all traffic generated by RNs in A_{out}. We will explore the optimal value of h in Section 6.3. Also, the average intra-cluster traffic volume handled by the RNs in any sub-area is proportional to the size of the sub-area under consideration. That is, the intra-cluster traffic handled by RNs in the shell A_m is the traffic originated by SNs located in the same shell. Following the same logic, the relay traffic transmitted from A_{out} to A_m is the sum of the aggregated traffic generated by SNs in A_{out}. The approximations on the inter-cluster and intra-cluster traffic volume of the shell A_m are the basis for the following derivation.

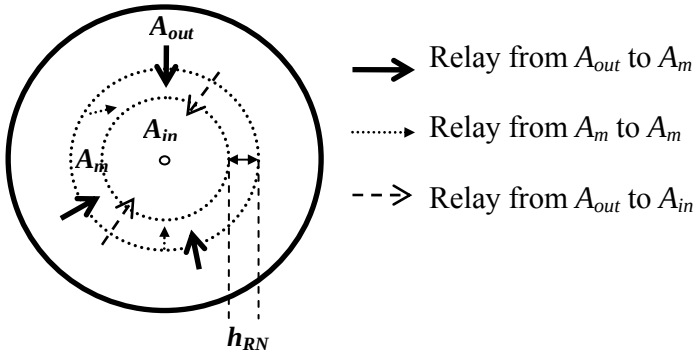

Figure 6.4 The physical meaning of the effective radius of RNs

With h_{RN}, we partition a sensing field with radius R into three areas as shown in Figure 6.5. The part which is surrounded by the inner broken circle of radius r_{RN} is the first area, denoted by A_1. In this area, an RN is able to transmit to the BS in one hop. The shell between the two broken circles of radius of R-h_{RN} and r_{RN} respectively, is the second area, denoted by A_2. In this area, traffic is relayed from far to near. The remaining part, which is between the bounding solid circle of radius R and the broken circle of radius R-h_{RN} , is the third area, denoted by A_3. The inter-cluster relay traffic is negligible in area A_3. The three areas are defined as,

$$A_1 = \{(d,\theta) \mid 0 \le d \le \min(r_{RN}, R), 0 \le \theta \le 2\pi\} \tag{6.15}$$

$$A_2 = \begin{cases} \{(d,\theta) \mid r_{RN} < d \le R - h_{RN}, 0 \le \theta \le 2\pi\} & \text{if } R > r_{RN} + h_{RN} \\ \phi & \text{otherwise} \end{cases} \tag{6.16}$$

$$A_3 = \begin{cases} \{(d,\theta) \mid \max(r_{RN}, R - h_{RN}) < d \le R, 0 \le \theta \le 2\pi\} & \text{if } R > r_{RN} \\ \phi & \text{otherwise} \end{cases} \tag{6.17}$$

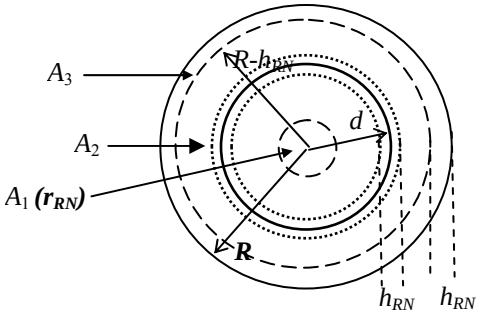

Figure 6.5 Partitioning of a sensing site

Note that, if $R \le r_{RN}$, A_2 and A_3 shrink to null sets, and if $r_{RN} < R \le h_{RN} + r_{RN}$, A_2 shrinks to a null set. Without loss of generality, we consider the case where $R > h_{RN} + r_{RN}$. The other two cases are easily addressed following the same line of logic.

In A_1, the expected number of SNs is $N_{SN} r_{RN}^2 / R^2$. Substituting for n in (3.7), the expected total energy spent on intra-cluster communication by all RNs in A_1 is

$$E_{\text{intra}}^{(1)} = \left(c_1 + g\alpha_2 r_{RN}^m\right) N_{SN} l r_{RN}^2 / R^2 \tag{6.18}$$

All traffic generated by SNs outside of A_1 must be relayed by a RN in A_1 to reach the BS. The expected traffic relayed by RNs in A_1 is $gN_{SN} l(R^2 - r_{RN}^2)/R^2$. Substituting for l_{relay} in (3.8), the expected total energy spent on inter-cluster relay by RNs in A_1 is

$$E_{\text{inter}}^{(1)} = c_2 g N_{SN} l(R^2 - r_{RN}^2)/R^2 \tag{6.19}$$

We make the approximation that the ECI at any position (d,θ) in A_1 is the same and so is given by

$$\mathrm{ECI}^{(1)}(d,\theta)=\left(\frac{E_{\mathrm{intra}}{}^{(1)}+E_{\mathrm{inter}}{}^{(1)}}{\pi r_{RN}^2}\right)=\frac{N_{SN}l}{\pi R^2}\left(c_1+g\alpha_2 r_{RN}^m+c_2 g\left(\frac{R^2}{r_{RN}^2}-1\right)\right) \tag{6.20}$$

The integral of $\mathrm{ECI}^{(1)}(d,\theta)$ over A_1, denoted by $J^{(1)}$, is

$$J^{(1)}=\frac{N_{SN}l}{R^2}\left(c_1 r_{RN}^2+g\alpha_2 r_{RN}^{2+m}+c_2 g\left(R^2-r_{RN}^2\right)\right) \tag{6.21}$$

In A_2, the ECI at different positions might be largely differentiated, as RNs at different positions relay different amounts of traffic. We propose to approximate the ECI at point (d,θ) by the ECI of the shell between the two dotted circles of radius *(d - h_{RN} /2)* and *(d +h_{RN} /2)* (see Figure 6.5), which is calculated as the sum of the energy consumption for intra-cluster communication, $E_{\mathrm{intra}}{}^{(2)}(d)$ and the energy consumption for the inter-cluster relay, $E_{\mathrm{inter}}{}^{(2)}(d)$, by RNs in the shell, divided by the size of the shell, i.e.,

$$\mathrm{ECI}^{(2)}(d,\theta)=\left(\frac{E_{\mathrm{intra}}{}^{(2)}(d)+E_{\mathrm{inter}}{}^{(2)}(d)}{\pi\left(\left(d+h_{RN}/2\right)^2-\left(d-h_{RN}/2\right)^2\right)}\right) \tag{6.22}$$

Similar to (6.18), the energy consumption for intra-cluster traffic in the shell for each round of data collection is approximated as

$$E_{\mathrm{intra}}{}^{(2)}(d)=\frac{2\left(c_1+g\alpha_2 r_{RN}^m\right)N_{SN}ldh_{RN}}{R^2} \tag{6.23}$$

The energy consumption for inter-cluster traffic in the shell for each round of data collection can be approximated by

$$E_{\text{inter}}{}^{(2)}(d) = c_2 g N_{SN} l \left(\frac{R^2 - (d + h_{RN}/2)^2}{R^2} \right) \tag{6.24}$$

Plugging (6.23) and (6.24) into (6.22), we have,

$$\text{ECI}^{(2)}(d,\theta) = \frac{N_{SN} l}{\pi R^2} \left[c_1 + g\alpha_2 r_{RN}^m + \frac{c_2 g}{2dh_{RN}} \left(R^2 - \left(d + \frac{h_{RN}}{2} \right)^2 \right) \right] \tag{6.25}$$

The integral of $\text{ECI}^{(2)}(d,\theta)$ over A_2, denoted by $J^{(2)}$, is

$$J^{(2)} = \frac{N_{SN} l}{R^2} \left[\begin{array}{l} \left(c_1 + g\alpha_2 r_{RN}^m \right) \left((R - h_{RN})^2 - r_{RN}^2 \right) \\ + c_2 g \left(R^2 \left(R - h_{RN} - r_{RN} \right) + \dfrac{\left(2r_{RN} + h_{RN} \right)^3 - \left(2R - h_{RN} \right)^3}{24} \right) \end{array} \right] \tag{6.26}$$

For A_3, the traffic of inter-cluster relaying is negligible. Similar to A_1, the ECI at any position (d,θ) in A_3 is

$$\text{ECI}^{(3)}(d,\theta) = \frac{\left(c_1 + g\alpha_2 r_{RN}^m \right) N_{SN} l}{\pi R^2} \tag{6.27}$$

The integral of $\text{ECI}^{(3)}(d,\theta)$ over A_3, denoted by $J^{(3)}$, is

$$J^{(3)} = \frac{\left(c_1 + g\alpha_2 r_{RN}^m \right) N_{SN} l (2R - h_{RN}) h_{RN}}{R^2} \tag{6.28}$$

Let $J = J^{(1)} + J^{(2)} + J^{(3)}$. We propose the density function for the three areas as follows.

$$f(d,\theta) = \begin{cases} \text{ECI}^{(1)}(d,\theta)/J, & \text{if } (d,\theta) \in A_1 \\ \text{ECI}^{(2)}(d,\theta)/J, & \text{if } (d,\theta) \in A_2 \\ \text{ECI}^{(3)}(d,\theta)/J & \text{if } (d,\theta) \in A_3 \end{cases} \tag{6.29}$$

In the following, we discuss the properties of the deployment density in (6.29) in terms of connectivity. If N_{RN} RNs are deployed according to the density function in (6.29), we use (6.5) to approximate the probability that an SN, at point (d,θ), can reach one or more RNs in one hop. For an SN whose transmission disk is in A_i, for i = 1, 2, 3, the connectivity probability is

$$p_R^{(i)}(d,\theta) = 1 - \left(1 - \pi r_{SN}^2 \mathrm{ECI}^{(i)}(d,\theta)/J\right)^{N_{RN}} \tag{6.30}$$

In A_1, if a connectivity probability σ_0 is required, letting $p_R^{(1)}(d,\theta) = \sigma_0$ and solving for N_{RN}, we have

$$N_{RN}^{w\{\min 1\}} = \ln(1-\sigma_0)/\ln\left(1 - \pi r_{SN}^2 \mathrm{ECI}^{(1)}(d,\theta)/J\right) \tag{6.31}$$

If $N_{RN} \geq N_{RN}^{w\{\min 1\}}$, the deployment according to (6.29) will be able to meet the connectivity requirement in A_1.

Now, $p_R^{(2)}(d,\theta)$ is a decreasing function in [r_{RN}, R-h_{RN}]. Thus, an SN at distance R-h_{RN} has the least connectivity probability, $p_R^{(2)}(R-h_{RN},\theta)$, while an SN at distance r_{RN} from the BS has the highest connectivity probability, $p_R^{(2)}(r_{RN},\theta)$. Following (6.31), we set

$$N_{RN}^{w\{\min 2\}} = \ln(1-\sigma_0)/\ln\left(1 - \pi r_{SN}^2 \mathrm{ECI}^{(2)}(R-h_{RN},\theta)/J\right) \tag{6.32}$$

$$N_{RN}^{w\{\min 2-\}} = \ln(1-\sigma_0)/\ln\left(1 - \pi r_{SN}^2 \mathrm{ECI}^{(2)}(r_{RN},\theta)/J\right) \tag{6.33}$$

If $N_{RN} < N_{RN}^{w\{\min 2-\}}$, the deployment according to (6.29) will not be able to meet the connectivity requirement anywhere in A_2 while if $N_{RN} \geq N_{RN}^{w\{\min 2\}}$, the connectivity requirement is met everywhere in A_2. If $N_{RN}^{w\{\min 2-\}} \leq N_{RN} < N_{RN}^{w\{\min 2\}}$, the connectivity requirement is only partially met in A_2. In this case, letting $p_R^{(2)}(d,\theta) = \sigma_0$, we can solve for d using Newton's method since $p_R^{(2)}(d,\theta)$ is a decreasing function of d on $[r_{RN}, R\text{-}h_{RN}]$. The solution d_0 defines a cutoff distance inside the sensing area A_2. We define the region B as

$$B = \{(d,\theta) \mid d_0 < d \leq R - h_{RN}\} \tag{6.34}$$

In the region B, the connectivity probability of an SN is less than σ_0 while in A_2 - B, an SN has connectivity probability at least σ_0. The cutoff circle and region B (tinted area) are illustrated in Figure 6.6.

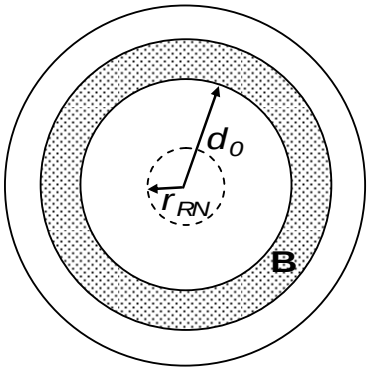

Figure 6.6 The connectivity in B is not satisfied

For A_3, we similarly define

$$N_{RN}^{w\{\min 3\}} = \ln(1-\sigma_0)/\ln\left(1-\pi r_{SN}^2 \mathrm{ECI}^{(3)}(d,\theta)/J\right) \tag{6.35}$$

Then letting $N_{RN}^{w\{\min\}} = \max\{N_{RN}^{w\{\min 1\}}, N_{RN}^{w\{\min 2\}}, N_{RN}^{w\{\min 3\}}\}$, if $N_{RN} \geq N_{RN}^{w\{\min\}}$ the connectivity of SNs is satisfied everywhere in the network.

6.2.3. Hybrid Deployment

For the same reason as stated in Section 6.1.3, we design a hybrid deployment for the multi-hop communication case. As in Section 6.1.3, the hybrid deployment is designed in two steps, where allocation of RNs for the two steps is a constrained optimization problem: as N_{RN}^{l} increases, N_{RN}^{c} has to be decreased. We next derive n_{RN}^{c} as a function of n_{RN}^{l}. In the set A_1, the number of RNs needed is

$$n_{RN}^{c1} = \max\left(0, \ln(1-\sigma_0)/\ln(1-r_{SN}^2/r_{RN}^2) - n_{RN}^{l} J^{(1)}/J\right) \tag{6.36}$$

Similarly, in A_3, the number needed is

$$n_{RN}^{c3} = \max\left(0, \ln(1-\sigma_0)/\ln(1-r_{SN}^2/(2Rh_{RN} - h_{RN}^2)) - n_{RN}^{l} J^{(3)}/J\right) \tag{6.37}$$

For the set A_2, we examine the compensation deployment in two cases. The first case is $N_{RN}^{w\{\min 2-\}} \leq N_{RN} < N_{RN}^{w\{\min 2\}}$ and the second case is $N_{RN} < N_{RN}^{w\{\min 2-\}}$. In the first case, the connectivity is partially satisfied in A_2. We define the RN density at a position (d,θ) as the product of the number of RNs deployed and the density function $f(d,\theta)$. To make the connectivity in the set B in (6.34) meet the minimum requirement, the RN density in B should be leveled up to the RN density level of points (d_0,θ) on the boundary of B. The number of RNs needed in the second step is

$$n_{RN}^{c2} = \left\lceil \int_B \left(n_{RN}^{l} \cdot f(d_0, v) - n_{RN}^{l} \cdot f(u, v) \right) u \, du \, dv \right\rceil \tag{6.38}$$

Plugging (6.22) and (6.29) into (6.38), we have

$$n_{RN}^{c2} = \left\lceil \begin{array}{l} \dfrac{c_2 g n_{RN}^{l} N_{SN} l}{R^2 J h_{RN}} \left(\dfrac{((R-h_{RN})^2 - d_0^2)(R^2 - (d_0 + h_{RN}/2)^2)}{2d_0} \right) - \\ \dfrac{c_2 g n_{RN}^{l} N_{SN} l}{R^2 J h_{RN}} \left(R^2 (R - h_{RN} - d_0) + \dfrac{(2d_0 + h_{RN})^3 - (2R - h_{RN})^3}{24} \right) \end{array} \right\rceil \tag{6.39-1}$$

In the second case, the connectivity is not satisfied anywhere in A_2. The number of RNs in the second step is

$$n_{RN}^{c2} = \left\lceil \left(N_{RN}^{u\{\min\}} - n_{RN}^{l} \right) \frac{\left((R - h_{RN})^2 - r_{RN}^2 \right)}{R^2} \right\rceil \tag{6.39-2}$$

Summing n_{RN}^{l} and n_{RN}^{ci}, the total number of RNs deployed is $n_{RN} = n_{RN}^{l} + n_{RN}^{c1} + n_{RN}^{c2} + n_{RN}^{c3}$.

Lemma 2: n_{RN} is a non-decreasing function of n_{RN}^{l}.

Proof: Pick two integers n_{RN}^{l1} and n_{RN}^{l2} where $n_{RN}^{l1} > n_{RN}^{l2}$. Consider two deployments in which n_{RN}^{l1} and n_{RN}^{l2} CHs are deployed in the first step, respectively. We have the following cases:

(1) If both deployments satisfy the connectivity requirement, i.e., $n_{RN}^{l1} > n_{RN}^{l2} \geq N_{RN}^{w\{\min\}}$, then no RNs are needed for the second step, and the argument holds.

(2) If the second deployment does not meet the connectivity requirement, while the first one does, then $n_{RN}^{c2} \leq N_{RN}^{w\{\min\}} - n_{RN}^{l2} \leq n_{RN}^{l1} - n_{RN}^{l2}$ RNs are needed to be deployed to compensate for the density in the sparse areas, and the argument holds.

(3) If both deployments do not satisfy the connectivity requirement, then deploy n_{RN}^{c1} and n_{RN}^{c2} RNs, respectively, to satisfy the connectivity requirements according to formulas (6.36), (6.37) and (6.39). As illustrated in Figure 6.7, a sensing field is partitioned into A_1, A_2 and A_3 as in Section 6.2.2 (see (6.15)-(6.17) and Figure 6.5). The area A_2 is further cut into three parts B_1, B_2, and B_3, where B_1 is the B area for the first deployment (Eq. (6.34)), B_1 and B_2 together are the B area for the second deployment, and B_3 is the rest of A_2. The expected number of RNs in B_1 is the same for both deployments since both deployments just meet the connectivity requirement. The expected number of RNs in B_2 of the first deployment is not less than that of the second deployment because the second deployment just meets the connectivity requirement while the first one provides better connectivity. The expected number of RNs in B_3 of the first deployment is again not less than that of the second deployment as both deployments provide good connectivity in the first place and $n_{RN}^{l1} > n_{RN}^{l2}$. For a similar reason, the expected number of RNs in the area

A_1 and A_3 of the first deployment is not less than that of the second deployment. Summing the numbers of RNs in all parts, the argument holds. ■

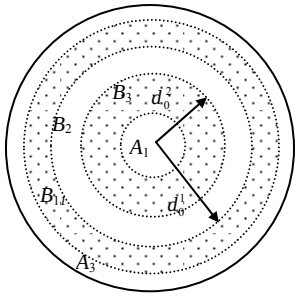

Figure 6.7 Comparison of two hybrid deployments

For the compensation deployment, the number of RNs for each part can be calculated using formulas (6.36), (6.37) and (6.39). The density function for areas A_1 and A_3 is uniform. The density function for the region B in A_2 in the first case is

$$g(d,\theta) = \frac{f(d_0,\theta) - f(d,\theta)}{\int_0^{2\pi} \int_{d_0}^{R-h_{RN}} (f(d_0,\theta) - f(u,v))\,u\,du\,dv} \tag{6.40-1}$$

In the second case, the density function for all of A_2 is

$$g(d,\theta) = \frac{N_{RN}^{u\{\min\}} / \pi R^2 - n_{RN}^l f(d,\theta)}{\int_0^{2\pi} \int_{d_0}^{R-h_{RN}} (N_{RN}^{u\{\min\}} / \pi R^2 - n_{RN}^l f(u,v))\,u\,du\,dv} \tag{6.40-2}$$

After the second step, the RN density becomes uniform everywhere in B and the connectivity is satisfied everywhere.

6.3. Performance Evaluation

In this section, we will evaluate the three deployment strategies using simulations. We are interested in the energy utilization and the system lifetime of the different deployment strategies. Therefore, two metrics are used to measure the performance. The first is the utilization of energy in the system, i.e., the ratio of the total consumed energy of RNs to the total initial energy. The other metric, denoted by Normalized DCR, is the number of data collection rounds normalized to the initial energy of a RN (the unit is Joul) before the network lifetime expires.

As RNs are densely deployed, energy is wasted if all of them work simultaneously. A clustering algorithm is used to select CHs from redundant RNs, so that some RNs can connect all SNs while other RNs go to sleep. Most existing clustering algorithms are designed for homogenous networks and they assign the role of CH to identical nodes in rotation [104, 122, 124, 125, 126]. Such schemes cannot be directly applied or extended to the case of heterogeneous networks. To conduct a convincing performance evaluation and a fair comparison of the deployment strategies, we propose a simple and effective idealized clustering scheme for heterogeneous WSNs.

6.3.1. Clustering Scheme

Assuming every RN sets up a neighboring SN table upon initialization, the operation of our scheme is briefly described as follows:

a) An RN is elected as a CH if it covers the most uncovered SNs, and it broadcasts an ADVERTISEMENT message to its neighboring RNs.

b) An RN goes to sleep if all of its neighboring SNs are covered by active CHs (known from the ADVERTISEMENT messages).
c) A CH keeps functioning until its energy is exhausted. In this case, the clustering scheme is locally invoked to select other CHs. The election gives preference to the RNs which cover the most uncovered SNs.
d) Depleted RNs will not be involved in any further operations.

The scheme has the following desirable properties. First, it ensures that each SN is able to reach a CH, unless all neighboring RNs are out of energy. Second, the clustering scheme tries to minimize the number of CHs. Third, the CH duty cycle is rotated in an on-demand manner. Only a CH which is going out of energy needs to invoke a local CH selection procedure.

After CHs have been locally selected in the network to connect SNs directly, the CHs execute the Bellman-Ford algorithm to set up the paths to the BS. For simplicity we use a constant link cost so shortest paths correspond to minimum hop paths. If there are two or more shortest paths to the BS, the one with less traffic is chosen.

6.3.2. Simulation Setup

We simulate a WSN of 10,000 SNs on a disk sensing field with radius 500m, in which the BS is located at the center. The parameters used in the simulations are listed in Table 6.1. Therein, σ_0 is calculated to ensure (with probability greater than 0.9999) that the

ratio of total connected SNs in an initial deployment is not less than *q*. All experimental results presented are the average of 30 runs.

Table 6.1 The parameters of the simulated WSN

α_1	50e-9 (J/bit)	m	2
α_2	10e-12 (J/bit/m^2)	g	0.2
β	50e-9 (J/bit)	γ	1e-12 (J/bit)
N_{SN}	10,000	R	500 (m)
r_{RN}	90 (m)	r_{SN}	30 (m)
q	0.8	σ_0	0.84
l	2000 (bits)		

6.3.3. Comparison of Deployment Strategies in the Single-hop Case

In this section, we explore and compare the performance of the three strategies in the single-hop communication case, as derived in Section 6.1. The three strategies are conducted on the same network while N_{RN} varies from 450 to 4000. The minimum numbers of RNs required to guarantee connectivity with a high probability (beyond 0.9999) in the connectivity-oriented deployment and the lifetime-oriented deployment are 509 (Eq. 9) and 2630 (Eq. 16), respectively. Figure 6.8 and Figure 6.9 present, respectively, the average energy utilization and system lifetime (Normalized DCR) by using the three strategies.

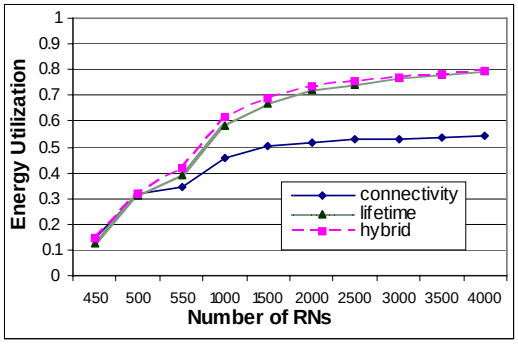

Figure 6.8 Comparison of three deployment strategies by energy utilization in the single-hop case

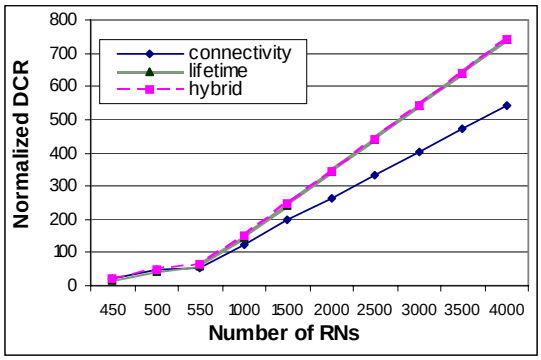

Figure 6.9 Comparison of three deployment strategies by DCR in the single-hop case

As can be seen in Figure 6.8 and Figure 6.9, the hybrid deployment strategy performs uniformly better than the connectivity-oriented deployment in terms of both energy utilization and normalized system lifetime, while its performance is also better, though quite similar to, that of the lifetime-oriented deployment strategy. For the connectivity-oriented deployment, when N_{RN} = 450, the energy utilization is only 14% and the DCR is only 21. The energy utilization climbs up to 32%, 34%, 45%, and 50% when N_{RN} increases to 500, 550, 1000, and 1500 respectively. Correspondingly, the normalized DCR increases to 49, 56, 124 and 196. After that, the growth of energy utilization becomes much slower as the number of RNs increases. The energy utilization reaches 54% when N_{RN} = 4000.

In our experiments, when N_{RN} is small, the lifetime-oriented deployment provides shorter lifetime and lower energy utilization than the connectivity-oriented deployment, since it provides only weak connectivity in the part of the sensing field nearer to the BS. For example, when N_{RN} = 450, in the 30 runs the connectivity is so poor in some cases that the deployment does not function at all. On the other hand, one should perhaps not expect improved energy utilization or extended system lifetime when the number of deployed sensors cannot even provide the desired connectivity using the connectivity-oriented deployment. When the number of RNs gets larger, the lifetime-oriented deployment enjoys fast performance improvement and outperforms the connectivity-oriented strategy on both lifetime and energy utilization. When N_{RN} = 4000, the lifetime-oriented deployment provides a normalized DCR lifetime of 741 and energy utilization of 79%, compared with a normalized DCR of 543 and energy utilization of 54% in case of the connectivity-oriented deployment. Both measurements are improved by more than 35%. Of course, using the lifetime-oriented deployment the desired connectivity is not achieved until at least 2630 RNs are deployed.

In these experiments the hybrid deployment is the preferred deployment strategy of the three, as it provides both energy efficiency and lifetime extension at least as good as that provided by the lifetime-oriented deployment, while also satisfying the connectivity requirement whenever the connectivity-oriented deployment does so. When $N_{RN} \leq 509$, the hybrid deployment is equal to the connectivity-oriented deployment as the number of RNs allocated for the first step will be 0. All RNs are used to meet the minimal

connectivity (Section 6.1.3). When $509 < N_{RN} < 2630$, the hybrid deployment provides better performance than the lifetime-oriented deployment since it reconciles the needs of lifetime extension and connectivity. The advantage becomes less significant as N_{RN} increases due to the fact that the connectivity issue becomes a less serious problem as N_{RN} approaches 2630. When $N_{RN} > 2630$, the hybrid deployment is reduced to the lifetime-oriented deployment.

We remark that, for all the deployment strategies, the energy utilization appears to approach a saturation level as the number of RNs increases, while the normalized DCR grows approximately linearly. Under this observation, the performance of the connectivity-oriented deployment can be characterized as having a lower energy utilization saturation level and a smaller DCR growth slope compared to the lifetime-oriented or hybrid deployment performance curves. The energy wastage from the connectivity-oriented deployment, exemplified by its low energy utilization saturation level, is due to the BECR problem.

6.3.4. Comparison of Deployment Strategies in the Multi-hop Case

The derivation of the lifetime-oriented deployment in Section 6.2.2 depends on an ad hoc parameter h. We first investigate how this design parameter affects the performance of the lifetime-oriented deployment strategy and determine the best value for the simulation setup above. We then present and discuss some simulation results on the performance of the three deployment strategies.

6.3.4.1. Impact of the Parameter h

We implement the lifetime-oriented deployment strategy using different values of *h* from 0.4 to 1.0. To make the comparison fair and effective, the number of RNs to be deployed is set to 2500, which is greater than $N_{RN}^{w\{\min\}}$ for all cases ($N_{RN}^{w\{\min\}}$ is a function of *h*). In other words, with 2500 RNs deployed by the weighted density function, the connectivity requirement is satisfied for all cases. The results are presented in Figure 6.10.

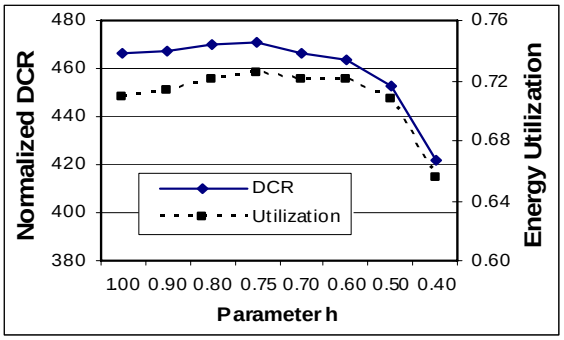

Figure 6.10 Comparison of the lifetime-oriented deployments with different *h* by energy utilization and DCR

The results for both the energy utilization and the system lifetime (Normalized DCR) indicate the same trend. First of all, the weighted random deployment performs the best at $h = 0.75$ for the given setup. Generally speaking, the performance varies slightly when *h* is between 0.6 and 1. From 0.75 to 1, the performance of the weighted random deployment degrades gradually as *h* increases. From 0.75 to 0.40, the performance degrades as *h* decreases and the drop accelerates for $h \leq 0.5$. We expect that the drop will continue as *h* decreases further. In the experiments which follow, we always use $h = 0.75$ for the weighted random strategy and corresponding hybrid strategy.

6.3.4.2. Comparison of Deployment Strategies

In this section, we explore and compare the performance of each of the strategies from Section 6.2. Some key properties of the connectivity-oriented deployment and the weighted deployment (when h = 0.75) are given in Table 6.2. Each of the three strategies is always implemented on the same network and we increase N_{RN} from 509 to 3000. (According to (6.2), if the number of RNs is less than 509, none of the strategies can provide a fully functioning network upon startup with high probability.)

Table 6.2 Key properties of deployment strategies.

$N_{RN}^{u\{\min\}}$	509	$N_{RN}^{w\{\min 1\}}$	98
$N_{RN}^{w\{\min 2\}}$	1181	$N_{RN}^{w\{\min 3\}}$	1495

Figure 6.11 and Figure 6.12 present the results for the average energy utilization and Normalized DCR by using the three strategies.

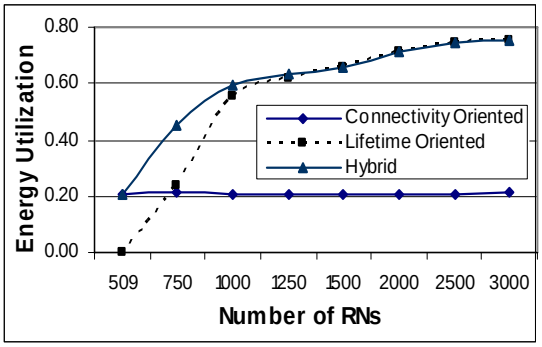

Figure 6.11 Comparison of three deployment strategies by energy utilization in the multi-hop case

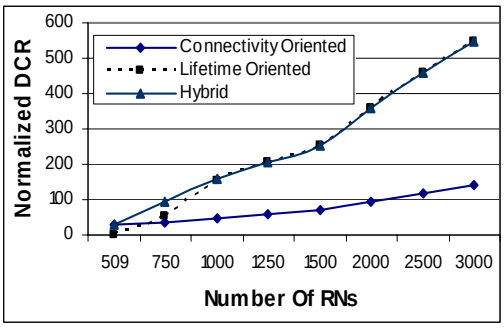

Figure 6.12 Comparison of three deployment strategies by DCR in the multi-hop case

For the connectivity-oriented deployment, the energy utilization is almost unchanged at around 21% as the number of RNs increases from 509 to 3000. The energy wastage due to the BECR problem is clearly exemplified. The Normalized DCR does increase, in an approximately linear fashion, as the number of RNs increases, though the increase is slow relative to the other strategies. The overall poor performance of the connectivity-oriented deployment illustrates the critical importance of the RNs closer to the BS when using multi-hop transmission.

In contrast, since the weighted density function reflects the energy consumption at different locations, not only from the local traffic, but also from the traffic relayed from far to near, the lifetime-oriented deployment exhibits much better performance as N_{RN} increases. The energy utilization increases rapidly from 24% when N_{RN} = 750 to 66% when N_{RN} = 1500. The rate of increase becomes less when N_{RN} > 1500 and reaches 75% when N_{RN} = 3000. Its benefits to the Normalized DCR are better realized when N_{RN} is larger and the connectivity is provided with high probability. As a result, the Normalized DCR increases much faster than for the connectivity-oriented deployment as N_{RN} gets larger. When N_{RN} = 3000, the utilization of the lifetime-oriented deployment is more than

three times of that of the connectivity-oriented deployment, and similarly for the Normalized DCR. However, when N_{RN} = 509, the deployment according to the weighted random density function cannot satisfy the connectivity requirement, and the initial network is unusable.

As in the single-hop case, the hybrid deployment is the preferred deployment strategy of the three. When N_{RN} = 509, the hybrid deployment is equal to the connectivity-oriented deployment as the number of RNs allocated for the first step is 0. In this case all RNs are used to meet the minimal connectivity (Section 6.2.3). When 509 < N_{RN} < 1500, the hybrid deployment provides better performance than the lifetime-oriented deployment since it reconciles the needs of lifetime extension with the connectivity. The advantage becomes less significant as N_{RN} increases due to the fact that the connectivity issue becomes a less serious problem as N_{RN} approaches $N_{RN}^{w\{\min\}}$ = 1495. When $N_{RN} > N_{RN}^{w\{\min\}}$, there is no difference between the hybrid deployment and lifetime-oriented deployment.

The general trend of the weighted density function is that positions farther away from the BS receive less density. It may be that there exist other decreasing functions in a simple form that can provide similar performance. If so, one can avoid going through the derivations of Section 6.2.2. We investigate this by considering two decreasing functions of simple form as optional deployment density functions. We conduct experiments using them and compare the results with those of the weighted density function.

The first is a quadratic density function. Consider a shell of width ε (a small value) at distance d. A quick estimate of the traffic passing by the RNs in the shell is

approximately equal to the traffic generated from SNs farther than d (from the BS). The expected number of SNs whose distance from the BS is equal to or greater than d is proportional to (R^2 - d^2), and so is the traffic volume passing by the shell. We therefore propose a quadratic density function given by

$$f(d,\theta) = \frac{2(R^2 - d^2)}{\pi R^4} \tag{6.41}$$

Another simple function we consider is the linear density function given by

$$f(d,\theta) = \frac{3(R - d)}{\pi R^3} \tag{6.42}$$

We implement the deployment according to the density functions (6.29), (6.41) and (6.42) with 2000, 2500 and 3000 RNs. The density functions are first plotted and compared in Figure 6.13. Results are presented in Figure 6.14 and Figure 6.15.

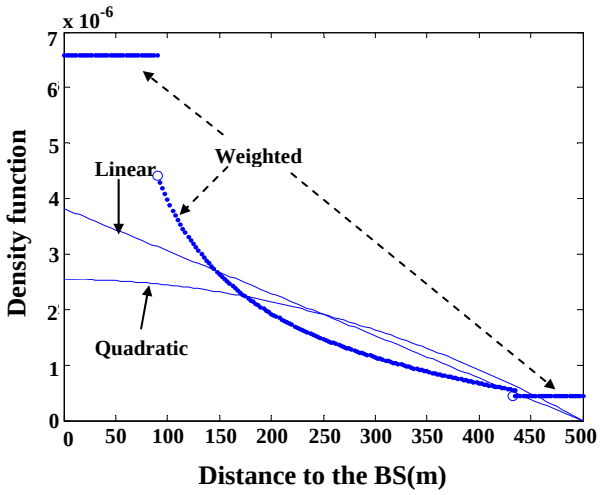

Figure 6.13 Three deployment density functions

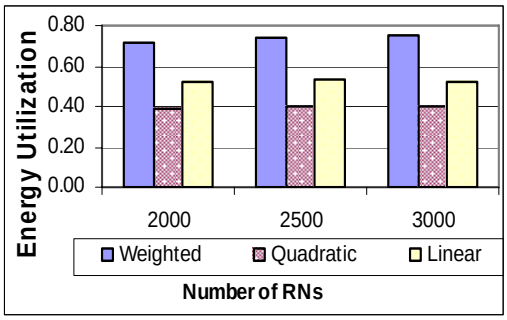

Figure 6.14 Comparison of three density functions by energy utilization

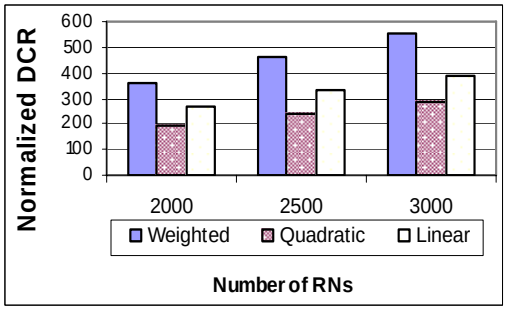

Figure 6.15 Comparison of three density functions by DCR

Generally speaking, the weighted density function given by (6.29) performs the best of the three functions in all cases. Both the linear density function and quadratic function overcome the BECR problem to some degree. However, the performance of the linear function performs always better than the quadratic function. Actually, the formula (6.25), which determines the deployment in A_2 (from radius 90m to 432.5m) is composed of a linear function of d and a inverse function of d. It partially explains the advantage of the linear function over the quadratic function.

6.4. Practical Issues

In this section, we address two practical issues with random deployment strategies. We first discuss how to apply the derivations in Sections 6.1 and 6.2 to a sensing field of a more general shape. We then briefly discuss the implementation of random deployment strategies in practice.

6.4.1. General Sensing Field

We first remark that the validity of the derivations for the deployment strategies in the single-hop communication case is not limited to any particular shape of the sensing field. On the other hand, the derivations in Sections 6.2.2 and 6.2.3 assume a sensing field which is a disk with the BS at the center. However, the method and the derivations can be extended to the case where the sensing field is of arbitrary convex shape and the BS is at an arbitrary position or even outside the sensing field, as long as RNs can be deployed anywhere on the same planar (not restricted to the sensing field). For example, in Figure 6.16(a), SNs are uniformly deployed in a sensing field *S*, represented by the solid irregularly shaped region, and the BS is outside of *S*. In such a case, draw two lines (broken lines in Figure 6.16(a)) from the BS tangent to the boundary of *S*. Thus, we can determine a RN deployment density function for the area surrounded by the irregular curve and the tangent lines, denoted by *S'*, which encompasses the sensing field *S*. We first derive the ECI of each position in *S'*, which indicates the expected energy consumption rate. The overall deployment density function is the ECI divided by the integral of ECI over *S'*.

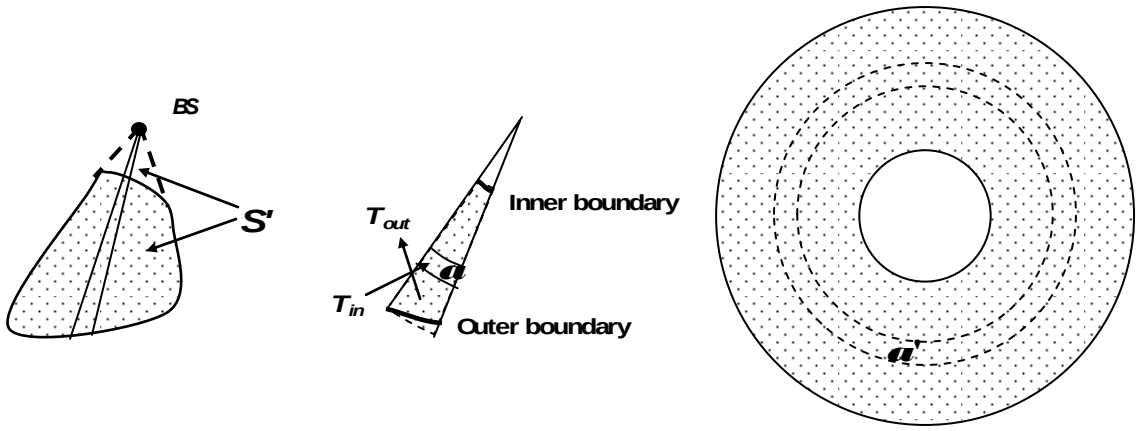

(a) RNs are to be deployed in *S'*. **(b)** A wedge contains a slide out of *S'* **(c)** The wedge is expanded to a full disk.

Figure 6.16 Irregularly shaped sensing site with the BS is outside of it.

To find the ECI function, we start by cutting *S'* into "pie slices" by drawing line segments from the BS to the boundary of *S'* such that in any given slice the points on the same boundary of *S* (there are two boundaries in figure 6.16(b)) are all at a similar distance from the BS. As such, we can approximate the intersection of a slice with *S'* by an arced wedge which just contains the intersection, as magnified in Figure 6.16(b). In order to obtain the ECI for a point *a* in Figure 6.16(b), we first construct a (in-wedge) shell around *a* of width h_{RN} so that *a* has an equal distance to the two sides of the shell, similar to Figure 6.4. The energy consumption of RNs inside the wedge is due to the local intra-cluster traffic, and the inter-cluster traffic from the area which are further away, either inside or outside of the wedge. Note that in practice, traffic inside the wedge would be partially routed through RNs outside the wedge. On the other hand, some traffic outside the wedge will be routed through the RNs in the shell. We argue that these two inverse traffic flows would be largely cancelled out. Therefore, we can approximate that the energy consumption at points in the wedge is due to receiving, transmitting and

relaying information from (some) sensors contained in wedge, but not from sensors outside the wedge. Now imagine expanding the wedge into a disk, as denoted by the dotted circle in Figure 6.16(c). As the traffic amount increases proportionally to the size of the field, in other words, when the wedge is expanded into a full disk, the energy consumption rate and the area are amplified by the same factor. According to the Eqs. (6.18)-(6.27), the ECI of the shell around *a* in Figure 6.16(b) is equal to the ECI of the shell centered at *a'* in Figure 6.16(c) as long as their distances to the BS are the same. As we use the ECI of the shell to approximate the ECI of the point, the ECI at the point *a* in Figure 6.16(b) is the same as the ECI at the point *a'* in Figure 6.16(c) The ECI function as derived in (6.18)-(6.27) in Section 6.2.2 can now be used for the disk in Figure 6.16(c) without modification except for the non-sensing sub area between the *S* area and the BS. For the non-sensing part, the derivation is essentially the same; except that the expected intra-cluster traffic comes from this part is 0.

The hybrid deployment can be further derived once the weighted density function is determined. As the lemma 2 holds for any disk sensing field, we argue it also holds for any wedges, except that the exact number of RNs scales with the angle of the wedge. Therefore, the lemma 2 holds for any convex sensing field which can be seen as a combination of a group of wedges. Therefore, to construct the hybrid deployment density function, we can start from a small n_{RN}^{l} and construct the lifetime-oriented deployment density function, and then evaluate the number of RNs, n_{RN}^{c}, required to compensate for the connectivity and the respective deployment density function. We then increment n_{RN}^{l} iteratively until the sum of n_{RN}^{l} and n_{RN}^{c} is equal to a given number N_{RN}.

To verify this idea, a group of experiments is conducted on a square sensing field. The side length is set to be 886.2 so that the area of the square field is the same as that of the disk field considered in Section 6.3. The BS is fixed at the middle of one edge. All other parameters are kept the same as in Section 6.3. Figure 6.17 and Figure 6.18 present the results of the three strategies. We observe that the performance improvement by the lifetime-oriented deployment and hybrid deployment over the connectivity-oriented deployment is more significant in the case of the square field compared to that in the case of the disk field. This may be due to the greater radial asymmetry of the square and therefore a higher degree of unbalance in the energy consumption rates.

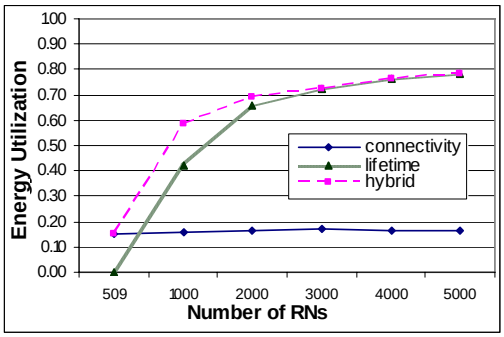

Figure 6.17 Comparison of three deployment strategies by energy utilization with the square sensing field (multi-hop communication)

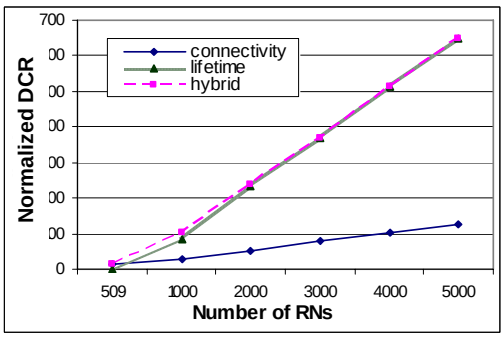

Figure 6.18 Comparison of three deployment strategies by DCR with the square sensing field (multi-hop communication)

6.4.2. Implementation

A few methods can be used in practice to implement random deployment as dictated by a density function. One is a variable rate leaky bucket method. For example, consider a transportation tool used to deploy N_{RN} RNs on a row-by-row basis. The transportation tool will keep track of the integral of the density function over the area it has swiped. If the increment of the integral reaches $1/N_{RN}$, the transportation tool drops one RN. As well, the movement of the RNs in the direction of inertia when traveling from the transportation tool to the sensing field should be taken into consideration. Figure 6.19 demonstrates the variable rate leaky bucket method.

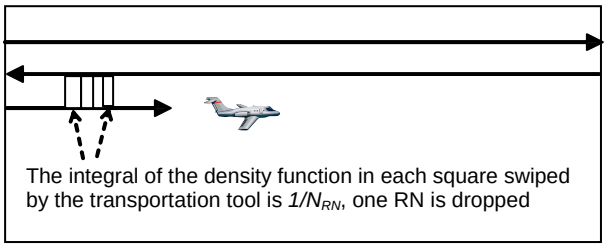

Figure 6.19 An illustration of the variable rate leaky bucket method

6.5. Summary

RN deployment is a fundamental issue in WSNs. The number and positions of RNs determine the usability of a system in terms of connectivity, lifetime, cost, etc. In this chapter, we study the impacts of random RN deployment on connectivity and lifetime in a large-scale heterogeneous WSN. We first examine the BECR problem with the uniform random deployment in both single-hop and multi-hop WSNs. This problem results in low energy utilization of RNs and unnecessarily short system lifetime. To overcome the

BECR problem, we propose two novel deployment strategies for each case, namely, lifetime-oriented deployment and hybrid deployment (balancing connectivity and lifetime goals). The performance study of the deployment strategies shows the new strategies have significant advantages to the connectivity-oriented deployment, which is the only random deployment strategy used in the literature. When the number of RNs is relatively small, the hybrid deployment is the preferred solution as it reconciles the concerns of lifetime with connectivity. When the number of RNs is large, the hybrid deployment is the same as the lifetime deployment, and they both significantly outperform the connectivity-oriented deployment. This chapter provides a guideline for non-deterministic RN deployment of typical large-scale heterogeneous WSNs.

Chapter 7. CONCLUSIONS & FUTURE WORK

7.1. Conclusions

Device deployment is an important engineering problem in implementing WSN applications. The types, numbers, and locations of devices have to be judiciously planned so that performance requirements such as sensing coverage quality, network connectivity, lifetime, and reliability are all met while keeping the cost affordable. This problem is particularly important for large-scale WSN applications, in which a large number of devices will be employed. Due to expensive labour cost, the inaccessibility of the sensing field, and the characteristics of terrain, deliberate placement of devices by humans or machines can be very difficult, or even completely infeasible. In these situations, deployment errors are inevitably incurred in the deployment exercise. As a result, it is necessary to take these deployment errors into consideration when the device deployment plan is conducted. In this thesis, we propose a large-scale WSN deployment framework under which deployment errors are incorporated into the deployment models and the problem formulations. We also propose a series of methods and tools to address a set of deployment problems.

We propose a deployment framework in the context of two-tier heterogeneous WSNs. The two-tier architecture associates different utilities to different types of devices and

allows for effectively utilizing the distinct functionalities, capacities, and features of different devices. As the two tiers accomplish non-overlapping functionalities, the optimization conducted for one tier has little impact on the performance of the other tier. One of the great benefits of this decoupling of functionalities into different tiers is that it encourages design reuse.

The lower tier of the network, which consists of sensor nodes (SNs), mainly addresses sensing coverage concerns. On the other hand, network connectivity is facilitated by the upper tier of the network, which is essentially a communication backbone composed of RNs. At the same time, the deployment of relay nodes (RNs) has to take into consideration energy consumption due to data transmission so as to satisfy system lifetime requirements. Although reliability is not explicitly addressed, the large-scale deployment methods examined in this thesis, i.e., random deployment and grid-based deployment, are highly reliable in practice. First, for the SN deployment of the first tier, coverage reliability is achieved naturally by addressing deployment errors with a grid-based SN deployment. Second, for random RN deployment in the second tier, we craft the deployment density function so that an SN is connected to RNs at a very high and quantified probability. At the same time, our proposed density function extends the lifetime of the communication backbone in a probabilistic sense. In other words, the network connectivity and the system lifetime would be little affected if one or a few RNs malfunction or are misplaced.

In this research, we propose appropriate deployment methods for four distinct deployment problems.

In the first problem (Chapter 4), we assume SNs are deployed in a grid pattern. We first address deployment errors, aiming at providing complete sensing coverage even in the worst-case error scenario. By examining the causes of deployment errors and their characteristics, a reduced length/increased deployment density is derived. While this method provides complete sensing coverage, the significant cost increase makes it inapplicable or less favoured in many applications.

In the second deployment problem (Chapter 5), we attempt to reduce the grid-based SN deployment cost. Our objective is to provide high quality sensing coverage at an affordable cost when complete coverage is not necessary and would prove expensive. Therefore, we have to examine the probabilistic properties of sensing coverage. We first propose a generic approach to deriving the average and variances of the sensing coverage area. This generic approach can apply to a wide spectrum of deployment scenarios, including all shapes of deployment grids, all kinds of deployment error models, and various sensing models. We then prove that the sensing coverage provided by grid-based SN deployment in the presence of deployment errors follows approximately a normal distribution. We observe that the grid-based SN deployment is resilient to deployment errors in terms of reasonable degradation of the quality of sensing coverage. Based on our study, we strongly advocate a grid-based deployment of SNs in practice whenever it is possible.

We further study RN deployment looking at concerns of connectivity and system lifetime extension. The Biased Energy Consumption Rate (BECR) problem with uniform deployment is examined. The location-dependent unbalanced energy consumption rate problem cuts short the system lifetime; this is mainly due to different communication range in the single-hop communication case and/or various communication traffic loads in the multi-hop communication case. Therefore, RN deployment density functions are subject to optimization so as to provide robust connectivity to SNs and achieve balanced energy dissipation at the same time. The core of the optimization is that the density function is designed to reflect the energy dissipation rate. To do so, we approximate the energy consumption rate of RNs as a function of their locations. The single hop case and multi-hop case are both addressed in Chapter 6.

7.2. Technical Trends and Future Work

Recently, we have witnessed a fast growth in the portfolio of WSN devices. These devices can sense different physical characteristics, have different power supplies, have different communication capabilities, and can be used in a large variety of applications. By adopting compatible communication protocols, these devices can work together to fulfill various application requirements. This trend towards diverse devices with compatible communication will continue. Evidence of this is the industry Zigbee alliance, whose members focus on IEEE802.15.4-based WSN systems and applications, which has expanded from 15 promoters in 2002 to more than 200 members in 2007. The availability of these diverse devices and their proliferation in the near future not only makes the

heterogeneous network composition we describe in this thesis not only feasible, but also a favourable design choice.

Another technical trend of WSNs is the vast expansion of the scale of the network in trial deployments. Some of the examples include the Trio testbed reported in [127] and VigilNet, studied in [84]. The Trio tested is composed of 557 Telos sensor devices [128], 7 gateway nodes, and a base station. The VigilNet consists of 200 XSM motes [129]. These outdoor deployments stress the system software, networking protocols, and management tools for large scale WSNs. However, we argue that in a practical large scale deployment, the overall system effectiveness is highly affected by the deployment strategy, which are not stressed by these trial deployments. Our research serves as complementary work towards large-scale WSN applications.

It is very encouraging to observe the robustness of the sensing area coverage provided by the grid-based SN deployment with random errors in Chapter 5. Moreover, the grid-based deployment is simple and efficient. In the future, it would be desirable to extend our work in three aspects. First, we would like to extend our study of probabilistic properties of the sensing area coverage to incorporate other types of deployment errors identified in Chapter 4, including horizontal misalignment and vertical misalignment. Such an extension will provide a complete insight into the SN deployment in practice. Second, in Chapter 5 we implicitly assume all sensor nodes are operational all the time. It is interesting to investigate the coverage property if sensor nodes work in duty cycles. We

would like to examine this deployment approach for other sensing coverage criteria, such as discrete point coverage and crossing coverage.

We derived density functions to control RN deployment so as to provide sound connectivity and extend the system lifetime. Our design is simple and efficient. However, the engineering implementation of the density function is yet to be solved. We envision that the actual deployment exercise will be conducted in some sort of grid pattern, but further studies along these lines are necessary to turn our theory into practice.

Furthermore, we are also interested in developing an automotive network planning software package that utilizes the research in this thesis. This software package will allow the WSN solution providers and WSN system integrators to provide cost-effective, lifetime-guaranteed and application-specific network planning solutions for various application scenarios. The software package will include (1) the provisioning plan engine; (2) a user-friendly interface to display the provisioning solution; (3) an API interface that enables a provisioning control system to instruct the deployment efforts according to the optimized deployment plans. Upon successful completion of this project, we will promote the simulation-proven techniques to a commercially viable stage.

7.3. Concluding Remarks

While there is clearly more work to be done, this thesis presents significant technical advances in the device deployment design of large-scale WSN applications. Among other things, our research is pioneering in three aspects. First, our research is the only program

we are aware of that addresses the coverage-guaranteed grid-based SN deployment problem. Second, for the first time, we find and prove that the sensing coverage provided by grid-based SN deployment with random errors has approximately a normal distribution. Moreover, the formulas to evaluate the average and the variance of the normal distribution are so generic that they can be applied to a wide spectrum of deployment scenarios. Third, our RN deployment proposals can effectively balance the energy consumption rate across the network. Both the single-hop communication case and the multi-hop communication case are addressed, with no dependence on the availability of device location information. In short, the model presented in this thesis represents a significant advance in balancing communication, lifetime, and coverage requirements for large-scale WSN deployments in the face of device deployment errors.

BIBLIOGRAPHY

[1] S. Ganeriwal, A. Kansal, and M. B. Srivastava, "Self Aware Actuation for Fault Repair in Sensor Networks," in *Proceedings of IEEE International Conference on Robotics and Automation (ICRA)*, New Orleans, LA, USA, April 2004, pp. 5244-5249.

[2] M. Leoncini, G. Resta, and P. Santi, "Analysis of a Wireless Sensor Dropping Problem in Wide-area Environmental Monitoring " in *Proceedings of the 4th ACM International Conference on Information Processing in Sensor Networks (IPSN)*, Los Angeles, CA, USA, April 2005, pp. 239-245.

[3] *Opto 22* [Online]. Available: http://www.opto22.com

[4] Intel. *Autonomic Computing* [Online]. Available: http://www.intel.com/technology/itj/2006/v10i4/6-monitoring/6-usage-models.htm

[5] G. Tolle, J. Polastre, R. Szewczyk, D. Culler, N. Turner, K. Tu, S. Burgess, T. Dawson, P. Buonadonna, D. Gay, and W. Hong, "A Macroscope in the Redwoods," in *Proceedings of the 3rd ACM International Conference on Embedded Networked Sensor Systems (SenSys)*, San Diego, CA, USA, November 2005, pp. 51-64.

[6] A. Mainwaring, D. Culler, J. Polastre, R. Szewczyk, and J. Anderson, "Wireless Sensor Networks for Habitat Monitoring," in *Proceedings of the 1st ACM International Workshop on Wireless Sensor Networks and Applications (WSNA)*, Atlanta, GA, USA, September 2002, pp. 88 - 97.

[7] Wireless Sensing at Camalie Vineyards, 2003, http://camalie.com/WirelessSensing/WirelessSensors.htm.

[8] Crossbow Technology Inc, 2006, http://www.xbow.com/.

[9] Moteiv Corporation, 2007, http://www.moteiv.com/.

[10] L. Krishnamurthy, R. Adler, P. Buonadonna, J. Chhabra, M. Flanigan, N. Kushalnagar, L. Nachman, and M. Yarvis, "Design and Deployment of Industrial Sensor Networks: Experiences from A Semiconductor Plant and the North Sea," in *Proceedings of the 3rd ACM International Conference on Embedded Networked Sensor Systems (SenSys)*, San Diego, CA, USA, November 2005, pp. 64-75.

[11] S. Kim, S. Pakzad, D. Culler, J. Demmel, G. Fenves, S. Glaser, and M. Turon, "Health Monitoring of Civil Infrastructures Using Wireless Sensor Networks," in *Proceedings of the 6th ACM International Conference on Information Processing in Sensor Networks (IPSN)*, Cambridge, MA, USA, April 2007, pp. 254-263

[12] N. Xu, S. Rangwala, K. K. Chintalapudi, D. Ganesan, A. Broad, R. Govindan, and D. Estrin, "A Wireless Sensor Network for Structural Monitoring," in *Proceedings of the 2nd ACM International Conference on Embedded Networked Sensor Systems (SenSys)*, Baltimore, Maryland, USA, November 2004, pp. 13-24.

[13] V. A. Petrushin, Y. Wei, O. Shakil, D. Roqueiro, and V. Gershman, "Multiple-Sensor Indoor Surveillance System," in *Proceedings of the 3rd Canadian Conference on Computer and Robot Vision (CRV)*, Quebec City, QC, Canada, June 2006, pp. 53-60.

[14] P. B. Gibbons, B. Karp, Y. Ke, S. Nath, and S. Seshan, "IrisNet: An Architecture for a World-Wide Sensor Web," *IEEE Pervasive Computing*, vol. 2, pp. 22-33, October.-December 2003.

[15] I. F. Akyildiz, X. Wang, and W. Wang, "Wireless Mesh Networks: a Survey," *Computer Networks*, vol. 47, pp. 445-487, September 2005.

[16] I. F. Akyildiz, W. Su, Y. Sankarasubramaniam, and E. Cayirci, "A Survey on Sensor Networks," *IEEE Communications Magazine*, vol. 40, pp. 102-114, August 2002.

[17] G. Pottie and W. Kaiser, "Wireless Integrated Network Sensors," *Communications of the ACM*, vol. 43, pp. 51-58, May 2000.

[18] M. Conti and S. Giordano, "Multihop Ad Hoc Networking: The Reality," *Communications Magazine, IEEE*, vol. 45, pp. 88-95, April 2007.

[19] F. Hoffmann, M. Kaufmann, and K. Kriegel, "The Art Gallery Theorem for Polygons with Holes," in *Proceedings of the 32nd Annual Symposium on Foundations of Computer Science*, October 1991, pp. 39-48.

[20] J. N. Al-Karaki and A. E. Kamal, "Routing Techniques in Wireless Sensor Networks: A Survey," *IEEE Wireless Communications*, vol. 11, pp. 6-28, December 2004.

[21] M. Younis and K. Akkaya, "Strategies and Techniques for Node Placement in Wireless Sensor Networks: A Survey," *Ad Hoc Networks, In Press*.

[22] B. Wang, W. Wang, V. Srinivasan, and K. C. Chua, "Information Coverage and its Applications in Sensor Networks," *IEEE Communications Letters*, vol. 9, pp. 967-969, November 2005.

[23] N. Ahmed, S. S. Kanhere, and S. Jha, "Probabilistic Coverage in Wireless Sensor Networks," in *Proceedings of the 30th Annual IEEE Conference on Local Computer Networks (LCN)*, Sydney, Australia, November 2005, pp. 672-679.

[24] C.-F. Huang and Y.-C. Tseng, "The Coverage Problem in a Wireless Sensor Network " in *Proceedings of the 2nd ACM International Conference on Wireless Sensor Networks and Applications (WSNA)*, Atlanta, GA, USA, September 2003, pp. 115-121.

[25] W. Wang, V. Srinivasan, B. Wang, and K.-C. Chua, "Coverage for Target Localization in Wireless Sensor Networks," in *Proceedings of the 5th ACM International Conference on Information Processing in Sensor Networks (IPSN)*, Nashville, TN, USA, April 2006, pp. 118-125.

[26] S. Meguerdichian, F. Koushanfar, M. Potkonjak, and M. B. Srivastava, "Coverage Problems in Wireless Ad-hoc Sensor Networks," in *Proceedings of the 20nd Annual Joint Conference of the IEEE Computer and Communications Societies (INFOCOM)*, Anchorage, AK, USA, April 2001, pp. 1380-1387.

[27] S. Meguerdichian, F. Koushanfar, G. Qu, and M. Potkonjak, "Exposure in Wireless Ad-Hoc Sensor Networks " in *Proceedings of the 7th Annual International Conference on Mobile Computing and Networking (MobiCom)*, Rome, Italy, July 2001, pp. 139-150.

[28] T. Clouqueur, V. Phipatanasuphorn, P. Ramanathan, and K. K. Saluja, "Sensor Deployment Strategy for Target Detection " in *Proceedings of the 1st ACM International Workshop on Wireless Sensor Networks and Applications (WSNA)*, Atlanta, GA, USA, September 2002, pp. 42 - 48.

[29] T. Clouqueur, V. Phipatanasuphorn, P. Ramanathan, and K. K. Saluja, "Sensor Deployment Strategy for Detection of Targets Traversing a Region," *Mobile Networks and Applications*, vol. 8, pp. 453-461, August 2003.

[30] S. Kumar, T. H. Lai, and A. Arora, "Barrier Coverage with Wireless Sensors," in *Proceedings of the 11th Annual International Conference on Mobile Computing and Networking (MobiCom)*, Cologne, Germany, August 2005, pp. 284 - 298.

[31] K. Chakrabarty, S. Iyengar, H. Qi, and E. Cho, "Grid Coverage or Surveillance and Target Location in Distributed Sensor Networks," *IEEE Transactions on Mobile Computers*, vol. 51, pp. 1448-1453, December 2002.

[32] C.-F. Huang and Y.-C. Tseng, "The Coverage Problem in a Wireless Sensor Network," *Mobile Networks and Applications*, vol. 10, pp. 519-528, August 2005.

[33] G. Xing, X. Wang, Y. Zhang, C. Lu, R. Pless, and C. Gill, "Integrated Coverage and Connectivity Configuration for Energy Conservation in Sensor Networks," *ACM Transactions on Sensor Networks* vol. 1, pp. 36-72, August 2005.

[34] P.-J. Wan and C.-W. Yi, "Coverage by Randomly Deployed Wireless Sensor Networks," *IEEE/ACM Transactions on Networking*, vol. 14, pp. 2658-2669, June 2006.

[35] S. Toumpis and L. Tassiulas, "Optimal Deployment of Large Wireless Sensor Networks," *IEEE Transactions on Information Theory*, vol. 52, pp. 2935-2953, July 2006.

[36] T. Armstrong, "Wake-up Based Power Management in Multi-hop Wireless Networks," Term Survey Paper for ECE1717 Quality of Service Provisioning in Mobile Networks course, 2005, Available: http://www.eecg.toronto.edu/~trevor/Wakeup/survey.pdf.

[37] A. Keshavarzian, H. Lee, and L. Venkatraman, "Wakeup Scheduling in Wireless Sensor Networks," in *Proceedings of the 7th ACM International Symposium on Mobile Ad Hoc Networking and Computing (MobiHoc)*, Florence, Italy, May 2006, pp. 322-333

[38] W. Ye, F. Silva, and J. Heidemann, "Ultra-low Duty Cycle MAC with Scheduled Channel Polling," in *Proceedings of the 4th ACM International Conference on Embedded Networked Sensor Systems (SenSys)*, Boulder, Colorado, USA, November 2006, pp. 321-334

[39] A. Efrat, S. Har-Peled, and J. S. B. Mitchell, "Approximation Algorithms for Two Optimal Location Problems in Sensor Networks," in *Proceedings of the 2nd International Conference on Broadband Networks (Broadnets)*, Boston, MA, USA, October 2005, pp. 714-723.

[40] K. L. Clarkson, "Algorithms for Polytope Covering and Approximation," in *Proceedings of the 3rd Workshop on Algorithms and Data Structures*, Montréal, QC, Canada, August 1993, pp. 246-252.

[41] X. Zhang and S. B. Wicker, "How to Distribute Sensors in a Random Field?," in *Proceedings of the 3rd ACM International Conference on Information Processing in Sensor Networks (IPSN)*, Berkeley, CA, USA, April 2004, pp. 243-250.

[42] X. Zhang and S. B. Wicker, "On the Optimal Distribution of Sensors in a Random Field," *ACM Transactions on Sensor Networks*, vol. 1, pp. 301-306, November 2005.

[43] D. Ganesan, R. Cristescu, and B. Beferull-Lozano, "Power Efficient Sensor Placement and Transmission Structure for Data Gathering under Distortion Constraints," in *Proceedings of the 3rd ACM International Conference on Information Processing in Sensor Networks (IPSN)*, Berkeley, California, USA, April 2004, pp. 142-150.

[44] X. Liu and P. Mohapatra, "On the Deployment of Wireless Sensor Netowrks," in *Proceedings of the 3rd International Workshop on Measurement, Modelling, and Performance Analysis of Wireless Sensor Networks (SenMetrics)*, San Diego, CA, USA, July 2005, pp. 78-85.

[45] M. G. Karpovsky, K. Chakrabarty, and L. B. Levitin, "On a New Class of Codes for Identifying Vertices in Graphs," *IEEE Transactions on Information Theory*, vol. 44, pp. 599-611, March 1998.

[46] F. Y. S. Lin and P. L. Chiu, "A Near-optimal Sensor Placement Algorithm to Achieve Complete Coverage-Discrimination in Sensor Networks," *IEEE Communications Letters*, vol. 9, pp. 43-45, January 2005.

[47] S. S. Dhillon, K. Chakrabarty, and S. S. Iyengar, "Sensor Placement for Grid Coverage under Imprecise Detections " in *Proceedings of the 5th International Conference on Information Fusion*, Annapolis, MD, USA, July 2002, pp. 1581-1587.

[48] S. S. Dhillon and K. Chakrabarty, "Sensor Placement for Effective Coverage and Surveillance in Distributed Sensor Networks," in *Proceedings of Wireless Communications and Networking Conference (WCNC)*, New Orleans, LO, USA, March 2003, pp. 1609-1614.

[49] K. Kar and S. Banerjee, "Node Placement for Connected Coverage in Sensor Networks," in *Proceedings of the Modeling and Optimization in Mobile, Ad Hoc and Wireless Networks Conference (WiOpt)*, INRIA Sophia-Antipolis, France, March 2003, pp. 2.

[50] R. Iyengar, K. Kar, and S. Banerjee, "Low-coordination Topologies for Redundancy in Sensor Networks," in *Proceedings of the 6th ACM International Symposium on Mobile Ad Hoc Networking and Computing (MobiHoc)*, Urbana-Champaign, IL, USA, May 2005, pp. 332-342

[51] X. Bai, S. Kumar, D. Xuan, Z. Yun, and T. H. Lai, "Deploying Wireless Sensors to Achieve Both Coverage and Connectivity," in *Proceedings of the 7th ACM International Symposium on Mobile Ad Hoc Networking and Computing (MobiHoc)*, Florence, Italy, May 2006, pp. 131-142.

[52] E. S. Biagioni and G. Sasaki, "Wireless Sensor Placement for Reliable and Efficient Data Collection," in *Proceedings of IEEE Hawaii International Conference on System Sciences(HICSS)*, Hawaii, USA, January 2003, pp. 127b.

[53] D. Wang, Y. Cheng, Y. Wang, and D. P. Agrawal, "Lifetime Enhancement of Wireless Sensor Networks by Differentiable Node Density Deployment," in *Proceedings of the 3rd IEEE International Conference on Mobile Ad-hoc and Sensor Systemsthe (MASS)*, Vancouver, BC, Canada, October 2006, pp. 546-549.

[54] S.-C. Liu, "A Lifetime-Extending Deployment Strategy for Multi-Hop Wireless Sensor Networks," in *Proceedings of the 4th Annual IEEE Communication Networks and Services Research Conference (CNSR)*, Moncton, NB, Canada, May 2006, pp. 53-60

[55] K. Xu, Q. Wang, H. Hassanein, and G. Takahara, "Optimal Wireless Sensor Networks (WSNs) Deployment: Minimum Cost with Lifetime Constraint," in *Proceedings of 2nd IEEE International Conference on Wireless and Mobile Computing, Networking and Communications (WiMob)*, Montreal, QC, Canada, August 2005, pp. 454-461.

[56] T. H. Cormen, C. E. Leiserson, R. L. Rivest, and C. Stein, *Introduction to Algorithms*, 2nd ed: The MIT Press, 2001.

[57] X. Cheng, D.-Z. Du, L. Wang, and B. Xu, "Relay Sensor Placement in Wireless Sensor Networks " *ACM WINET*.

[58] B. Hao, J. Tang, and G. Xue, "Fault-tolerant Relay Node Placement in Wireless Sensor Networks: Formulation and Approximation," in *Proceedings of Workshop on High Performance Switching and Routing (HPSR)*, Phoenix, AZ, USA, April 2004, pp. 246-250.

[59] J. Tang, B. Hao, and A. Sen, "Relay Node Placement in Large Scale Wireless Sensor Networks," *Computer Communications*, vol. 29, pp. 490-501, Febuary 2005.

[60] E. L. Lloyd and G. Xue, "Relay Node Placement in Wireless Sensor Networks," *IEEE Transactions on Computers*, vol. 56, pp. 134-138, January 2007.

[61] J. L. Bredin, E. D. Demaine, M. Hajiaghayi, and D. Rus, "Deploying Sensor Networks with Guaranteed Capacity and Fault Tolerance," in *Proceedings of the 6th ACM International Symposium on Mobile Ad Hoc Networking and Computing (MobiHoc)*, Urbana-Champaign, IL, USA, May 2005, pp. 309-319.

[62] X. Han, X. Cao, E. L. Lloyd, and C.-C. Shen, "Fault-tolerant Relay Nodes Placement in Heterogeneous Wireless Sensor Networks," in *Proceedings of the 26th Annual Joint Conference of the IEEE Computer and Communications Societies (INFOCOM)*, Anchorage, AK, USA, May 2007, pp. 1667-1675.

[63] E. I. Oyman and C. Ersoy, "Multiple Sink Network Design Problem in Large Scale Wireless Sensor Networks," in *Proceedings of the IEEE International Conference on Communications (ICC)*, Paris, France, June 2004, pp. 3663-3667.

[64] Q. Wang, K. Xu, G. Takahara, and H. Hassanein, "Locally Optimal Relay Node Placement in Heterogeneous Wireless Sensor Networks," in *Proceedings of the 48th annual IEEE Global Telecommunications Conference(GlobeCom)*, St. Louis, MO, USA, November 2005, pp. 3549-3553.

[65] Q. Wang, K. Xu, H. Hassanein, and G. Takahara, "Minimum Cost Guaranteed Lifetime Design for Heterogeneous Wireless Sensor Networks," in *Proceedings*

of the 24th IEEE International Performance Computing and Communications Conference (IPCCC), Phoenix, AZ, USA, April 2005, pp. 599-604.

[66] A. Iranli, M. Maleki, and M. Pedram, "Energy Efficient Strategies for Deployment of a Two-Level Wireless Sensor Network," in *Proceedings of ACM/IEEE International Symposium on Low Power Electronics and Design (ISLPED)*, San Diego, CA, USA, August 8-10, 2005, pp. 233-238.

[67] Q. Wang, G. Takahara, H. Hassanein, and K. Xu, "On Relay Node Placement and Locally Optimal Traffic Allocation in Heterogeneous Wireless Sensor Networks," in *Proceedings of the 30th Annual IEEE Conference on Local Computer Networks (LCN)*, Sydney, Australia, November 2005, pp. 656-664.

[68] I. Stojmenovic and X. Lin, "Power-aware Localized Routing in Wireless Networks," *IEEE Transactions on Parallel and Distributed Systems*, vol. 12, pp. 1122-1133, November 2001.

[69] Y. Xin, T. Guven, and M. Shayman, "Relay Deployment and Power Control for Lifetime Elongation in Sensor Networks," in *Proceedings of the IEEE International Conference on Communications (ICC)*, Istanbul, Turkey, June 2006, pp. 3461-3466.

[70] A. Bogdanov, E. Maneva, and S. Riesenfeld, "Power-aware Base Station Positioning for Sensor Networks," in *Proceedings of the 23rd Annual Joint Conference of the IEEE Computer and Communications Societies (INFOCOM)*, Hong Kong, China, March 2004, pp. 575-585.

[71] J. Pan, L. Cai, Y. T. Hou, Y. Shi, and S. X. Shen, "Optimal Base-Station Locations in Two-tiered Wireless Sensor Networks," *IEEE Transactions on Mobile Computing*, vol. 4, pp. 458-473, September/October 2005.

[72] M. Younis, M. Bangad, and K. Akkaya, "Base-station Repositioning for Optimized Performance of Sensor Networks," in *Proceedings of the 58th IEEE Vehicular Technology Conference (VTC)*, Orlando, FL, USA October 2003, pp. 2956-2960.

[73] Y. Shi, Y. T. Hou, and A. Efrat, "Algorithm Design for Base Station Placement Problems in Sensor Networks " in *Proceedings of the 3rd International Conference on Quality of Service in Heterogeneous Wired/Wireless Networks* Waterloo, ON, Canada, August 2006, pp. 11 pps.

[74] P. Maulin, R. Chandrasekaran, and S. Venkatesan, "Energy Efficient Sensor, Relay and Base Station Placements for Coverage, Connectivity and Routing," in *Proceedings of 24th IEEE International Performance Computing and Communications Conference (IPCCC)*, Phoenix, AZ, USA, April 2005, pp. 581-586.

[75] J. Pan, Y. T. Hou, L. Cai, Y. Shi, and S. X. Shen, "Topology Control for Wireless Sensor Networks " in *Proceedings of the 9th Annual International Conference on Mobile Computing and Networking (MobiCom)*, San Diego, CA, USA September 2003, pp. 286-299

[76] Y. Zou and K. Chakrabarty, "Sensor Deployment and Target Localization Based on Virtual Forces," in *Proceedings of the 22nd Annual Joint Conference of the IEEE Computer and Communications Societies (INFOCOM)*, San Franciso, CA, USA, March 2003, pp. 1293-1303.

[77] G. Wang, G. Cao, and T. L. Porta, "Movement-Assisted Sensor Deployment," in *Proceedings of the 23rd Annual Joint Conference of the IEEE Computer and Communications Societies (INFOCOM)*, Hong Kong, China, March 2004, pp. 2469-2479.

[78] G. Wang, G. Cao, and T. LaPorta, "A Bidding Protocol for Deploying Mobile Sensors," in *Proceedings of the 11th IEEE International Conference on Network Protocols*, Atlanta, GA, USA, November 2003, pp. 315-324.

[79] G. Wang, G. Cao, and T. L. P. Porta, "Proxy-Based Sensor Deployment for Mobile Sensor Networks," in *Proceedings of the 1st IEEE International Conference on Mobile Ad-hoc and Sensor Systemsthe (MASS)*, Fort lauderdale, FL, USA, October 2004, pp. 493-502.

[80] J. Wu and S. Yang, "SMART: a Scan-based Movement-assisted Sensor Deployment Method in Wireless Sensor Networks," in *Proceedings of the 24th Annual Joint Conference of the IEEE Computer and Communications Societies (INFOCOM)*, Miami, FL, USA, March 2005, pp. 2313-2324.

[81] K. Akkaya and M. Younis, "Relocation of Gateway for Enhanced Timeliness in Wireless Sensor Networks," in *Proceedings of IEEE Workshop on Energy-Efficient Wireless Communications and Networks (EWCN)*, Phoenix, AZ, USA, April 2004, pp. 471-476.

[82] S. R. Gandham, M. Dawande, R. Prakash, and S. Venkatesan, "Energy Efficient Schemes for Wireless Sensor Networks With Multiple Mobile Base Stations," in *Proceedings of the 46th annual IEEE Global Telecommunications Conference(GlobeCom)*, San Francisco, CA, USA, December 2003, pp. 377-381.

[83] K. Akkaya, M. Younis, and M. Bangad, "Sink Repositioning for Enhanced Performance in Wireless Sensor Networks," *Computer Networks*, vol. 49, pp. 512-534, November 2005.

[84] T. He, P. Vicaire, T. Yan, Q. Cao, G. Zhou, L. Gu, L. Luo, R. Stoleru, J. A. Stankovic, and T. F. Abdelzaher, "Achieving Long-Term Surveillance in VigilNet," in *Proceedings of the 25th Annual Joint Conference of the IEEE Computer and Communications Societies (INFOCOM)*, Barcelona, Spain, April 2006, pp. 1-12.

[85] V. Mhatre and C. Rosenberg, "Homogeneous vs Heterogeneous Clustered Sensor Networks," in *Proceedings of the IEEE International Conference on Communications (ICC)*, Paris, France, June 2004, pp. 3646-3651.

[86] A. Boulis, S. Ganeriwal, and M. B. Srivastava, "Aggregation in Sensor Networks: An Energy-Accuracy Trade-off," in *Proceedings of the 1st IEEE International Workshop on Sensor Network Protocols and Applications*, Anchorage, AK, USA, May 2003, pp. 128-138.

[87] B. Krishnamachari, D. Estrin, and S. Wicker, "The Impact of Data Aggregation in Wireless Sensor Networks," in *Proceedings of the 22nd International Conference on Distributed Computing Systems*, Vienna, Austria, July 2002, pp. 575-578.

[88] K. Kalpakis, K. Dasgupta, and P. Namjoshi, "Efficient Algorithm for Maximum Lifetime Data Gathering and Aggregation in Wireless Sensor Networks," Computer Science and Electrical Engineering Department, University of Maryland, Baltimore County, Technical Report UMBC-TR-02-13, 2002, Available: http://citeseer.ist.psu.edu/kalpakis02efficient.html

[89] B. Greenstein, C. Mar, A. Pesterev, S. Farshchi, E. Kohler, J. Judy, and D. Estrin, "Capturing High-frequency Phenomena using a Bandwidth-limited Sensor Network," in *Proceedings of the 4th ACM International Conference on Embedded Networked Sensor Systems (SenSys)*, Boulder, Colorado, USA Nov. 2006, pp. 279-292.

[90] B. Aoun and R. Boutaba, "Clustering in WSN with Latency and Energy Consumption Constraints," *Journal of Network and Systems Management*, vol. 14, pp. 415-439, September 2006.

[91] Q. Wang, K. Xu, H. Hassanein, and G. Takahara, "SWATCH: a StepWise AdapTive Clustering Hierarchy for Energy-Efficient Communication in Wireless Sensor Network (WSNs)," in *Proceedings of IFIP International Conferences on Networking*, Waterloo, Ontario, Canada, May 2005, pp. 1422-1425.

[92] O. Younis and S. Fahmy, "Distributed Clustering in Ad-hoc Sensor Networks: a Hybrid, Energy-efficient Approach," in *Proceedings of the 23rd Annual Joint Conference of the IEEE Computer and Communications Societies (INFOCOM)*, Hong Kong, China, March 2004, pp. 629-640.

[93] Q. Wang, H. Hassanein, and G. Takahara, "Stochastic Modeling of Distributed, Dynamic, Randomized Clustering Protocols for Wireless Sensor Networks," in *Proceedings of International Conference on Parallel Processing (ICPP)*, Montreal, QC, Canada, August 2004, pp. 456-463.

[94] V. Mhatre and C. Rosenberg, "Design Guideline for Wireless Sensor Networks: Communication, Clustering and Aggregation," *Ad Hoc Networks Journal, Elsevier Science*, vol. 2, pp. 45-63, January 2004.

[95] V. Mhatre, C. Rosenberg, D. Kofman, R. Mazumdar, and N. Shroff, "A Minimum Cost Heterogeneous Sensor Network with a Lifetime Constraint," *IEEE Transactions on Mobile Computing*, vol. 4, pp. 4-15, January-Febuary, 2005.

[96] C.-H. Wu and Y.-C. Chung, "Heterogeneous Wireless Sensor Network Deployment and Topology Control Based on Irregular Sensor Model," in *Proceedings of International Conference on Grid and Pervasive Computing*, Paris, France, May 2007, pp. 12 pps

[97] W. Hu, C. T. Chou, S. Jha, and N. Bulusu, "Deploying Long-lived and Cost-effective Hybrid Sensor Networks," in *Proceedings of the 1st Workshop on Broadband Advanced Sensor Networks*, San Jose, CA, USA, October 2004 pp. 10 pps.

[98] X. Wu, G. Chen, and S. K. Das, "On the Energy Hole Problem of Nonuniform Node Distribution in Wireless Sensor Networks," in *Proceedings of the 3rd IEEE International Conference on Mobile Ad-hoc and Sensor Systemsthe (MASS)*, Vancouver, BC, Canada, October 2006, pp. 180-187.

[99] L. Nachman, R. Kling, R. Adler, J. Huang, and V. Hummel, "The Intel Mote Platform: a Bluetooth-based Sensor Network for Industrial Mnitoring," in *Proceedings of the 4th ACM International Conference on Information Processing in Sensor Networks (IPSN)*, Los Angeles, CA, USA, April 2005, pp. 437-442.

[100] I. Zeevo. *TC2001P Product Brief* [Online]. Available: http://www.zeevo.com/pdf_files/TC2001P_HCI_prodbrief_v1.2.pdf

[101] IEEE Standard for Information Technology - Telecommunications and Information Exchange between Systems - Local and Metropolitan Area Networks

Specific Requirements Part 15.4: Wireless Medium Access Control (MAC) and Physical Layer (PHY) Specifications for Low-rate Wireless Personal Area Networks (LR-WPANs), 2003.

[102] S.-P. Kuo, Y.-C. Tseng, F.-J. Wu, and C.-Y. Lin, "A Probabilistic Signal-Strength Based Evaluation Methodology for Sensor Network Deployment," *International Journal of Ad Hoc and Ubiquitous Computing*, vol. 1, pp. 3-12, 2005.

[103] Q. Wang, K. Xu, H. Hassanein, and G. Takahara, "Deployment for Information Oriented Sensing Coverage in Wireless Sensor Networks," in *Proceedings of the 49th annual IEEE Global Telecommunications Conference(GlobeCom)*, San Francisco, CA, USA, November 2006, pp. 1-5.

[104] W. B. Heinzelman, A. P. Chandrakasan, and H. Balakrishnan, "An Application-Specific Protocol Architecture for Wireless Microsensor Networks," *IEEE Tranactions on Wireless Communications*, vol. 1, pp. 660-670, October 2002.

[105] J.-J. Lee, B. Krishnamachari, and C.-C. J. Kuo, "Impact of Heterogeneous Deployment on Lifetime Sensing Coverage in Sensor Networks," in *Proceedings of the 1st IEEE Communications Society Conference on Sensor and Ad Hoc Communications and Networks (SECON)*, San Jose, CA, USA, October 2004, pp. 367-376.

[106] A. Nasipuri and K. Li, "A Directionality based Location Discovery Scheme for Wireless Sensor Networks " in *Proceedings of the 1st ACM International Workshop on Wireless Sensor Networks and Applications (WSNA)*, Atlanta, GA, USA September 2002, pp. 105-111

[107] C. Savarese, J. Rabay, and K. Langendoen, "Robust Positioning Algorithms for Distributed Ad-Hoc Wireless Sensor Networks," in *USENIX Technical Annual Conference*, Monterey, CA, USA, June 2002, pp. 317-327.

[108] A. Savvides, C. C. Han, and M. Srivastava, "Dynamic Fine-Grained Localization in Ad-Hoc Networks of Sensors," in *Proceedings of the 7th Annual International Conference on Mobile Computing and Networking (MobiCom)*, Rome, Italy, July 2001, pp. 166-179.

[109] K. Xu, G. Takahara, and H. Hassanein, "On the Robustness of Grid-based Deployment in Wireless Sensor Networks," in *Proceedings of International Wireless Communications and Mobile Computing Conference (IWCMC)*, Vancouver, BC, Canada, July 2006, pp. 1183-1188.

[110] Y. Liu and W. Liang, "Approximate Coverage in Wireless Sensor Networks," in *Proceedings of the 30th Annual IEEE Conference on Local Computer Networks (LCN)*, Sydney, Australia, November 2005, pp. 68-75.

[111] T. He, S. Krishnamurthy, J. A. Stankovic, T. Abdelzaher, L. Luo, R. Stoleru, T. Yan, L. Gu, J. Hui, and B. Krogh, "Energy-Efficient Surveillance System Using Wireless Sensor Networks," in *Proceedings of the 2nd International Conference on Mobile Systems, Applications, and Services (MobiSys)*, Boston, MA, USA, June 2004, pp. 270-283

[112] S. Megerian, F. Koushanfar, M. Potkonjak, and M. B. Srivastava, "Worst and Best-Case Coverage in Sensor Networks," *IEEE Transactions on Mobile Computing*, vol. 4, pp. 84-92, January-Febuary 2002.

[113] G. Takahara, K. Xu, and H. Hassanein, "How Resilient is Grid-based WSN Coverage to Deployment Errors?," in *Proceedings of IEEE Wireless*

Communications and Networking Conference (WCNC), Hongkong, China, March 2007, pp. 6 pps.

[114] G. Takahara, K. Xu, and H. Hassanein, "Efficient Coverage Planning for Grid-Based Wireless Sensor Networks," in *Proceedings of the IEEE International Conference on Communications (ICC)*, Glasgow, Scotland, June 2007, pp. 5 pps.

[115] B. Rosen, "A Note on Asymptotic Normality of Sums of Higher Dimensionally Indexed Random Variables," *Ark. Mat.*, vol. 8, pp. 33-43, 1969.

[116] A. V. Bulinskii and I. G. Zurbenko, "The Central Limit Theorem for Random Fields," *Soviet Math. Dokl.*, vol. 17, pp. 14-17, 1976.

[117] H. Takahata, "On the Rates in the Central Limit Theorem for Weakly Dependent Random Fields," *Zeitschrift für Wahrscheinlichkeitstheorie und Verwandte Gebiete*, vol. 64, pp. 445-456, 1983.

[118] L. Wang and S. S. Kulkarni, "Sacrificing a Little Coverage Can Substantially Increase Network Lifetime," in *Proceedings of the 3rd IEEE Communications Society Conference on Sensor, Mesh and Ad Hoc Communications and Networks (SECON)*, Reston, VA, USA, September 2006, pp. 326-335.

[119] K. Xu, H. Hassanein, G. Takahara, and Q. Wang, "Relay Node Deployment Strategies in Heterogeneous Wireless Sensor Networks: Single Hop Communication Case," in *Proceedings of the 48th annual IEEE Global Telecommunications Conference(GlobeCom)*, St. Louis, MO, USA, November-December 2005, pp. 21-25.

[120] K. Xu, H. Hassanein, and G. Takahara, "Relay Node Deployment Strategies in Heterogeneous Wireless Sensor Networks: Multiple-Hop Communication Case," in *Proceedings of the 2nd IEEE Communications Society Conference on Sensor and Ad Hoc Communications and Networks (SECON)*, San Jose, CA, USA, September 2005, pp. 575-585.

[121] D. Ganesan, R. Cristescu, and B. B. Lozano, "Power Efficient Sensor Placement and Transmission Structure for Data Gathering under Distortion Constraints," *ACM Transactions on Sensor Networks*, vol. 2, pp. 155-181.

[122] A. D. Amis, R. Prakash, T. H. P. Vuong, and D. T. Huynh, "Max-Min D-Cluster Formation in Wireless Ad Hoc Networks," in *Proceedings of the 19th Annual Joint Conference of the IEEE Computer and Communications Societies (INFOCOM)*, Tel-Aviv, Israel, March 2000, pp. 32-41.

[123] P. Cheng, C.-N. Chuah, and X. Liu, "Energy-aware Node Placement in Wireless Sensor Networks," in *Proceedings of the 47th annual IEEE Global Telecommunications Conference(GlobeCom)*, Dallas, TX, USA, pp. 3210-3214.

[124] M. Chatterjee, S. K. Das, and D. Turgut, "WCA: A Weighted Clustering Algorithm for Mobile Ad Hoc Networks," *Clustering Computing, special issue on mobile ad hoc networking*, vol. 5, pp. 193-204, November 2004.

[125] O. Younis and S. Fahmy, "HEED: A Hybrid, Energy-Efficient, Distributed Clustering Approach for Ad Hoc Sensor Networks," *IEEE Transactions On Mobile Computing*, vol. 3, pp. 366-379, 2004.

[126] S. Bandyopadhyay and E. J. Coyle, "An Energy Efficient Hierarchical Clustering Algorithm for Wireless Sensor Networks," in *Proceedings of the 22nd Annual Joint Conference of the IEEE Computer and Communications Societies (INFOCOM)*, San Franciso, CA, USA, March 2003, pp. 1713-1723.

[127] P. Dutta, J. Hui, J. Jeong, S. Kim, R. Shah, J. Taneja, G. Tolle, K. Whitehouse, and D. Culler, "Trio: Enabling Sustainable and Scalable Outdoor Wireless Sensor Network Deployments," in *Proceedings of the 5th ACM International Conference on Information Processing in Sensor Networks (IPSN)*, Nashville, TN, USA, April 2006, pp. 407- 415.

[128] J. Polastre, R. Szewczyk, and D. Culler, "Telos: Enabling ultra-Low Power Wireless Research," in *Proceedings of the 4th ACM International Conference on Information Processing in Sensor Networks (IPSN)*, Los Angeles, CA, USA, April 2005, pp. 364-369.

[129] P. Dutta, M. Grimmer, A. Arora, S. Bibyk, and D. Culler, "Design of a Wireless Sensor Network Platform for Detecting Rare, Random and Ephemeral Events," in *Proceedings of the 4th ACM International Conference on Information Processing in Sensor Networks (IPSN)*, Los Angeles, CA, USA, April 2005, pp. 497-502.

A list of publications resulted from this research

[1] Q. Wang, H. Hassanein, and K. Xu, "A Practical Perspective on Wireless Sensor Networks," in *Handbook of Sensor Networks: Compact Wireless and Wired Sensing Systems*, M. Ilyas and I. Mahgoub, Eds., CRC press, 2004, pp. 28 pps.

[2] G. Takahara, K. Xu, and H. Hassanein, "Efficient Coverage Planning for Grid-Based Wireless Sensor Networks," in *Proceedings of the IEEE International Conference on Communications (ICC)*, Glasgow, Scotland, June 2007, pp. 5 pps.

[3] G. Takahara, K. Xu, and H. Hassanein, "How Resilient is Grid-based WSN Coverage to Deployment Errors?," in *Proceedings of IEEE Wireless Communications and Networking Conference (WCNC)*, Hongkong, China, March 2007, pp. 6 pps.

[4] K. Xu, H. Hassanein, G. Takahara, and Q. Wang, "Differential Random Deployment for Sensing Coverage in Wireless Networks," in *Proceedings of the 49th annual IEEE Global Telecommunications Conference(GlobeCom)*, San Francisco, CA, USA, November 2006, pp. 1-5.

[5] K. Xu, G. Takahara, and H. Hassanein, "On the Robustness of Grid-based Deployment in Wireless Sensor Networks," in *Proceedings of International Wireless Communications and Mobile Computing Conference (IWCMC)*, Vancouver, BC, Canada, July 2006, pp. 1183-1188.

[6] K. Xu, H. Hassanein, G. Takahara, and Q. Wang, "Relay Node Deployment Strategies in Heterogeneous Wireless Sensor Networks: Single Hop Communication Case," in *Proceedings of the 48th annual IEEE Global Telecommunications Conference(GlobeCom)*, St. Louis, MO, USA, November-December 2005, pp. 21-25.

[7] K. Xu, H. Hassanein, and G. Takahara, "Relay Node Deployment Strategies in Heterogeneous Wireless Sensor Networks: Multiple-Hop Communication Case," in *Proceedings of the 2nd IEEE Communications Society Conference on Sensor and Ad Hoc Communications and Networks (SECON)*, San Jose, CA, USA, September 2005, pp. 575-585.